UNCLASSIFIED

MARTIN MARIETTA ENERGY SYSTEMS LIBRARIES
3 4456 0050902 8

ORNL 865
Series A 8
Progress Report
Physics

PHYSICS DIVISION

QUARTERLY PROGRESS REPORT FOR PERIOD ENDING SEPTEMBER 20, 1950

CENTRAL RESEARCH LIBRARY
DOCUMENT COLLECTION

LIBRARY LOAN COPY

DO NOT TRANSFER TO ANOTHER PERSON

If you wish someone else to see this document, send in name with document and the library will arrange a loan.

OAK RIDGE NATIONAL LABORATORY
OPERATED BY
CARBIDE AND CARBON CHEMICALS DIVISION
UNION CARBIDE AND CARBON CORPORATION
UCC
POST OFFICE BOX P
OAK RIDGE, TENNESSEE

UNCLASSIFIED

UNCLASSIFIED

ORNL 865
Progress
This document consists of 107 pages.
Copy 8 of 220. Series A.

Contract No. W-7504, eng 26

PHYSICS DIVISION

A. H. Snell, Director
E. O. Wollan, Associate Director

QUARTERLY PROGRESS REPORT
for Period Ending September 20, 1950

DATE ISSUED: JAN 8 1951

OAK RIDGE NATIONAL LABORATORY
operated by
CARBIDE AND CARBON CHEMICALS DIVISION
Union Carbide and Carbon Corporation
Post Office Box P
Oak Ridge, Tennessee

UNCLASSIFIED

MARTIN MARIETTA ENERGY SYSTEMS LIBRARIES
3 4456 0050902 8

ORNL-865
Progress Report
Physics

INTERNAL DISTRIBUTION:

1	G. T. Felbeck (C&CCD)	30	M. T. Kelley
2-3	706-A Library	31	W. H. Pennington
4	706-B Library	32	R. S. Livingston
5	Biology Library	33	C. D. Susano
6	Health Physics Library	34	E. O. Wollan
7	Metallurgy Library	35	D. W. Cardwell
8-9	Training School Library	36	A. S. Householder
10-13	Central Files	37	L. D. Roberts
14	C. E. Center	38	J. A. Lane
15	C. E. Larson	39	M. M. Mann
16	W. B. Humes (K-25)	40	R. N. Lyon
17	W. D. Lavers (Y-12)	41	W. C. Koehler
18	A. M. Weinberg	42	W. K. Ergen
19	J. A. Swartout	43	E. P. Blizard
20	E. D. Shipley	44	M. J. Skinner
21	E. J. Murphy	45	G. E. Boyd
22	F. C. VonderLage	46	Lewis Nelson
23	A. H. Snell	47	R. W. Stoughton
24	E. H. Taylor	48	C. E. Winters
25	A. Hollaender	49	W. H. Jordan
26	K. Z. Morgan	50	E. C. Campbell
27	F. L. Steahly	51	D. S. Billington
28	G. H. Clewett	52	M. A. Bredig
29	C. P. Keim	53-61	Central Files (Off-Plant)

EXTERNAL DISTRIBUTION:

62-73	Argonne National Laboratory
74	Armed Forces Special Weapons Project
75-80	Atomic Energy Commission, Washington
81	Battelle Memorial Institute
82	Brush Beryllium Company
83-86	Brookhaven National Laboratory
87	Bureau of Medicine and Surgery
88	Bureau of Ships
89-92	Carbide and Carbon Chemicals Division (K-25 Plant)
93	Columbia University (J. R. Dunning)
94	Columbia University (G. Failla)
95-98	General Electric, Richland
99-102	Idaho Operations Office
103-104	Iowa State College
105	Kansas City Operations Branch
106	Kellex Corporation
107-108	Kirtland Air Force Base
109-112	Knolls Atomic Power Laboratory
113-115	Los Alamos Scientific Laboratory

EXTERNAL DISTRIBUTION (Cont'd)

116 Mallinckrodt Chemical Works
117 Massachusetts Institute of Technology (A. Gaudin)
118 Massachusetts Institute of Technology (A. R. Kaufmann)
119-121 Mound Laboratory
122 National Advisory Committee for Aeronautics
123 National Bureau of Standards (R. D. Huntoon)
124 Naval Medical Research Institute
125-126 Naval Radiological Defense Laboratory
127 New Brunswick Laboratory
128-130 New York Operations Office
131 North American Aviation, Inc.
132-135 Carbide and Carbon Chemicals Division (Y-12 Area)
136 Patent Branch, Washington
137 RAND Corporation
138 Sandia Corporation
139 Santa Fe Operations Office
140-154 Technical Information Service, Oak Ridge
155-157 USAF, NEPA Office
158-159 U. S. Geological Survey (T. B. Nolan)
160-161 U. S. Public Health Service
162 University of California at Los Angeles
163-167 University of California Radiation Laboratory
168-169 University of Rochester
170 University of Washington
171 Western Reserve University
172-175 Westinghouse Electric Corporation
176-179 Atomic Energy Project, Chalk River
180 Chief of Naval Research
181 H. K. Ferguson Company
182 Harshaw Chemical Company
183 Isotopes Division (Mr. McCormick)
184-185 Library of Congress, Acquisition Department (J. W. Cormn)
186 National Bureau of Standards
187 National Research Council, Ottawa
188 Naval Research Laboratory
189-190 Nevis Cyclotron Laboratories
191 Nucleonics
192-193 Oak Ridge Institute of Nuclear Studies
194-203 United Kingdom Scientific Mission (M. Greenhill)
204 USAF, Eglin Air Force Base (Technical Library)
205 USAF, Wright-Patterson Air Force Base (Rodney Nudenberg)
206-210 USAF, Wright-Patterson Air Force Base (CADO)
211 U. S. Army, Army Field Forces (Captain James Kerr)
212 U. S. Army, Atomic Energy Branch (Lt. Col. A. W. Betts)
213 U. S. Army, Director of Operations Research (Dr. Ellis Johnson)
214 U. S. Army, Office, Chief of Ordnance (Col. A. R. Del Campo)
215-216 U. S. Army, Office of the Chief Signal Officer (Curtis T. Clayton thru Major George C. Hunt)
217-219 U. S. Army, Technical Command (Col. J. H. Rothschild Attn: Technical Library)
220 UT-AEC Agricultural Research Program (Charles S. Hobbs)

TABLE OF CONTENTS

INTRODUCTION AND SUMMARY 8

PUBLICATIONS 11

RADIOACTIVITY STUDIES 12

- Short-lived Isomers 12
- X Rays from Radioactive Nuclei 16
- Short-period Radioactivity in In and Yb 19
- Split-crystal Scintillation Spectrometer 21
- Spectrometry and Coincidence Spectrometry of Cadmium Activities 21
- Total-absorption Spectrometer 24
- Single-channel Analyzer 27

NEUTRON PHYSICS AND LOW TEMPERATURES 32

- Nuclear Alignment 32
- Production of Polarized Neutrons for Nuclear Alignment 34
- Neutron Polarization by Transmission Through Magnetized Iron 35

NEUTRON DIFFRACTION 49

- Polarization of Bragg-reflected Neutrons 49
- Scattering of Neutrons by Iron and Its Isotopes 51
- Crystal Monochromators 55
- Tables of Trigonometric Functions 55

HIGH-VOLTAGE ACCELERATOR PROGRAM 56

- Reactions with Protons on B^{11} 56

SEARCH FOR A PERMANENT ELECTRIC DIPOLE MOMENT OF THE NEUTRON 62

THERMAL NEUTRON DIFFUSION IN WATER 63

THEORETICAL PHYSICS 64

- Introduction 64
- Theoretical Problems Concerning Paramagnetic Substances 65
- Internal Conversion 66
- Zero-Zero Transitions 66
- Reactions 67
- Angular Dependence in Gamma Emission 72
- Collecting Efficiency in Neutron Decay Studies 73

TABLE OF CONTENTS (cont'd)

PHYSICS OF SOLIDS 77

Phase Transition on Neutron Bombardment 77
X-Ray Diffraction and Crystal Structure 78

Remote Control X-ray-diffraction Spectrometer for High-level Radioactive Specimens 78
Determination of the Crystal Structure of the Tutton Salts 78
Line-broadening in Electron-bombarded Copper-Beryllium Alloy 79
Search for Hypothetical Cubic Modification of Beryllium Oxide 79
High-temperature Crystal Structure of Uranium Dicarbide 81
Growing of Single Crystals 83
Miscellaneous X-ray-diffraction Work 83

Heavy Positive Ion Bombardment Studies 84
Electron Bombardment of Be-Cu 87
Semiconductor Bombardment Research 87

Experiments on Cuprous Oxide 87
Experiments on Germanium 92

Physics of Solids New Hot Laboratory 95
Cryostat for Pile Irradiations 95

Bonded Wire Resistance Strain Gages 98
Effect of Pile Radiation on Performance of Electrical Leads 106

LIST OF FIGURES

Fig. 1	Delayed-coincidence Scintillation Spectrometer	13
Fig. 2	Decay of Eu^{153*}	15
Fig. 3	Decay of $_{68}Er^{166*}$	17
Fig. 4	X Rays from Radioactive Nuclei	18
Fig. 5	P^{32} β Spectrum, Split-crystal Spectrometer	22
Fig. 6	Kurie Plot of P^{32}; Split-anthracene-crystal Spectrometer	23
Fig. 7	Kurie Plot of Long-lived Cd^{113}; Split-crystal Spectrometer	25
Fig. 8	Cs^{137} Gamma Ray as Measured with Total Absorption Spectrometer	26
Fig. 9	Co^{60} Gamma Ray as Measured with Total Absorption Spectrometer	28
Fig. 10	Single-channel Analyzer—Preliminary	29
Fig. 11	Experimental Arrangement for Measuring Single-transmission Effect at a Given Neutron Energy	39
Fig. 12	Curves for Values of $F(l)$ for Three Cases	45
Fig. 13	Curve of j/j_0 vs. Iron Thickness	46
Fig. 14	Neutron Scattering Data Obtained from Polycrystalline Fe	52
Fig. 15	α-Particle Energy Distribution for the Reaction $B^{11}(p, 3\alpha)$	58
Fig. 16	Yield Curves of $B^{11}(p, 3\alpha)$ Reactions; Effect of Target Contamination	59
Fig. 17	Angular Distribution of the 12.2-Mev γ Ray from $B^{11} + H^1$ with Respect to the Beam	61
Fig. 18	Drawing Showing Angle Between Incident and Scattered Particles	68
Fig. 19	Schematic Drawing Showing Various Components of Heavy Positive Ion Source	85

LIST OF FIGURES (Cont'd)

Fig. 20	Cu_2O Plate Conductance vs. Bombardment Time (Constant Pile Power)	89
Fig. 21	Cu_2O Rectifier—Effect of Pile Irradiation	91
Fig. 22	Germanium Sample 44x-9, Hall Coefficient vs. Temperature	93
Fig. 23	Germanium Sample 44x-9, Current Carrier Change Due to Transmutations	94
Fig. 24	Physics of Solids Building—Cell Section	96
Fig. 25	Physics of Solids Building—Horizontal Section and South Elevation of Cells 4, 5 and 6	97
Fig. 26	Apparent Radiation Damage to Copper as Measured by SR-4 Bakelite-bonded 100-ohm Dual Lead-strain Gage No. 1, Water-cooled, Neutron Converter, Hole No. 51; Temperature Maintained at 34°C	99
Fig. 27	Apparent Radiation Damage to Copper as Measured by SR-4 Bakelite-bonded 100-ohm Dual Lead-strain Gage No. 2, Water-cooled, Neutron Converter, Hole No. 51; Temperature Maintained at 34°C	100
Fig. 28	Apparent Radiation Damage to Nilvar as Measured by SR-4 Bakelite-bonded 100-ohm Dual Lead-strain Gage No. 3, Water-cooled, Neutron Converter, Hole No. 51; Temperature Maintained at 34°C	101
Fig. 29	Apparent Radiation Damage to Nilvar as Measured by SR-4 Bakelite-bonded 100-ohm Dual Lead-strain Gage No. 4, Water-cooled, Neutron Converter, Hole No. 51; Temperature Maintained at 34°C	102
Fig. 30	Apparent Radiation Damage to 2S Aluminum as Measured by SR-4 Bakelite-bonded 100-ohm Dual Lead-strain Gage No. 5, Water-cooled, Neutron Converter, Hole No. 51; Temperature Maintained at 34°C	103
Fig. 31	Apparent Radiation Damage to 2S Aluminum as Measured by SR-4 Bakelite-bonded 100-ohm Dual Lead-strain Gage No. 6, Water-cooled, Neutron Converter, Hole No. 51; Temperature Maintained at 34°C	104

INTRODUCTION AND SUMMARY

The following report covers unclassified work for the interval June 15 to September 20, 1950. The classified section of the quarterly report appears separately (ORNL-864).

The Division has had several visiting members during the summer months, a few of whom have been or will be with the Division for a longer period. Drs. J. M. Jauch, University of Iowa, and Sidney D. Drell, new appointee at Stanford, were in the theoretical group. In experimental physics were L. W. Cochran (Kentucky), Dr. Max Goodrich (Louisiana), Dr. J. I. Hopkins (Vanderbilt), Dr. Darrell Hughes (University of Texas), F. I. Magee (Mississippi), Dr. Otto Meier, Jr. (Duke), Dr. J. R. Risser (Rice), and R. H. Rohrer (Duke). In training from Cornell's Engineering-Physics program were F. J. Loeffler and J. W. Schwartz.

As Physics Division members of the Reactor Training program, Dr. R. J. Stephenson (Wooster College) will be with the laboratory for a year and Dr. T. R. Cuykendall (Cornell) for six months. Dr. H. H. Hubbell (Middleburg College), in Physics for the summer, has joined Health Physics as a permanent member.

The ORINS Fellows now doing graduate work in the division include R. A. Erickson (Texas A. and M.), J. H. Kahn and W. E. Kunz (Tennessee), S. F. Malaker and G. S. Pawlicki (Catholic University), and, on a special fellowship arrangement, J. H. Smith (Harvard)

New additions to the Physics staff who have so far arrived are Drs. G. B. Arfken, L. C. Biedenharn, J. L. Meems, A. Simon, E. C. Smith, G. T. Trammell, and T. A. Welton.

Short-lived Isomers. The delayed coincidence technique has been improved so that delays in the region of about 5×10^{-10} sec can now be detected. An excited state in Eu^{153} (3×10^{-9} sec) has been observed, the half-life of the 80-Kev transition in Er^{166} has been measured (1.7×10^{-9} sec), and energy measurements have been made.

Short-period Activities. A study is being made with krypton and xenon containing proportional counters of the X rays and low-energy γ rays emitted

by radioactive nuclei. Many of the X rays result from the conversion of the low-energy γ rays. γ rays have been found associated with short-period activities in In and Yb, the investigation, in this case, being made with a NaI scintillation counter.

Scintillation Spectrometry. A split-crystal spectrometer has been developed in which a β-ray source is completely surrounded by the crystal and essentially all the radiation from the source can be measured. It is useful for absolute β-ray counting and also for the study of spectra, in which case the usual difficulties at low energies can to a great extent be eliminated.

Large crystals of NaI are now being used in γ-ray studies where it is desired to absorb almost completely the γ-ray energy. This has obvious applications in disintegration-scheme studies and in the study of complicated γ-ray spectra.

Instruments. A new single-channel analyzer has been built which has some advantages over previous models.

Nuclear Alignment. Test runs have been made in an experiment to align the manganous ion nuclei in manganous ammonium sulfate by aligning the electrons in a magnetic field at low temperatures and relying on the hyperfine coupling to affect the nuclei. The degree of alignment, if any, is detected by activation with polarized neutrons from the reactor.

Measurements on the specific heat of manganous ammonium sulfate below 1°K are found to be in good accord with Casimir's theory.

A study has been made of the polarization of neutrons by transmission through iron as a function of the neutron wavelength. The crystal discontinuity effects are observed, and it is suggested that this method may throw light on the nature of the form factor for the magnetic electrons.

Neutron Diffraction. Polarized beams of monochromatic neutrons have been obtained by Bragg reflection from magnetized single crystals of Fe. Studies have been made to see whether the theoretical value of about 60% polarization is realized experimentally.

The magnetic and nuclear cross sections for normal Fe and the isotopes Fe^{54}, Fe^{56}, and Fe^{57} have been measured.

Improvement in the monochromatic beam intensity by the use of a copper crystal has been effected.

High-voltage Accelerator Program. The Cockcroft-Walton generator has been used in the study of reactions involving protons on B^{11}. The energies and the yield as a function of voltage of the α particles have been measured. The yield with energy and the angular correlation of the γ rays from two of the four competing processes have been investigated with a scintillation spectrometer.

Search for a Permanent Electric Dipole Moment of the Neutron. As a joint project of Harvard University and this Laboratory, an experiment is underway to determine, if possible, whether or not the neutron possesses a permanent electric dipole moment. Results so far indicate an upper limit for such a moment as the electron charge multiplied by 10^{-18} cm.

Neutron Diffusion in Water. The thermal flux distribution has been measured in water in the vicinity of a large plane cadmium absorber. The theoretically determined curve, when fitted to the data, gives good values for the scattering and absorption cross sections.

Physics of Solids. A number of crystal-structure problems have been investigated. Some results have been obtained relative to the structure of cobalt ammonium sulfate. Diffraction-line broadening has been observed in electron-bombarded Cu-Be alloy. A neutron-diffraction study at high temperatures aimed at observing structure transitions in UC_2 has not yet been successful.

Equipment for heavy positive-ion-bombardment studies is nearing completion.

Tests on wire-insulation performance under pile irradiation show polyethylene to stand up better over long periods than other insulators so far tested.

A number of semiconductor neutron-bombardment studies have been carried out on cuprous oxide and germanium. In the case of germanium, the effective impurity concentration is varied by neutron capture toward P-type, and this permits a study of the variations of the Fermi level with impurity concentration which can then be compared with theory.

Theory. A number of problems have been treated by the theoretical physicists. The L-shell conversion problem has been reviewed relative to carrying out the computing-machine work. Several problems have arisen in connection with the work of the Particle Acceleration program, one of which is concerned with the angular dependence of γ emission from protons on B^{11}.

PUBLICATIONS

The following contributions by members of the Physics Division have appeared in the open literature between July 1 and September 30, 1950:

"Gamma-Rays from Po-Be Neutron Source and the Excited State of C^{12}," P. R. Bell and W. H. Jordan, *Phys. Rev.* **79**, 392 (1950).

"Coherent Neutron Scattering Cross Sections of Nickel and Its Isotope," W. C. Koehler, E. O. Wollan, and C. G. Shull, *Phys. Rev.* **79**, 395 (1950).

"A 5.7×10^{-9}-Sec. Isomeric State in $_{77}Ir^{191}$," F. K. McGowan, *Phys. Rev.* **79**, 404 (1950).

"Thermal Equilibrium in Neutron-Irradiated Semiconductors," J. H. Crawford, Jr., and K. Lark-Horovitz, *Phys. Rev.* **79**, 889 (1950).

"Electronic Pile Simulator," P. R. Bell and H. A. Straus, *Rev. Sci. Instruments* **21**, 760 (1950).

"Pair Production and Photoelectric Effect in Scintillation Phosphors," P. R. Bell, *Science* **112**, 7 (1950).

"Neutrons as Waves and Particles," E. O. Wollan and C. G. Shull, *Physics Today* **3**, 20 (1950).

"Measurement of the Gamma-Ray Energy of K^{40}," P. R. Bell and Judith M. Cassidy, *Phys. Rev.* **79**, 173 (1950).

RADIOACTIVITY STUDIES

Short-lived Isomers (F. K. McGowan). Both the radiation announcing the formation of the isomeric state and the radiation resulting from its decay have been studied with a delayed-coincidence scintillation spectrometer for the following nuclei: Ge^{72*}, Ta^{181*}, and Re^{187*}. The results of these measurements will be included and discussed fully as a part of a doctoral dissertation which is being written by the author.

The method of delayed coincidences between scintillation detectors employing anthracene and 5819 photomultipliers has been extended to measure time intervals in the region 5×10^{-10} to 1×10^{-8} sec. This extension has been made possible through the use of Hewlett Packard 460A wide-band amplifiers, the scintillation spectrometer, and improved methods of analysis[1] of delayed-coincidence resolution curves. A block diagram of the apparatus is shown in Fig. 1. With this apparatus the trailing edge of a resolution curve for prompt events has a slope corresponding to a half-period of 4×10^{-10} sec. Owing to the preliminary nature of the delay-line plumbing, optimum operating conditions have not yet been realized. However, the existence of the short-lived isomeric state of Yb^{170} (1.6×10^{-9} sec)[2] was confirmed.

An excited state in Eu^{153} with a half-life of $(3.0 \pm 0.3) \times 10^{-9}$ sec has been observed with the delayed-coincidence scintillation spectrometer. The position of the metastable state in the disintegration scheme has been determined.

Sm^{153} (47 hr) is known to decay by a 0.78 Mev β-ray branch leading to an excited state of Eu^{153}. This state is de-excited by γ-ray transitions in cascade[3] corresponding to 69 and 103 Kev which are strongly converted.[4]

(1) Newton, T. D., "Decay Constants from Coincidence Experiments," *Phys. Rev.* 78, 490 (1950).

(2) Bell, R. E., and Graham, R. L., "Measurement of a Second Half-Life in Yb^{170}," *Phys. Rev.* 78, 490 (1950).

(3) Burson, S. B., and Muelhause, C. O., "The Decay Scheme of 47-hr Sm^{153}," (abstract), *Phys. Rev.* 74, 1264 (1948).

(4) Hill, R. D., "Internal Conversion Electrons from Sm^{153} - 47 Hour," *Phys. Rev.* 74, 78 (1948).

UNCLASSIFIED
DWG. 9774

FIG. 1

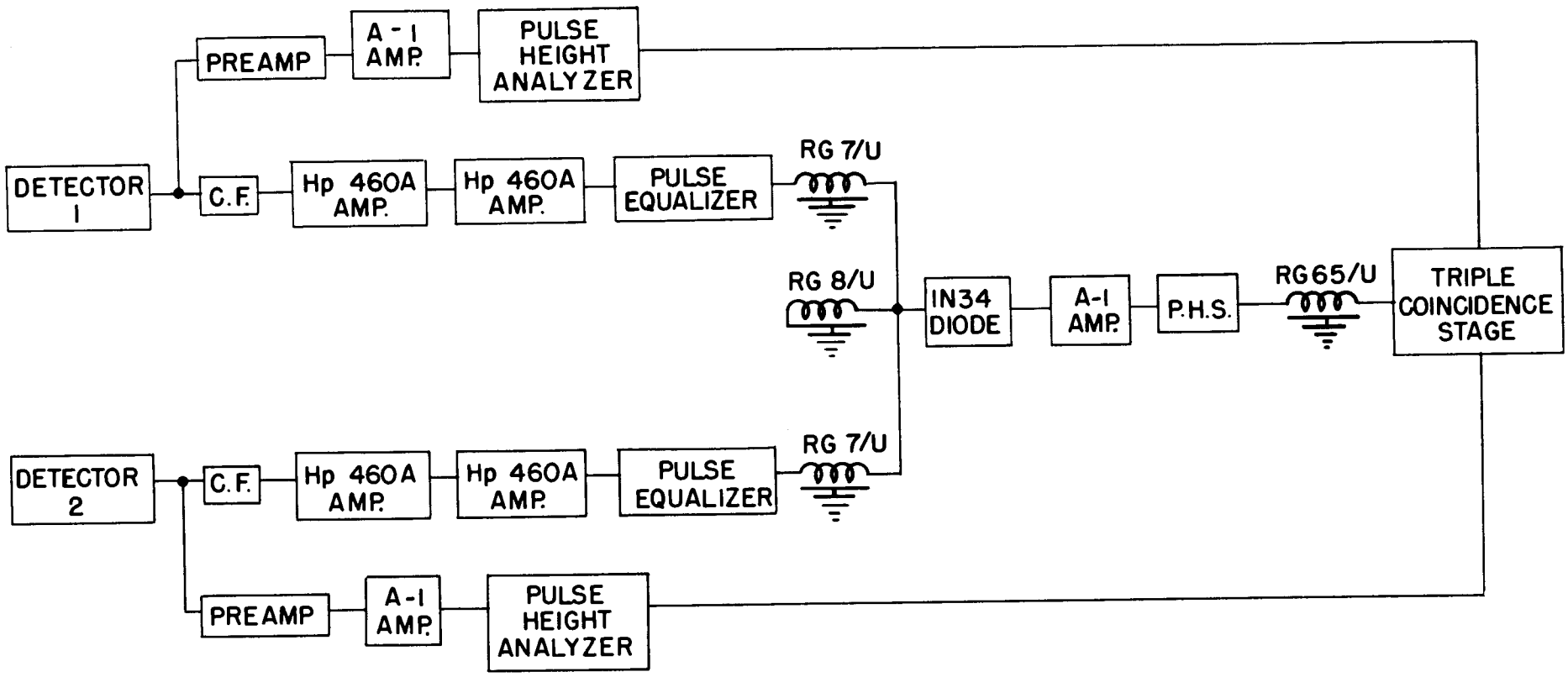

DELAYED COINCIDENCE SCINTILLATION SPECTROMETER

In Fig. 2, curve 1, the number of coincidences are plotted as a function of delay time obtained with a source of Sm^{153}. This delayed-coincidence resolution curve was recorded by exciting one channel of the delayed-coincidence apparatus by the nuclear β rays and the other channel by the L, M, or N internal conversion electrons of the 103-Kev γ rays. Without changing the apparatus a resolution curve for prompt coincidences was obtained between 411-Kev γ rays or internal conversion electrons and 85- to 110-Kev nuclear β rays with a source of Au^{198}. Curve 2 shows the result of such a measurement. Thus, for delay $T \gtrsim 8 \times 10^{-9}$ sec, the half-life of Eu^{153*} may be determined from the slope of curve 1.

The spectrum of the radiation announcing the formation of the metastable state appears to be a simple β-ray distribution unaccompanied by γ rays. This information, plus the fact that the decay curve for Eu^{153*} was obtained by selecting coincidences between the nuclear β rays and the L, M, or N internal conversion electrons of the 103 Kev-γ ray, fixes the position of the metastable state at 172 Kev above the ground state of Eu.

Measurements of the internal conversion electron spectrum of the delayed radiation indicate the presence of the 69- and 103-Kev γ rays. The relative heights of the K conversion peak of the 103 Kev γ ray (superimposed on the L, M, and N conversion lines of the 69-Kev γ ray) and the L + M + N conversion peak of the 103-Kev γ ray indicate that the amount of internal conversion in the L shell is comparable to that in the K shell. Also, the spectrum of the unconverted and delayed electromagnetic radiation shows the presence of two peaks which are attributed to the K X-ray of Eu and the 69-Kev γ ray. These observations favor the idea that the isomeric transition is the 103-Kev transition.

From the energy and half-life of this isomeric state the transition is probably electric quadrupole or a combination of electric quadrupole and magnetic dipole radiation.

The half-life of the 80-Kev transition in Er^{166} has been measured as $(1.7 \pm 0.2) \times 10^{-9}$ sec with the delayed-coincidence scintillation spectrometer.

The β spectrum of Ho^{166} (27 hr) is known to consist of two components of 1.84 and 0.55 Mev maximum energy and intensities 89% and 11%, respectively.[5]

(5) Siegbahn, K., and Slätis, H., "Ho^{166} Disintegration," *Arkiv Fysik* 1, 559 (1950).

UNCLASSIFIED
DWG 9562

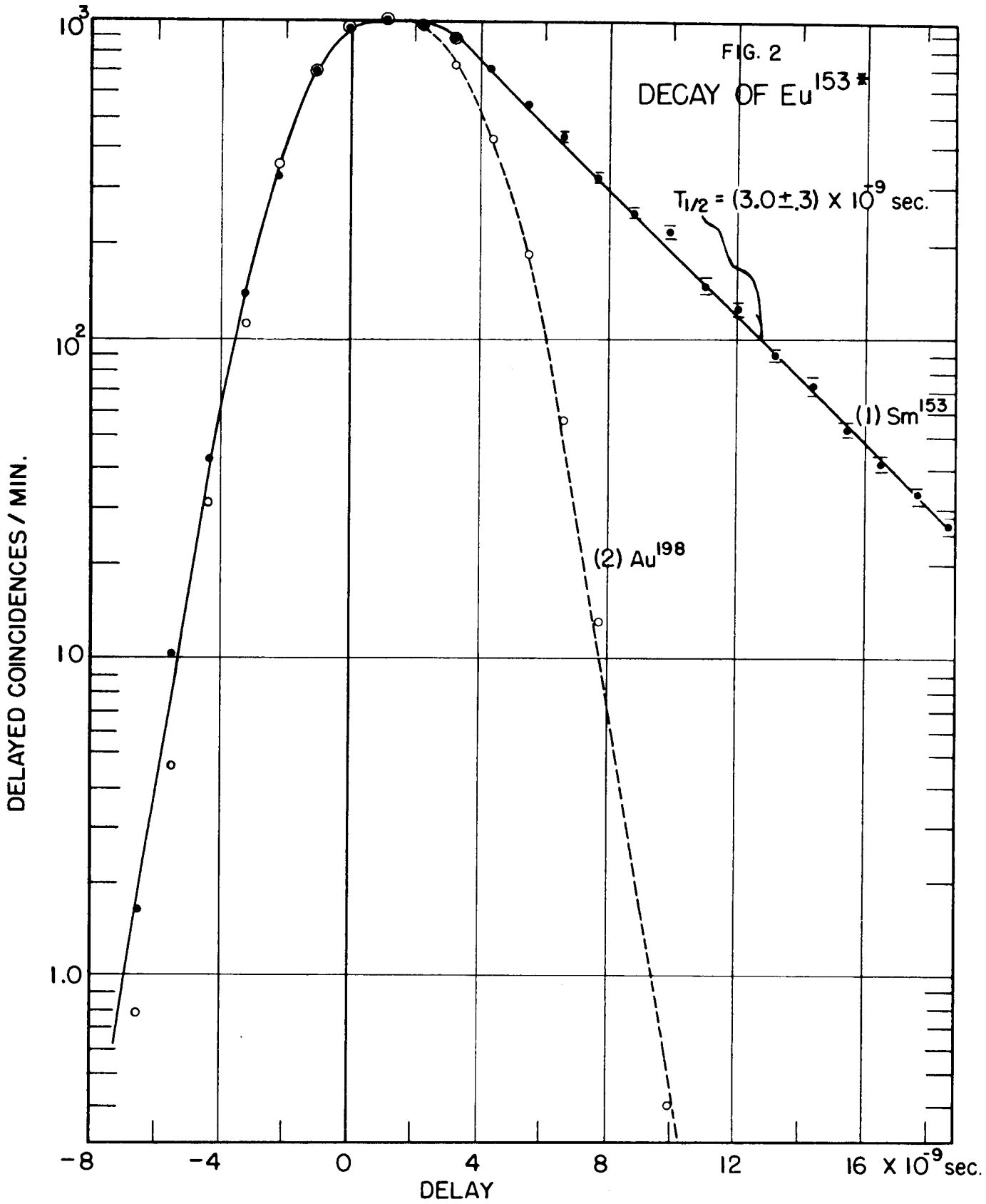

Siegbahn and Slätis showed that the 80 Kev transition follows the higher energy component of the β spectrum and that the L-shell conversion coefficient is ~ 0.4.

Figure 3 shows the number of coincidences as a function of delay time obtained with a source of Ho^{166}. This delayed coincidence resolution curve was recorded by exciting one channel of the delayed coincidence apparatus by 600- to 900-Kev nuclear β rays and the other channel by the L, M, or N internal conversion electrons of the 80 Kev transition. With a source of Au^{198} a resolution curve (not shown) for prompt events was obtained between 600 to 900 Kev β rays and 60 to 90 Kev Compton recoil electrons from the 411 Kev γ radiation. This measurement showed that, for delay $T \geqslant 8 \times 10^{-9}$ sec, the half-life of Er^{166*} may be determined from the slope of the curve in Fig. 3. However, for half-lives less than 10^{-9} sec it would be necessary to analyze the data by the methods of Newton[6] and Bay.[7]

The energy and half-life of this isomeric state suggest that the transition is probably electric quadrupole or a combination of electric quadrupole and magnetic dipole radiation.

It is interesting to note the distinct similarity of the short-lived isomeric states of $_{70}Yb^{170}$ (1.6×10^{-9} sec)[8] and $_{68}Er^{166}$. They occur in neighboring nuclei with an even number of protons and neutrons. The energies of the isomeric transitions are 83 and 80 Kev, respectively, and the half-lives are the same within the experimental error.

X Rays from Radioactive Nuclei (E. C. Campbell and J. H. Kahn*). As part of an extensive and systematic investigation, with the proportional counter spectrometer, of the X rays emitted by radioactive nuclei, the photographs reproduced in Fig. 4 were obtained. All pictures were enlarged to the same scale by using energy calibrations obtained from each set of negatives. These

(6) Newton, T. D., *op. cit.*

(7) Bay, Z., "Calculation of Decay Times from Coincidence Experiments," *Phys. Rev.* 77, 419 (1950).

(8) Bell, R. E., and Graham, R. L., *op. cit.*

* ORINS Fellow, University of Tennessee.

UNCLASSIFIED
DWG. 9654

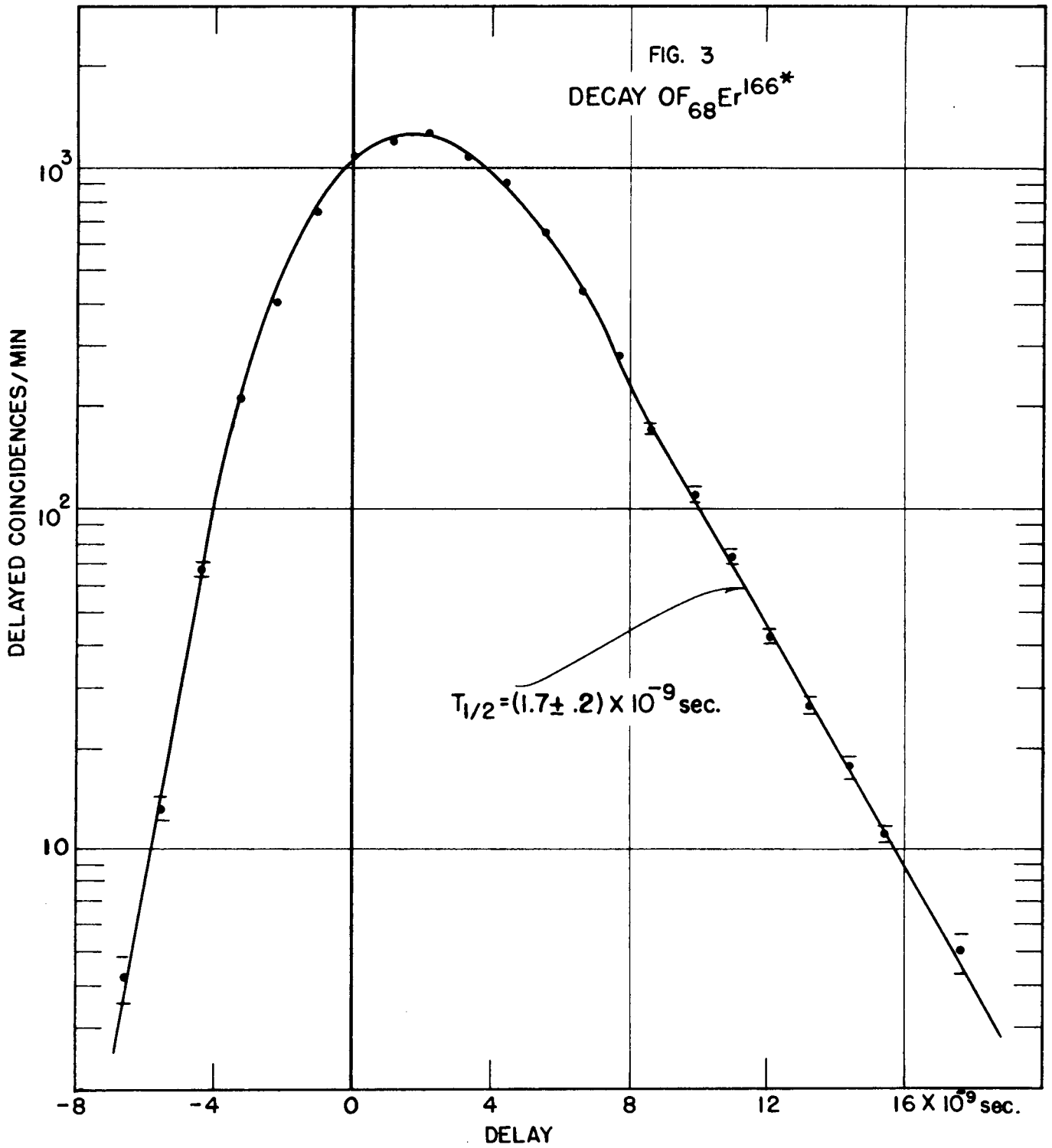

UNCLASSIFIED
DWG. 9801

FIG. 4

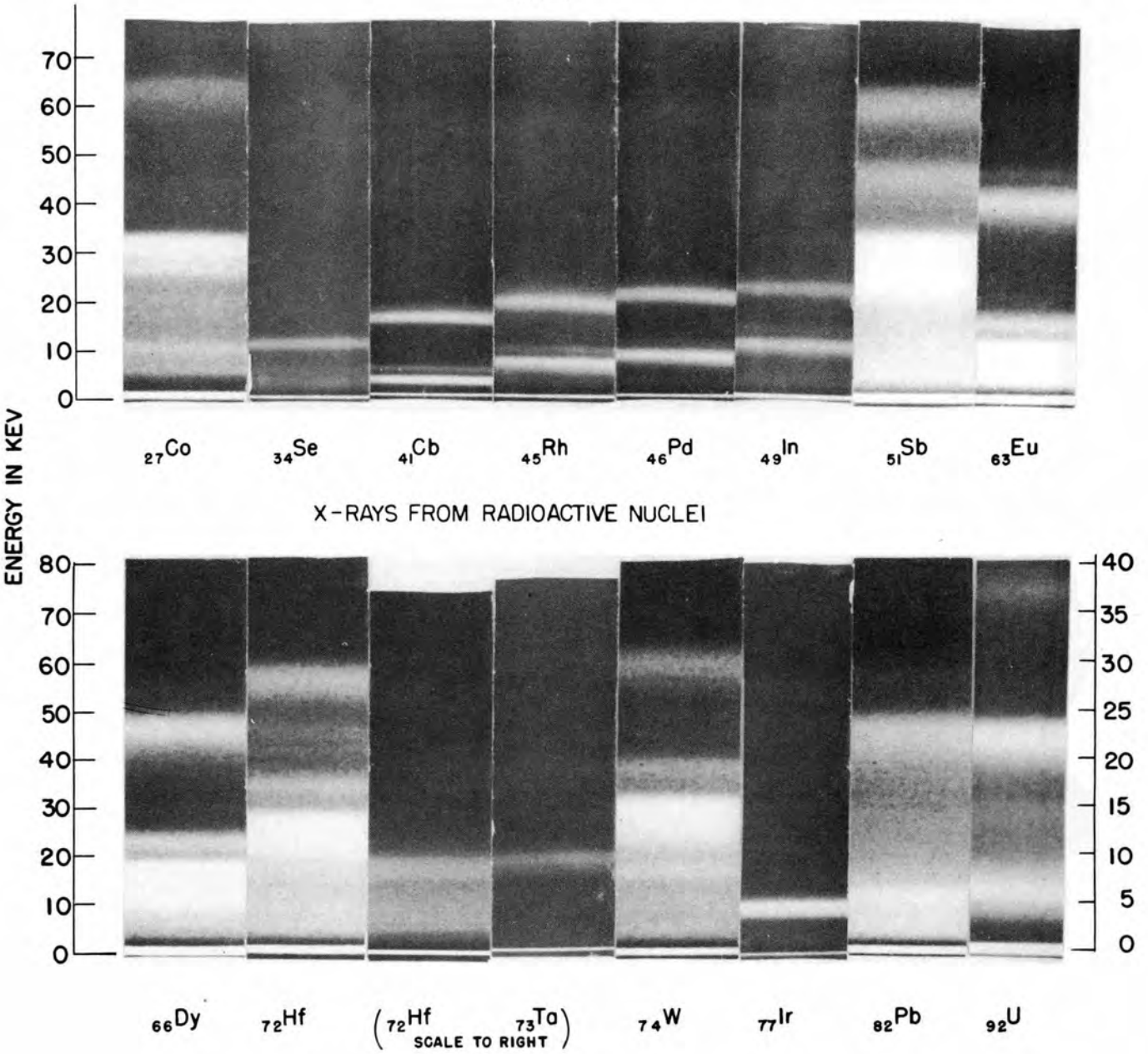

are sections from short-time-exposure photographs of an oscilloscope screen on which self-triggered pulses from a proportional counter are displayed. In three of the photographs, pulses due to low-energy nuclear γ rays are observed in addition to the characteristic X ray. The origin and energy of the lines seen in the photographs are listed in Table 1.

For calibration purposes, as a first approximation it was assumed that the element irradiated emitted X rays characteristic of that element. In the case of nuclear isomers this is certainly the case; it is expected, however, that in cases when irradiation of element Z leads to a β transition, characteristic X rays of elements Z - 1 or Z + 1 will be emitted. To test this point, calibrations are now being made with the fluorescent characteristic X rays of samples used as radiators. It appears that the X rays associated with the decay of Eu^{152} really belong to Sm and are those emitted following K capture.

The X rays observed are believed to be produced mainly following the emission of a nuclear γ ray which is internally converted either in the K- or the L-electron shell. As a result of the loss of an electron, the atom is in an excited state and returns to normal either by the emission of its characteristic X ray or through the emission of Auger electrons. A lucite absorber is introduced between the radioactive source and the counter in order to stop all β rays and conversion electrons given off by the source. For X-ray energies between 10 and 30 Kev a krypton-methane-filled counter is used, and for energies between 30 and 75 Kev a xenon-methane counter is used.

The operation of the krypton counter was discussed in ORNL-782. The xenon counter operates in a similar manner. In the detection of X rays from elements having a higher atomic number than xenon, extra lines are observed owing to the possibility of two different events occurring inside the counter. If the photoelectron produced in the counter by the absorption of an X ray in the K shell of xenon is followed by the emission of Auger electrons which are absorbed in the counter, the entire energy of the detected X ray is measured by the counter. If, however, the photoelectron ejected from the K shell of the xenon is followed by the emission of a xenon K X-ray, there is a good probability that this X ray will escape from the counter. Thus the energy measured by the counter will be less than that observed when the Auger process occurs by an amount equal to the xenon K X-ray energy.

Short-period Radioactivity in In and Yb. Through the use of the NaI scintillation counter located at the fast pneumatic tube, unreported γ rays

TABLE I

ISOTOPE	HALF-LIFE	ENERGY OF LINES (Kev) OBSERVED	ENERGY OF LINES (Kev) EXPECTED	COUNTER GAS	ASSUMED ORIGIN OF LINES
$_{27}Co^{60}$	10.7 m	62.0 30.5 9.5	58.9 29.2 10.6	Xe	Nuclear γ ray γ minus $(K\alpha)_{Xe}$ Probably Pb L X-rays
$_{34}Se^{77}$	17.5 s	11.1	11.2	Kr	Se $K\alpha$ X-ray
$_{41}Cb^{94}$	6.6 m	16.5 5.4 3.2	16.6 5.9 3.9	Kr	Cb $K\alpha$ X-ray $(K\beta)_{Cb}$ minus $(K\alpha)_{Kr}$ $(K\alpha)_{Cb}$ minus $(K\alpha)_{Kr}$
$_{45}Rh^{104}$	44 s	20.4 9.8 7.2	20.2 10.0 7.5	Kr	Rh $K\alpha$ X-ray $(K\beta)_{Rh}$ minus $(K\alpha)_{Kr}$ $(K\alpha)_{Rh}$ minus $(K\alpha)_{Kr}$
$_{46}Pd$	~10 m	21.8 8.2	21.2 8.5	Kr	Pd $K\alpha$ X-ray $(K\alpha)_{Pd}$ minus $(K\alpha)_{Kr}$
$_{49}In$	2.5 s	24.2 11.3	24.2 11.5	Kr	In $K\alpha$ X-ray $(K\alpha)_{In}$ minus $(K\alpha)_{Kr}$
$_{51}Sb^{122}$	3.5 m	59.8 44.8 29.7 26.5	 45.3 30.1 26.4	Xe	Nuclear γ ray $(K\alpha)_{Pb}$ minus $(K\alpha)_{Xe}$ γ minus $(K\alpha)_{Xe}$ Sb $K\alpha$ X-ray
$_{63}Eu^{152}$	9.2 h	40.8 15.0 10.0	41.6 17.4 11.9	Xe	Eu $K\alpha$ X-ray $(K\beta)_{Eu}$ minus $(K\alpha)_{Xe}$ $(K\alpha)_{Eu}$ minus $(K\alpha)_{Xe}$
$_{66}Dy^{165}$	1.3 m	46.2 22.2 16.1	46.0 22.5 16.3	Xe	Dy $K\alpha$ X-ray $(K\beta)_{Dy}$ minus $(K\alpha)_{Xe}$ $(K\alpha)_{Dy}$ minus $(K\alpha)_{Xe}$
$_{72}Hf$	19 s	56.0 34.0 25.8	55.8 33.7 26.1	Xe	Hf $K\alpha$ X-ray $(K\beta)_{Hf}$ minus $(K\alpha)_{Xe}$ $(K\alpha)_{Hf}$ minus $(K\alpha)_{Xe}$
$_{72}Hf^{181}$	46 d		8.1-10.9	Kr	For comparison with Ta
$_{73}Ta^{182}$	0.3 s	9.3	8.1-10.9	Kr	Ta L X-ray
$_{74}W$	5.5 s	59.4 37.1 29.7	59.4 37.6 29.7	Xe	W $K\alpha$ X-ray $(K\beta)_{W}$ minus $(K\alpha)_{Xe}$ $(K\alpha)_{W}$ minus $(K\alpha)_{Xe}$
$_{77}Ir^{192}$	1.5 m	10.4		Kr	Ir L X-ray
$_{82}Pb$ (fluorescent X rays from Se γ ray)		76.8 56.6 45.1 11.1	75.0 55.1 45.3 11.2	Xe	Pb $K\alpha$ X-ray $(K\beta)_{Pb}$ minus $(K\alpha)_{Xe}$ $(K\alpha)_{Pb}$ minus $(K\alpha)_{Xe}$ Se $K\alpha$ X-ray
$_{92}U^{239}$	23.5 m	75.0 45.1 12.7	73.3 43.6 13.6	Xe	Nuclear γ ray γ minus $(K\alpha)_{Xe}$ U $L\alpha$ X-ray

have been found in In and in Yb. Upon neutron bombardment inside the pile, In gives a 152-Kev γ ray with a 2.5-sec half-life, and Yb emits a 455-Kev γ ray with a half-life of the order of 0.5 sec. Characteristic X rays from these two elements were also detected which had the same half-lives as the γ rays.

Split-crystal Scintillation Spectrometer (P. R. Bell, J. M. Cassidy, and R. C. Davis). After the first good results obtained by B. H. Ketelle in the Chemistry Division, a split-crystal spectrometer was constructed. Anthracene crystals ½ in. thick, 1 in. high, and 1½ in. long were cut from adjacent parts of a larger crystal. The two crystals were placed on their long faces on a standard 1½ in. diameter by ½ in. thick light piper so that their largest faces were almost in contact. β-ray samples on very thin foils were placed between the crystals. The light piper was joined to the crystals and 5819 photomultiplier tube with Canada balsam, and the whole crystal assembly was enclosed in an aluminum light-reflector box. With this arrangement all the β rays leaving the source can be counted, and the spectrum measured. Absolute β counting can be done easily with the split-crystal spectrometer, and, by extrapolating the Kurie plot data to zero energy, an accurate value of all the β rays can be obtained with a minimum of assumptions.

The Kurie plots obtained with the split-crystal unit do not show much of the turnup at low electron energies which characterize the single-crystal spectrometer and which would be acceptable on magnetic instruments. Figure 5 shows the β spectrum, and Fig. 6 the Kurie plot obtained using a P^{32} source, which was thin but was mounted on 100 $\mu g/cm^2$ Formvar-polystyrene film and covered by a similar film. The plot still deviates somewhat at low energies, but at least a part of the deviation is due to the source film. The source can, of course, be evaporated directly on the crystal surface so that no mounting foil is needed.

Spectrometry and Coincidence Spectrometry of Cadmium Activities. The long-lived β activity previously reported[9] has been further investigated. Samples of separated cadmium isotopes 108, 112, and 114 were irradiated in the X pile for 12 days, and their activities have been followed since their removal in July. The 1.59-Mev β ray assigned[10] to Cd^{115} has been confirmed, and the

(9) Cassidy, J. M., and Bell, P. R., "Long-Lived Cadmium Activities" (abstract), *Phys. Rev.* 79, 418 (1950).

(10) Seren, L., Engelkemeier, D., Sturm, W., Friedlander, H. N., and Turkel, S., "Forty-three-day $_{48}Cd^{115}$," *Phys. Rev.* 71, 409 (1947).

UNCLASSIFIED
DWG. 9769

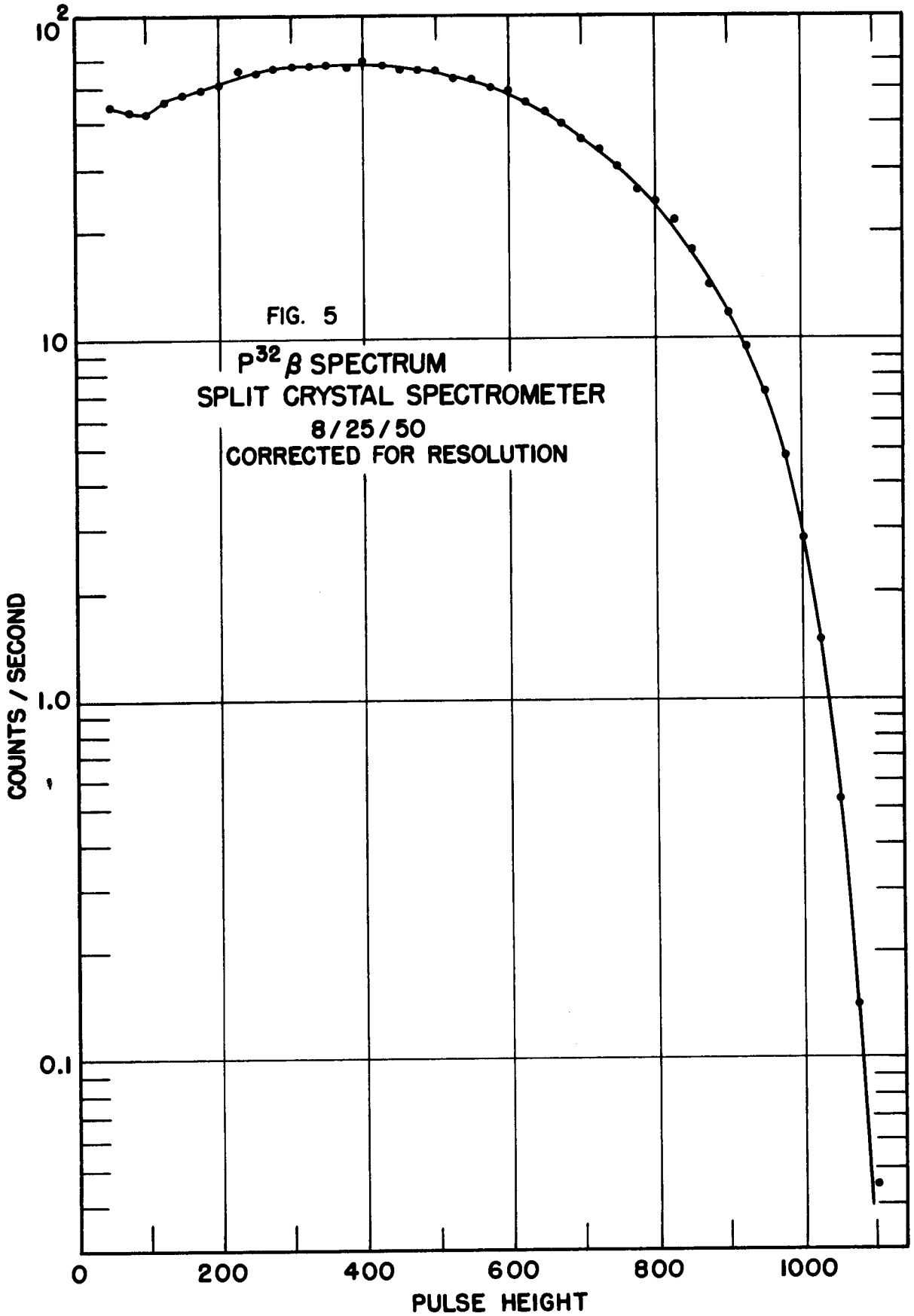

UNCLASSIFIED
DWG. 9770

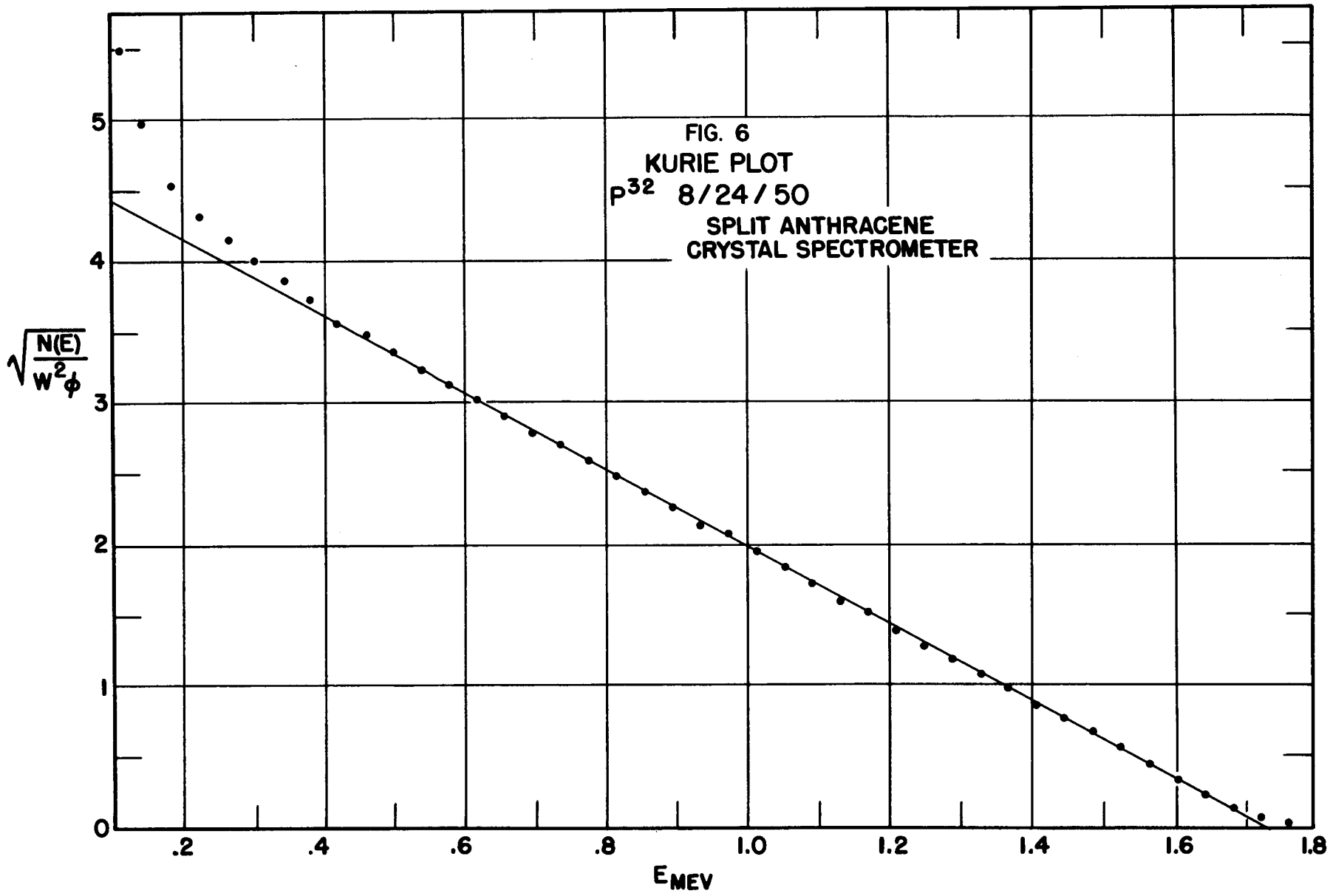

330-day K-capture isotope[11] giving an 88-Kev γ ray has been confirmed as Cd^{109}. The 580-Kev β emitter was found, as suspected, to be Cd^{113}. This is a previously unreported activity. The split-crystal scintillation spectrometer was applied to a very old cadmium sample which also showed this activity. The sample was chemically separated from Ag, Sn, In, Fe, and Co. The spectrum was found to be complex with an inner β group at 350 Kev and the outer group at 580 Kev. About 20% of the disintegrations are involved in the inner group. A typical Kurie plot is shown in Fig. 7. The strong turnup below 130 Kev is probably due to the very strong radiations from 330-day Cd^{109} present in the sample. The γ radiation from the sample was measured, and a γ ray at 270 ± 15 Kev was found. The quantity seems to be too small (2 to 3%) to correspond to the inner β-ray group. A higher energy γ ray is also seen, but, since the activity is quite low for the whole sample, it is not certain that it is not an impurity. From the sample activations, accepting 0.14 barn for the isotopic cross section leading to the production of the 43-day Cd^{115} and using the tentative half-life of 300 to 600 days, we find the slow-neutron isotopic cross section for the production of Cd^{113} to be 0.008 ± 0.003 barn.

The coincidence spectrometer was used this quarter to study the γ ray spectrum of the 43-day cadmium. Many effects not generally noticeable are evident while doing γ-γ coincidences, especially the scattering by the Compton process of photons from crystal to crystal. A lead-diaphragm shield with a central hole for the sample was found to be necessary. The decay scheme for four or more γ rays present with the 0.7% abundant β group is still not complete.

Total-absorption Spectrometer. Tests of very large crystals as total-absorption scintillation spectrometers have met with some success. A 4-in.-diameter 2-in.-thick NaI-TlI crystal was tested, and the resolution was found to be poor. Its failure was attributed to poor activation, as the pulses are also rather small (20% of the height produced by small crystals). A crystal 3 in. in diameter and 3 in. high gives much better results. A central hole 1¾ in. deep and ½ in. in diameter allows samples to be inserted into the crystal. Figure 8 shows the response to the 0.661-Mev γ ray of Cs^{137}. The peak contains six-tenths of all the counts. The resolution is considerably poorer than with the smaller crystals, which will give about 11% width of peak while the 3-in. crystal gives 27%. The resolution improves as the energy increases so that the crystal is adequate for some high-energy work.

(11) Helmholz, A. C., "Isotopic Assignment of Cadmium and Silver Activities," *Phys. Rev.* 70, 982 (1946).

UNCLASSIFIED
DWG. 9767

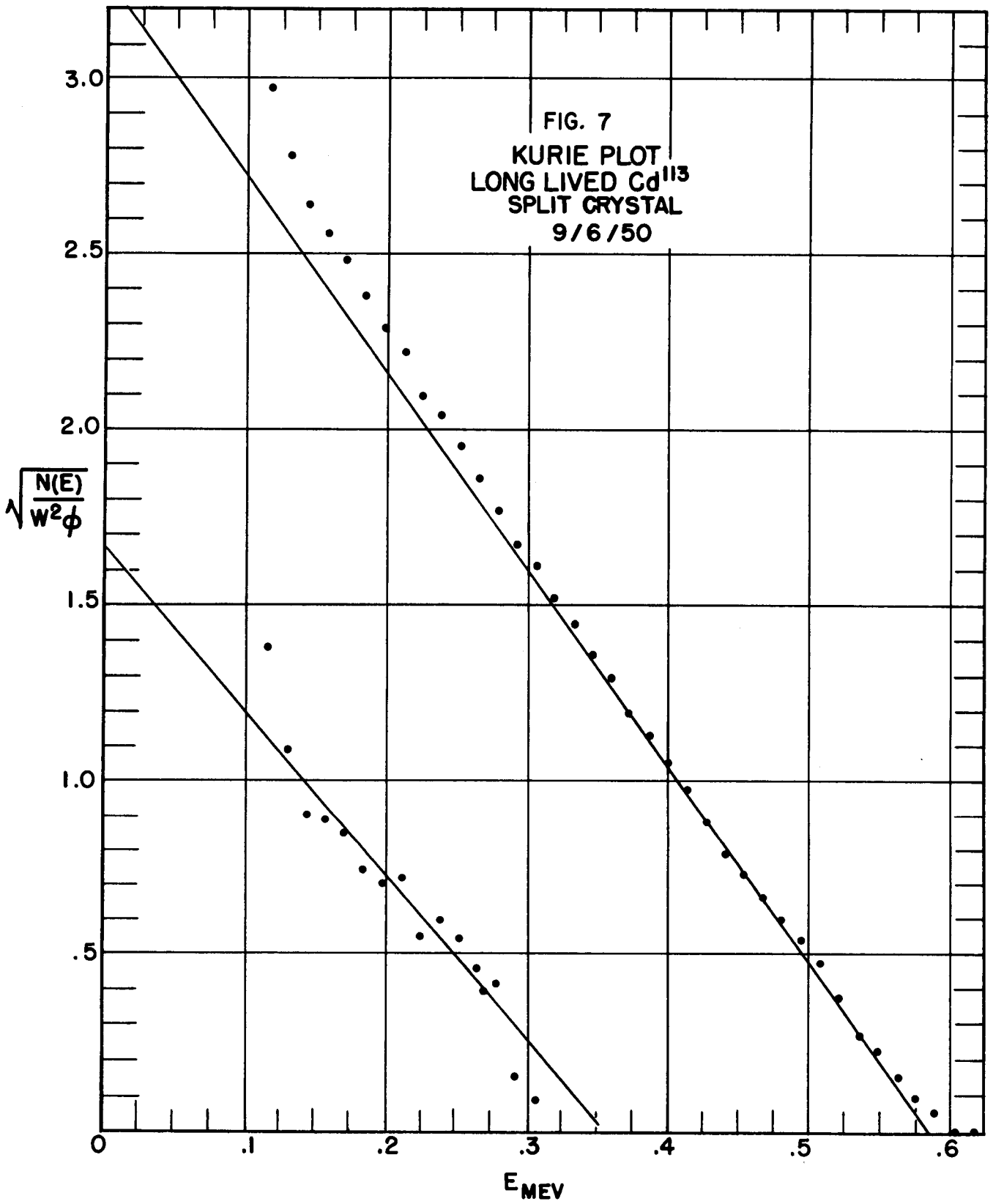

UNCLASSIFIED
DWG. 9768

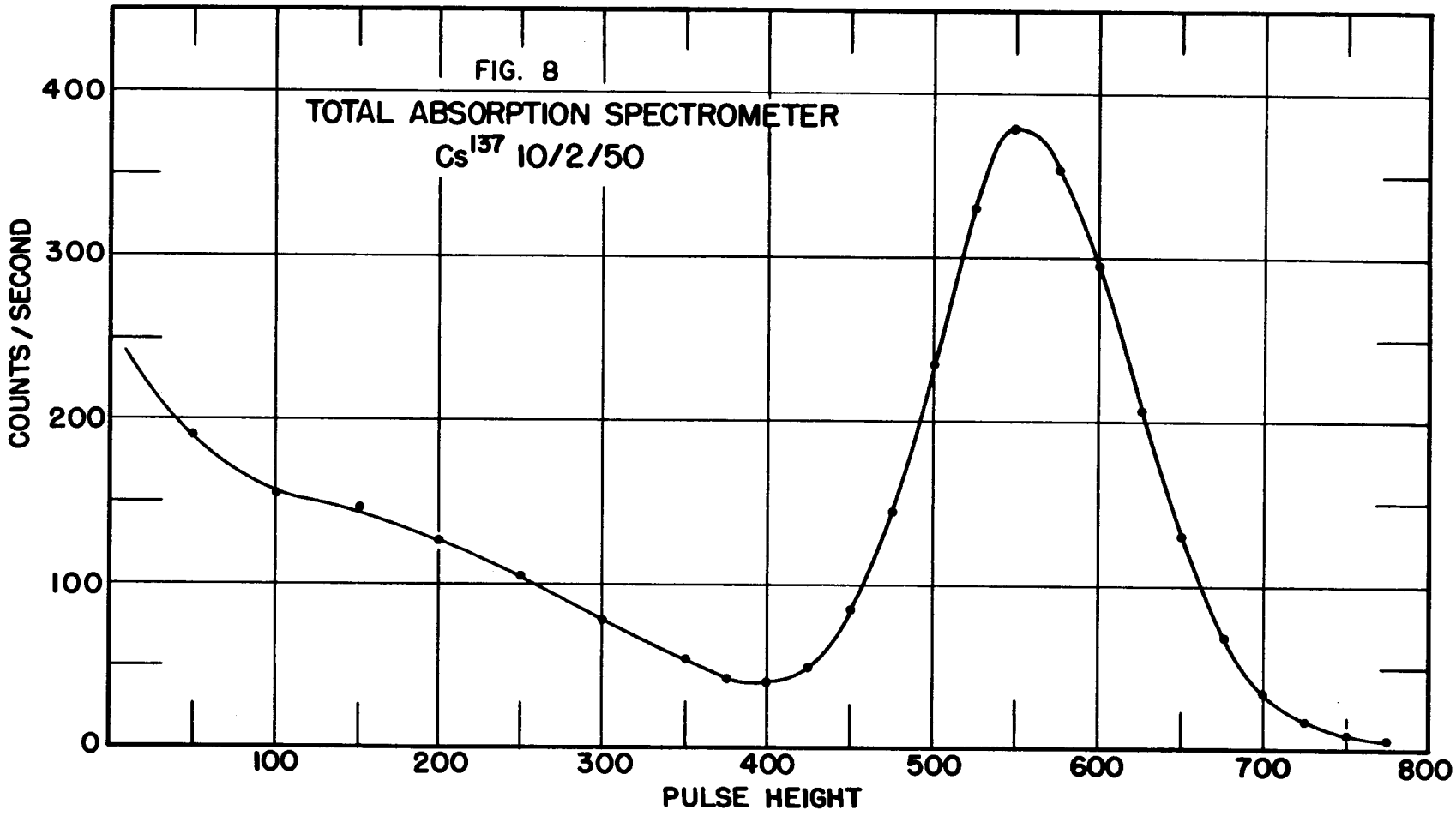

To show the use of the total-absorption spectrometer in decay-scheme determination, a sample of Co^{60} was run. Curve A in Fig. 9 is for a source inside the crystal, and curve B is for a larger source outside. The two γ rays of Co^{60} at 1.16 and 1.32 Mev are unresolved, but a strong peak at 2.5 Mev can be seen for curve A; there is only a very weak peak due to random coincidences for the outside source. This shows that the two γ rays are in coincidence (an already known fact), since a peak at an energy equal to their sum is seen.

A γ-ray continuum can be analyzed with this crystal, but the resolution is poor.

Single-channel Analyzer (J. E. Francis and P. R. Bell). A single-channel analyzer has been built for measuring the pulse spectrum from proportional and scintillation counters; it counts the number of pulses between E and $E + \Delta E$. This analyzer has the advantage of using fewer tubes and components than previous models. It contains a pulse-height-selecting amplifier, followed by two pulse-height selectors, a memory circuit, and an anticoincidence circuit.

A circuit diagram of the analyzer is shown in Fig. 10. The pulse-height-selecting amplifier amplifies a segment of the pulse distribution. A helipot at the beginning of the amplifier determines which segment will be amplified and thus sets the minimum value that a pulse must have to give an output signal. V-1 is a cathode follower whose grid bias can be varied over a range of 100 volts. This allows the d-c level of an input pulse to be varied over the same range. The signal is fed from the cathode of V-1 to the grid of V-3 through a current-limiting resistor. The grid of V-3 is prevented from going too far in the positive direction by a 6AL5 diode, which starts to conduct after the signal on the grid of V-3 has reached a certain value. The two IN38A diodes in series between the plates of V-3 and V-4 hold the plate of V-3 constant until V-3 is drawing 2 ma and is on the linear portion of its characteristic. The IN38A diode in parallel with the 8.2K resistor limits the size of the output from V-3 so that the grid of V-4 is not driven very far in a negative direction. This shortens the recovery time of the grid considerably. Tubes V-3, V-4, and V-5 and associated components comprise a conventional feedback loop with a nominal gain of 2000 and a feedback gain of 10 to provide a stabilization factor of 200.

The signal from the amplifier is fed into two pulse-height selectors, the lower of which (V-8, V-9) is a long-tailed pair biased to trigger on very small

UNCLASSIFIED
DWG. 9808

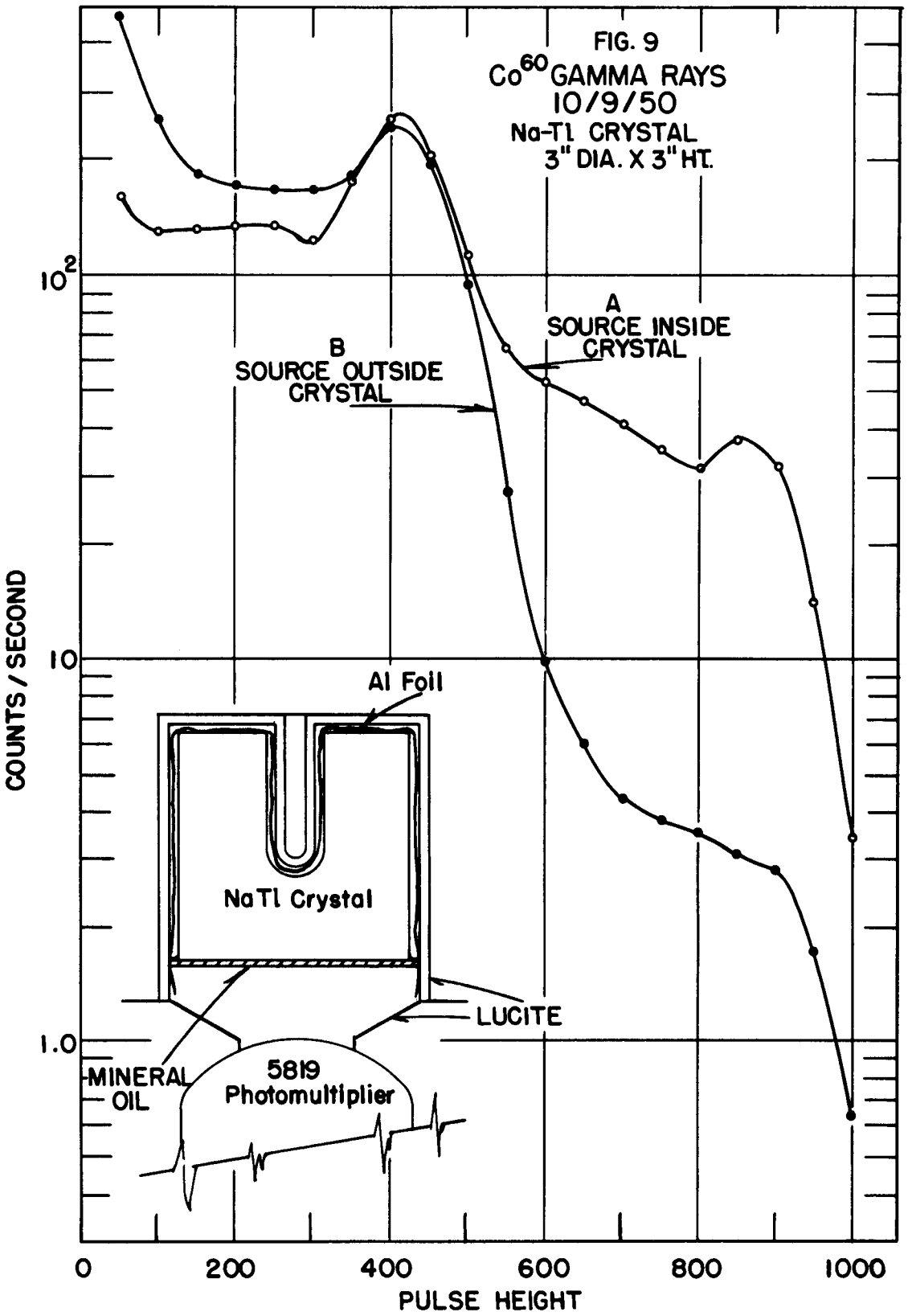

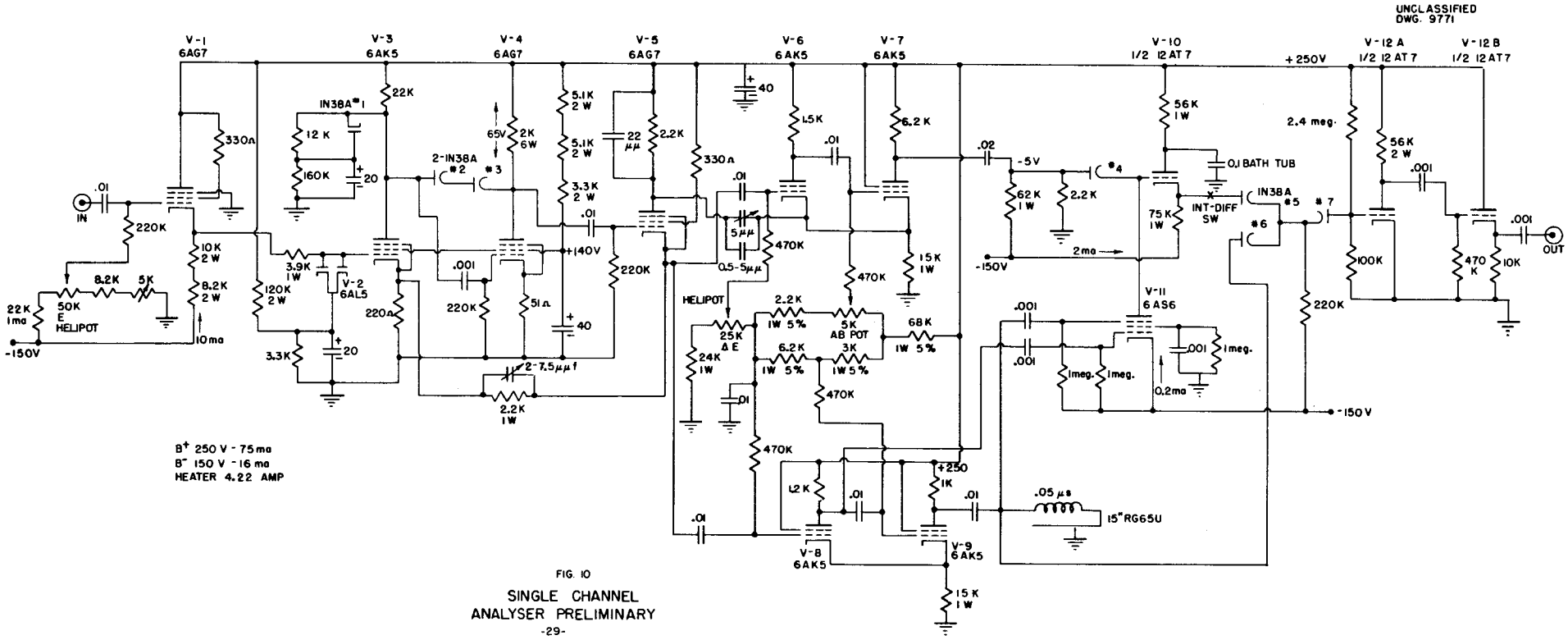

FIG. 10

SINGLE CHANNEL
ANALYSER PRELIMINARY

pulses from the amplifier. An output signal is taken from each plate of the pulse-height selector. The signal from V-8 is used to turn on the memory circuit by turning off V-11. The output signal from V-9 is differentiated by a shorted delay line to obtain two pulses, one which marks the beginning and one which marks the end of the input signal to the lower pulse-height selector. No use is made of the pulse marking the beginning. The pulse marking the end of the input pulse is used to hold the memory circuit on and is also fed to one input of the anticoincidence circuit.

The upper pulse-height selector (V-6, V-7) is similar to the lower one. It is biased to trigger only if the pulse is above a certain value determined by the bias on the grid of V-6. This determines the ΔE or "window width." The output signal from V-7 is fed into the memory circuit.

The memory circuit (V-10, V-11, and IN38A diode No. 4) provides a signal to one input of the anticoincidence circuit when the upper pulse-height selector triggers. Normally when there is no input to the circuit, the grid of V-10 is held down by current flowing through V-11, the diode, and the 2.2K resistor to ground. When a pulse triggers the lower pulse-height selector, V-11 is cut off and the grid of V-10 stays at approximately the same value. If, however, the upper pulse-height selector triggers, a pulse is placed on the plate of the IN38A diode. The diode lengthens the pulse and places it on the grid of V-10, which pulls up the plate of IN38A diode No. 5. The plate of diode No. 5 will stay up, preventing an output signal from the anticoincidence circuit. It will not come down until after the differentiated pulse from the lower pulse-height selector has disappeared from the grid of V-11. When the grid of V-11 no longer has a signal, V-11 starts to conduct and resets the memory circuit.

Therefore, if the upper pulse-height selector fires, the memory circuit provides a signal to one input of the anticoincidence circuit until after the differentiated pulse from the lower pulse-height selector has entered the second input of the anticoincidence circuit. When only the lower pulse-height selector triggers, there is no coincidence, and there is therefore an output pulse from the cathode of IN38A diode No. 6, which is lengthened by IN38A diode No. 7 and amplified by V-12A to make a longer and larger pulse. The output pulse from V-12A is fed into V-12B, which is a cathode follower to get a low impedance output.

The memory circuit is necessary because the pulse which triggers the upper pulse-height selector is of shorter duration and occurs after the pulse has entered the lower pulse-height selector. Without the memory circuit it is possible to get an anticoincidence when actually there is a coincidence.

A switch is placed between the memory circuit and the anticoincidence circuit so that it is possible to get the total number of counts above a certain value.

Preliminary tests indicate that the analyzer works as expected except for effects due to the grid-to-cathode capacity in the first tube of the upper pulse-height selector. Methods of compensating for this effect are now being tried.

NEUTRON PHYSICS AND LOW TEMPERATURES

L. D. Roberts
J. W. T. Dabbs, Jr.
T. E. Stephenson
S. Bernstein
C. P. Stanford
L. W. Cochran*

Nuclear Alignment. In the last quarterly report (ORNL-782) it was mentioned that several minor experimental difficulties had been encountered owing to the fact that pyrex glass was used in making our Dewar flasks. The pyrex, by virtue of its $1/v$ absorption, effectively removed the neutron polarization from the beam. The obvious solution to this problem was to make a metal Dewar-flask system, which has now been satisfactorily accomplished. When a beam of polarized neutrons is projected through the present metal Dewar-flask system, the neutron polarization remains essentially unaffected. The new Dewar flasks contain approximately 1 liter of liquid helium and have a satisfactorily low liquid-helium loss rate.

The equipment for the observation of nuclear alignment in a sample of manganous ammonium sulfate is now in operation. In using this equipment, a capsule, connected to a fast diffusion pump, is placed in the liquid helium and in the polarized neutron beam. A 3-g manganous ammonium sulfate pellet, in the shape of a short cylinder, is mounted on a very fine string suspension within the capsule with its circular face presented to the beam, and a manganese metal foil is placed inside the capsule immediately in front of the manganous ammonium sulfate. This foil serves as a beam monitor since all the neutrons which enter the manganous ammonium sulfate must first pass through the foil. The manganous ammonium sulfate used was hydrated with heavy water and sealed in a thin-walled aluminum container. The apparatus is so arranged that a partial demagnetization of this manganous ammonium sulfate can be carried out in the manner described in the last quarterly report (ORNL-782, *p.* 66). The demagnetized sample, with its nuclei either aligned to some extent, or not aligned (*loc. cit.*), is irradiated with a beam of polarized neutrons for one half-life. At the conclusion of the irradiation the capsule and its contents are removed as a unit from the liquid helium and warmed up to room temperature, which takes about 20 min. The sample and the monitor are then removed from the capsule, and their β activities are counted with a thin-walled

* Summer visitor.

glass β-ray counter. To observe nuclear alignment, the activity of the manganous ammonium sulfate activated with its nuclei presumably polarized is compared to the activity of the same manganous ammonium sulfate sample activated a second time with its nuclei unpolarized (*loc. cit.*). Two complete trial experiments of this type have been made, and the apparatus has been found to function quite satisfactorily.

In the last quarterly report (ORNL-782, *p.* 68) were discussed the results of a measurement of the specific heat of manganous ammonium sulfate in the temperature region below 1°K. It was shown that our experimental results approximately fitted the thermodynamic theory given by Casimir. However, there were several difficulties: (1) the signal-to-noise ratio was poor at some of the experimental points; (2) the thermodynamic theory was based on Curie's law, but the Weiss modification should have been used for manganous ammonium sulfate in the temperature region covered by the experiment; and (3) the values of H listed were not corrected for demagnetization effects. The experiment has been repeated and all three of these difficulties have been eliminated. First, the signal-to-noise ratio at all experimental points is now very favorable. Second, the experiment was performed in a slightly higher temperature region in which Curie's law is quite satisfactory. Third, a spherical sample was used so that there were no demagnetization corrections.

However, in the higher temperature region of 0.6 to 1°K, where this last experiment was performed, it was necessary to take into account the Debye specific heat. We have worked out this correction to Casimir's theory and fitted it to our results, obtaining a value of the ratio of the Curie constant to the specific heat constant, a/A (*loc. cit.*), of 1.56×10^{-6}; this agrees within 1% with the values given by Gorter[1] and by Benzie and Cooke.[2] A value was obtained for the Debye θ of about 25°K, which is quite low compared to the usual values of 200 to 400°K for the Debye θ for most substances. On the other hand, similarly low values of 30 to 40°K have been obtained for cobalt sulfate by Fritz and Giauque[3] and for iron ammonium alum by Van Dijk and Keesom.[4] Our value was obtained by a small-difference technique and is

(1) Gorter, C. J., *Paramagnetic Relaxation*, Elsevier Book Company, Inc., New York, 1947.

(2) Benzie, R. J., and Cooke, A. H., "Specific Heats of Some Paramagnetic Salts at Temperatures near 1°K," *Proc. Phys. Soc. London*, 63A, 213 (1950).

(3) Fritz, J. J., and Giauque, W. F., "Magnetism and the Third Law of Thermodynamics. Magnetic Properties and Heat Capacity of $CoSO_4 \cdot 7H_2O$ from 0.1 to 15°K," *J. Am. Chem. Soc.* 71, 2168 (1949).

(4) Van Dijk, H., and Keesom, W. H., "Measurements of Specific Heats of Iron Ammonium Alum in High Magnetic Fields and at Liquid Helium Temperatures," *Physica* 7, 970 (1940).

probably accurate to within a factor of 2. The agreement between the revised theory and this experiment is as follows:

H (gauss)	D_s (observed)	D_s (calculated)
0	21.14	21.14
404	15.02	15.18
531	12.27	12.42
814	7.25	7.82
1157	2.82	4.99

The observed and calculated values for D_s are seen to agree quite well at all but the last point. This disagreement seems to be real, but we are as yet unable to explain it. It does not seem to be due to spin lattice relaxation time, or to any relaxation-time phenomena occurring in the measuring equipment, and it may be that this disagreement, as well as the low value of the Debye θ, reflects the existence of a specific heat anomaly in the region 1 to 10°K.

As was stated in the last quarterly report, these low-temperature studies are being made in order to determine the temperature-magnetic field conditions leading to maximum nuclear alignment. The work is being continued.

Production of Polarized Neutrons for Nuclear Alignment. At the beginning of the nuclear alignment project, the decision was made to rely upon the method of producing a beam of polarized neutrons by transmission through magnetized iron, at least for the initial stages of the experiment, since it was thought that the transmission method could yield results in the shortest possible time. Such a system of neutron-polarizing equipment was set up along with the low-temperature apparatus and has been in use for some time.

Simultaneously, a long-range neutron-polarization program has been set up at another pile hole, the purpose of which has been twofold: (1) to permit acquiring skill in the handling of polarized neutrons without tying up the

entire nuclear-alignment apparatus, and (2) to test the possibilities of increasing the intensity and polarization of the neutron beam by other methods. Since the nuclear alignment studies have required most of the time of the group, work on improvement of the polarized-neutron setup has been limited. However, the following work may be reported:

(1) Neutron polarization by transmission using monochromatic neutrons has been studied in some detail, as described below.

(2) Equipment on hand for obtaining a 100% polarized neutron beam by total reflection from magnetized cobalt mirrors has been used but only to the extent of verifying that our mirrors do give a totally reflected beam.

(3) A single Fe crystal of acceptable size grown by F. A. Sherrill of the Solid-state Group has been obtained. This crystal has been cut so that it can be placed between the pole pieces of a magnet, magnetized in the 100 direction, and will give reflections from a set of 110 planes. It has been found that the intensities available by reflection from an iron crystal are at least as great as those available by transmission through 4 cm of iron. The use of Bragg reflection from a crystal has the advantage that the energy of the neutrons can be varied. Also, interpretation of the results of the overall nuclear alignment data should prove simpler if monochromatic neutrons are used. We are setting up equipment to measure the polarization of the Bragg-reflected beam.

(4) We have been very fortunate in procuring a good single crystal of magnetite from the Department of Geology of the University of Chicago. Shull and Wollan have calculated that reflection from the 220 planes of a magnetized magnetite crystal should give a 100% polarization. We hope to test this prediction soon. X-ray Laue spot pictures taken with the magnetite crystal show that it is a good single crystal.

The nuclear alignment experiment has reached the stage where increasing both the counting rates and the magnitude of the effect of the alignment are vital. It is therefore planned to concentrate more effort on increasing the intensity and polarization of the neutron beam.

Neutron Polarization by Transmission Through Magnetized Iron. Halpern and Holstein[5] give the following expression for the intensity and polarization of an initially unpolarized beam of neutrons after passing through a block of magnetized iron:

(5) Halpern, O., and Holstein, T., "On the Passage of Neutrons through Ferromagnets," *Phys. Rev.* 59, 960 (1941).

$$j = j_0 e^{-(px/2)} \left\{ \frac{\sinh \{ x [(p^2/4) + W^2]^{1/2} \}}{[(4W^2/p^2) + 1]^{1/2}} + \cosh \{ x [(p^2/4) + W^2]^{1/2} \} \right\} \quad (1)$$

$$\eta = j_0 e^{-(px/2)} \frac{\sinh \{ x [(p^2/4) + W^2]^{1/2} \}}{[(p^2/4W^2) + 1]^{1/2}} \quad (2)$$

where

j_0 = incident neutron particle current

j = emergent neutron particle current

η_0 = incident neutron spin current

η = emergent neutron spin current

x = thickness of iron sample, in centimeters

W = $N\sigma_p$

N = number of iron nuclei per cubic centimeter

σ_p = polarization cross section

p = ϵ/λ

ϵ = departure from magnetic saturation = $(M-M_\infty)/M_\infty$

λ = one-half the grain size of the iron or steel if the grain size is greater than the critical size; the critical size is equal to the distance traveled by a neutron while making a Larmor precession of 1 radian

If, in the above equation, q is substituted for $[(p^2/4) + W^2]^{1/2}$, then

$$j = j_0 e^{-(px/2)} \{ (p/2q) \sinh qx + \cosh qx \} \quad (3)$$

$$\eta = j_0 e^{-(px/2)} (W/q) \sinh qx \quad (4)$$

In these equations j and j_0 are measurable quantities, being the counting rates with iron magnetized and not magnetized, respectively. Also, N and x are known, but ϵ, λ, and σ_p are not known and are not directly determinable with sufficient accuracy. The quantity finally desired is η/j, the average spin per neutron in the emergent beam, or the polarization. One method for the determination of η/j is to measure j and j_0 for different thicknesses, x, of the same variety of iron, and, by fitting the data to Eq. (5), to determine the values of p and q. These will then determine ϵ/λ and σ_p, and the ratio η/j can be calculated. Since the various samples are all cut from the same piece of steel stock, λ will be a constant. If the measurements are made with the samples in a constant magnetic field, it is assumed that ϵ will remain constant. Since σ_p varies with neutron energy it is required that the measurements be made with a monoergic source of neutrons or that corrections involving the neutron-energy distribution, the hardening of the neutron beam by passage through the sample, and the efficiency of the detector be applied. Such transmission experiments with a heterogeneous beam were carried out by Hughes, Wallace, and Holtzman[6] and by Fleeman, Nicodemus, and Staub.[7]

Measurements of j and j_0 were made for five different thicknesses of steel at a neutron energy of 0.0261 ev. The steel samples were cut from 1018 cold-rolled steel so that the direction of the magnetic field was parallel to the direction of rolling. The samples were 1.25 in. high and 11/16 in. in the direction of the applied magnetic field, and had thicknesses in the direction of the neutron beam of 1.0, 1.5, 2.0, 2.5, and 3.0 cm. They were mounted in magnet-pole-piece adapters having plane surfaces 1.25 in. by 4 cm; the neutron beam was 1 in. high and ½ in. wide. The maximum magnetic field obtainable from the 1-kw magnet with the 3-cm sample between the pole faces was 10,500 gauss. For the smaller samples the magnet current was adjusted to give this field also.

The magnetic field was measured by locating a thin search coil, 1 cm by 1 cm by 0.1 cm and containing about 100 turns, flat up against the free faces of the polarizing sample of iron. This thin search coil was calibrated against a larger circular coil of known turns and cross section in the air gap of the magnet. It was found that the magnetic field as measured by the thin search coil was given by $H = 398D$, where H is the magnetic field in oersteds and D is the average flux-meter deflection for a current reversal in the magnet.

(6) Hughes, D. J., Wallace, J. R., and Holtzman, R. H., "Neutron Polarization," *Phys. Rev.* 73, 1277 (1948).

(7) Fleeman, J., Nicodemus, D. B., and Staub, H. H., "Neutron Polarization," *Phys. Rev.* 76, 1774 (1949).

The magnet currents required to produce a field of 10,500 gauss for each sample are given in Table II.

TABLE II

THICKNESS (cm)	MAGNET CURRENT (amp)
3.0	1.00
2.5	0.75
2.0	0.60
1.5	0.48
1.0	0.45

The experimental arrangement for measuring the single transmission effect at a given neutron energy is shown in Fig. 11. The sample of cold-rolled steel was mounted in the pole-face adapters of the magnet, and the field was adjusted to 10,500 gauss. The counting rate was then determined with the sample magnetized and not magnetized. The 111 plane of a LiF crystal mounted on a transit mount was used as an energy selector. For this crystal cut,

$$E = \frac{h^2}{8md^2 \sin^2 \theta} = \frac{0.003825}{\sin^2 \theta} \text{ ev}$$

Measurements were made with a crystal angle of 22.5°, corresponding to a neutron energy of 0.0261 ev (λ = 1.77 Å, neutron velocity of 2230 m/sec). The data are summarized in Table III.

TABLE III

x (cm)	j/j_0
1	1.023
1.5	1.046
2	1.085
2.5	1.128
3	1.184

UNCLASSIFIED
DWG. 9781

FIG. 11

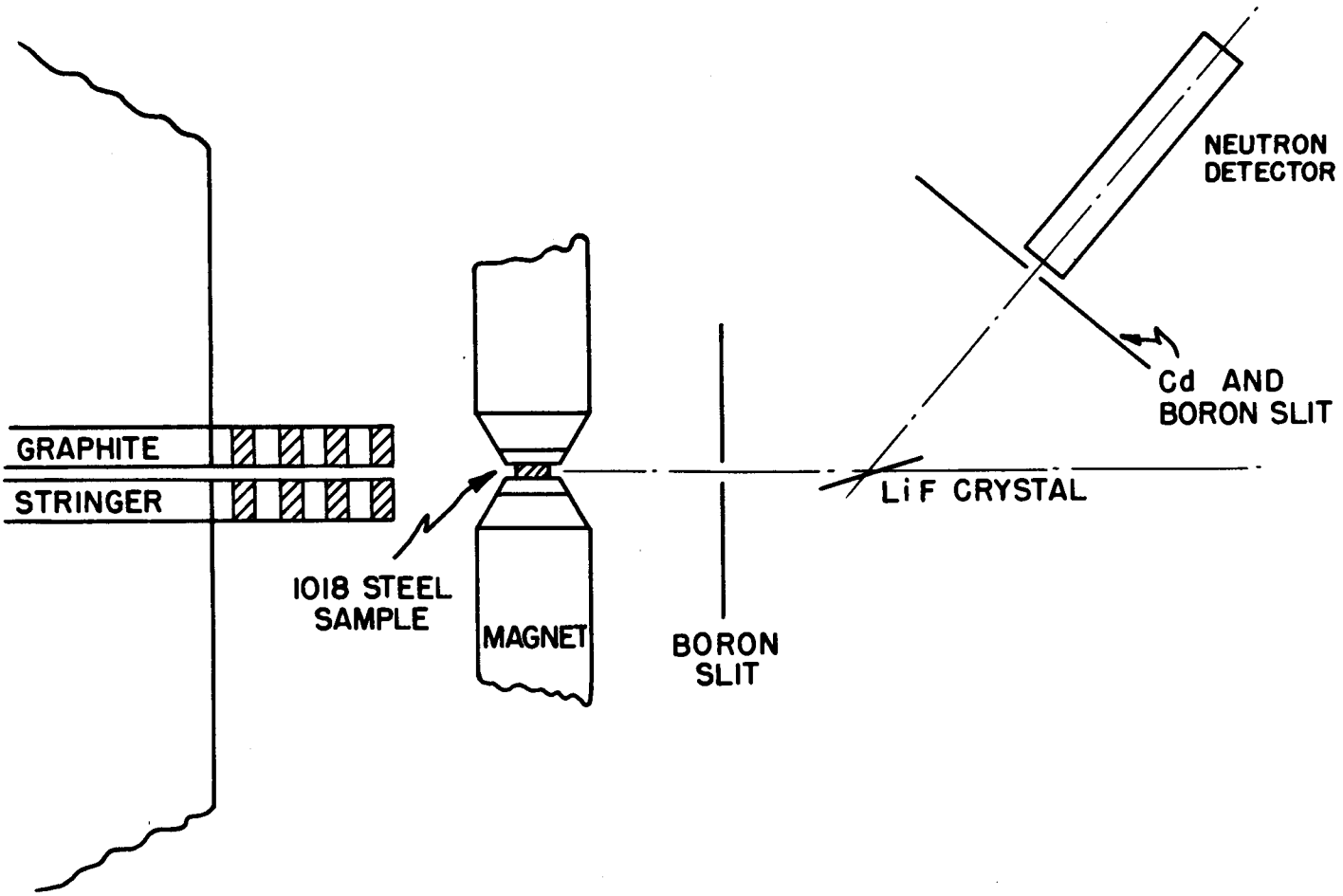

The data were fitted to Eq. (5) simply by trying various values of the two adjustable constants p and q. The values $p = 0.176$ and $q = 0.233$ seemed to fit the data best, corresponding to a value $\sigma_p = 2.55$ barns. Only the value ϵ/λ is determined by the data. However, if for convenience it is assumed that the average grain size of our 1018 cold-rolled steel samples is the same as found for Hughes' 1020 cold-rolled steel, and if λ is taken as 1.7×10^{-3} cm, then $\epsilon = 0.0003$. At essentially the same energy, Hughes, Wallace, and Holtzman found $\sigma_p = 3.15$ barns, while Fleeman, Nicodemus, and Staub found $\sigma_p = 2.35$ barns.

Having determined σ_p and ϵ/λ, we can then calculate η/j, the polarization, for the different thicknesses used, and it should be possible to predict the single transmission effect and polarization to be expected for other thicknesses of 1018 steel for a neutron energy of 0.0261 ev and in a magnetic field of 10,500 gauss. The values of η/j are given in Table IV. The P values are calculated from the expression $P = \sqrt{1-(j_0/j)^2}$, which is the polarization to be expected from the measured single transmission effect if it is assumed that the sample was magnetically saturated.

TABLE IV

x (cm)	η/j	P
1	0.196	0.211
1.5	0.276	0.293
2	0.347	0.389
2.5	0.405	0.463
3	0.456	0.546

It can be shown that Eq. (3) reduces to

$$\Delta j/j_0 = \tfrac{1}{2}\,(N\sigma_p x)^2 f(\xi) \qquad (5)$$

where

$$f(\xi) = 2\xi^2 \left[e^{-1/\xi} + (1/\xi) - 1 \right] \text{ and } \xi = \lambda/\epsilon x$$

Equation (5) is valid if $(N\sigma_p x) << 1$, $(\epsilon/\lambda)\, x \sim 1$, *i.e.*, $(\epsilon/\lambda) >> N\sigma_p$.

Though the conditions are not met for the values found in this experiment, $N\sigma_p = 0.216$ and $\epsilon/\lambda = 0.176$, it is found that Eq. (5) is equally as valid as Eq. (3) for x values up to 3 cm. It can also be shown that

$$\Delta j/j_0 = \tfrac{1}{2}\,(N\sigma_p x)^2 \tag{6}$$

if the steel sample is completely saturated. Therefore, if $\tfrac{1}{2}(N\sigma_p x)^2$ is calculated using $\sigma_p = 2.55$ barns for the values of x used, the ratio of $\Delta j/j_0$ measured to $\tfrac{1}{2}(N\sigma_p x)^2$ will give the value of $f(\xi)$ for that value of x. From Eq. (5) can be determined the corresponding value of ξ and hence of ϵ. This should give a measure of the constancy of ϵ, a condition assumed in the experiment. The results are shown in Table V.

TABLE V

x	$\tfrac{1}{2}(N\sigma_p x)^2$	$\Delta j/j_0$	$f(\xi)$	ξ	ϵ
1	0.0234	0.0230	0.983	22.00	0.77×10^{-4}
1.5	0.0526	0.0463	0.880	2.54	4.46×10^{-4}
2	0.0935	0.0848	0.907	3.30	2.58×10^{-4}
2.5	0.1461	0.1284	0.879	2.53	2.69×10^{-4}
3	0.2104	0.1841	0.875	2.44	2.32×10^{-4}

To determine the value of σ_p as a function of neutron energy the experimental arrangement shown in Fig. 11 was used. All measurements were made for a value of $x = 2$ cm and for the same value of ϵ as used previously. Since x, λ, and ϵ are constant, it follows from Eq. (5) that

$$\frac{(\Delta j/j_0)_1}{(\Delta j/j_0)_2} = \frac{(\sigma_{p_1})^2}{(\sigma_{p_2})^2}$$

At about this stage in the proceedings it was discovered that higher order reflections from the LiF 111 planes used for the velocity selector were affecting the measurements. This set of planes gives no second-order reflection. If it is assumed that only the first and third orders are important, the composition of the reflected beam can be determined as follows:

Let

T_0 = measured transmission of a $1/v$ absorber (BF_3) at an energy E_0 where higher orders can be neglected

T = measured transmission where the third-order component is to be determined

$T = a_1 T_1 + a_3 T_3;\ a_1 + a_3 = 1$

a_1 = fractional part of beam that is first order

a_3 = fractional part of beam that is third order

T_1 = transmission of BF_3 absorber due to first order

T_3 = transmission of BF_3 absorber due to third order

If

$$T_1 = T_0^{C}$$

then, because of the $1/v$ law,

$$T_3 = T_0^{C/3}$$

where

$$C = \sqrt{E_0/E_1}$$

E_1 = neutron energy of the first order

Therefore

$$T = T_0^C + a_3(T_0^{C/3} - T_0^C)$$

$$a_3 = \frac{T - T_0^C}{T_0^{C/3} - T_0^C}$$

$$a_1 = 1 - a_3$$

All the measurements discussed below were corrected using these relationships.

Steinberger and Wick[8] have given the following expression for the polarization cross section of iron:

$$\sigma_p = (\sigma_{coh}/4\pi)^{1/2} (e^2/mc^2) \mu_n\mu_e (\lambda/2a)^2 \sum_{l>2a/\lambda} [N(l)/l] \cdot [1 + (l^2\lambda^2/4a^2)] \cdot F(l)$$

where

σ_{coh} = coherent scattering cross section of the iron nucleus (here taken equal to 10 barns)

e = electronic charge

m = electronic mass

μ_n = neutron magnetic moment in nuclear magnetons (1.91)

μ_e = magnetic moment of all unpaired electrons, in electronic magnetons (2.18 for Fe)

λ = de Broglie wavelength of the neutrons

a_2 = lattice constant for iron = 2.86×10^{-8} cm

l^2 = $2n$; $n = 1, 2, 3, \ldots$

$N(l)$ = a weight factor for the Debye ring l, and is equal to twice the number of ways in which three integers—positive, negative, or zero—can be chosen such that the sum of their squares is equal to l^2

$F(l)$ = the form factor for the electrons of unpaired spin in the d shell

ϕ = wave function of the electrons of unpaired spin of the 3d shell

(8) Steinberger, J., and Wick, G. C., "On the Polarization of Slow Neutrons," *Phys. Rev.* 76, 994 (1949).

These authors give values of $F(l)$ for three cases: (1) free atom; (2) atom in solid, exchange forces taken into account, $\partial\phi/\partial r = 0$ at the atomic radius; (3) atom in solid, exchange taken into account, $\phi = 0$ at atomic radius. We have plotted curves for the three cases for wavelengths from 1.529 Å to 4.046 Å, using the form factors given by Steinberger and Wick. The results are shown in Fig. 12.

Our experimentally measured points are also shown in Fig. 12. In correcting the measured intensities for the presence of third-order reflection, it was assumed that the change in transmission on magnetization of the steel, Δj, was due entirely to first order. It follows that the corrected values of $\Delta j/j_0$ will be the measured value divided by a_1. The results of this correction for the measurements taken at 0.0261 ev are shown in Table VI.

TABLE VI

x (cm)	$\Delta j/j_0$ MEASURED	$\Delta j/j_0$ CORRECTED	$\Delta j/j_0$ BEST-FIT VALUE σ_p = 2.66 BARNS ϵ = 0.0003
1	0.0230	0.0253	0.0244
1.5	0.0463	0.0509	0.0526
2	0.0848	0.0932	0.0915
2.5	0.1284	0.1412	0.1423
3	0.1841	0.2024	0.2007

The best-fit curve to these corrected data is shown in Fig. 13. The result of the third-order correction is to increase the value of σ_p from 2.55 to 2.66 barns.

The third-order corrected values for the $\Delta j/j_0$ values as a function of λ for constant x and ϵ are shown in Table VII.

UNCLASSIFIED
DWG. 9782

FIG. 12

$$\sigma_p = \left(\frac{\sigma_c}{4\pi}\right)^{\frac{1}{2}} \frac{e^2}{mc^2}\, \mu_n\, \mu_e \left(\frac{\lambda}{2a}\right)^2 \sum_{\ell < \frac{2a}{\lambda}} \frac{N(\ell)}{\ell} \left[1 + \frac{\ell^2 \lambda^2}{4a^2} \right] F(\ell)$$

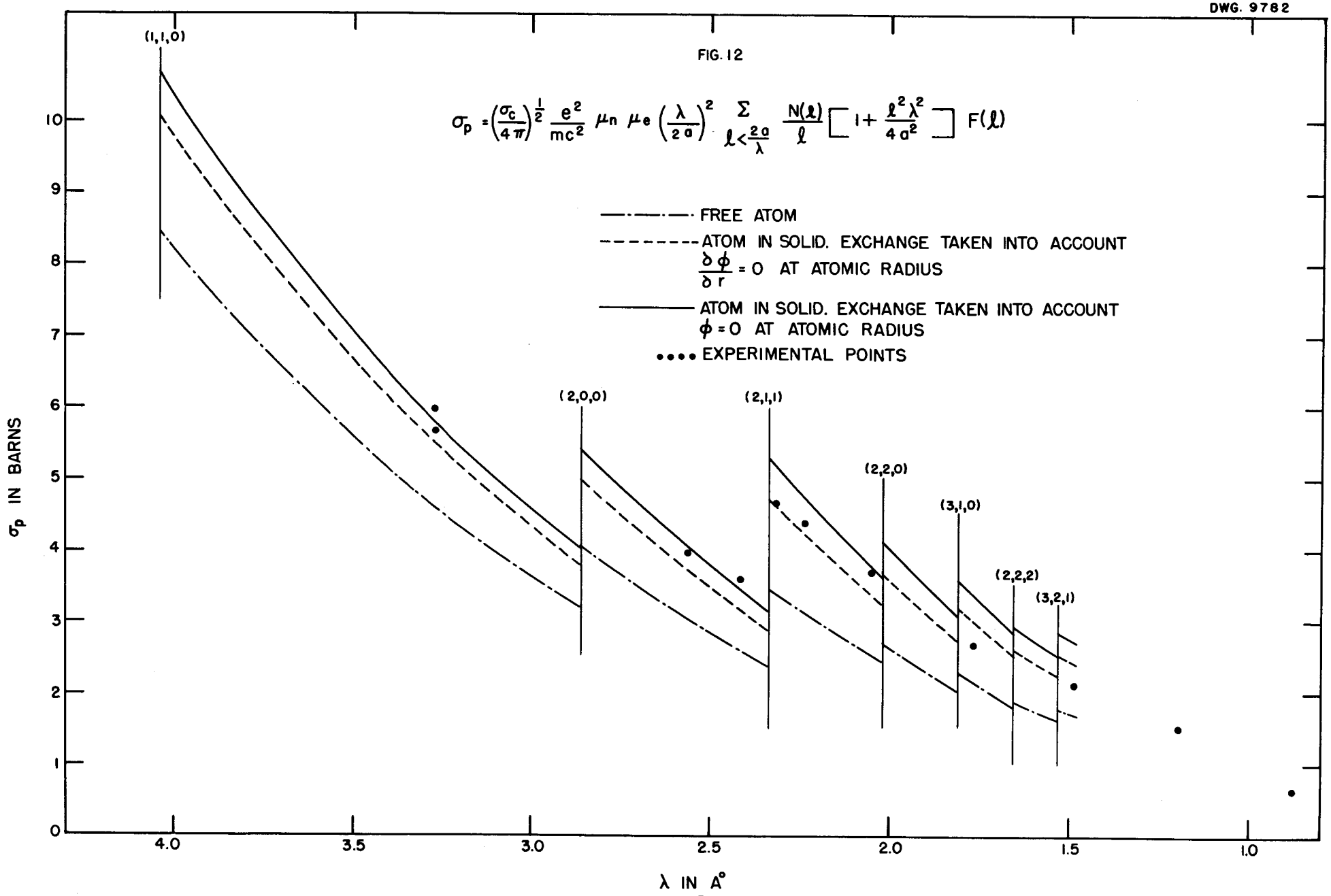

UNCLASSIFIED
DWG. 9794

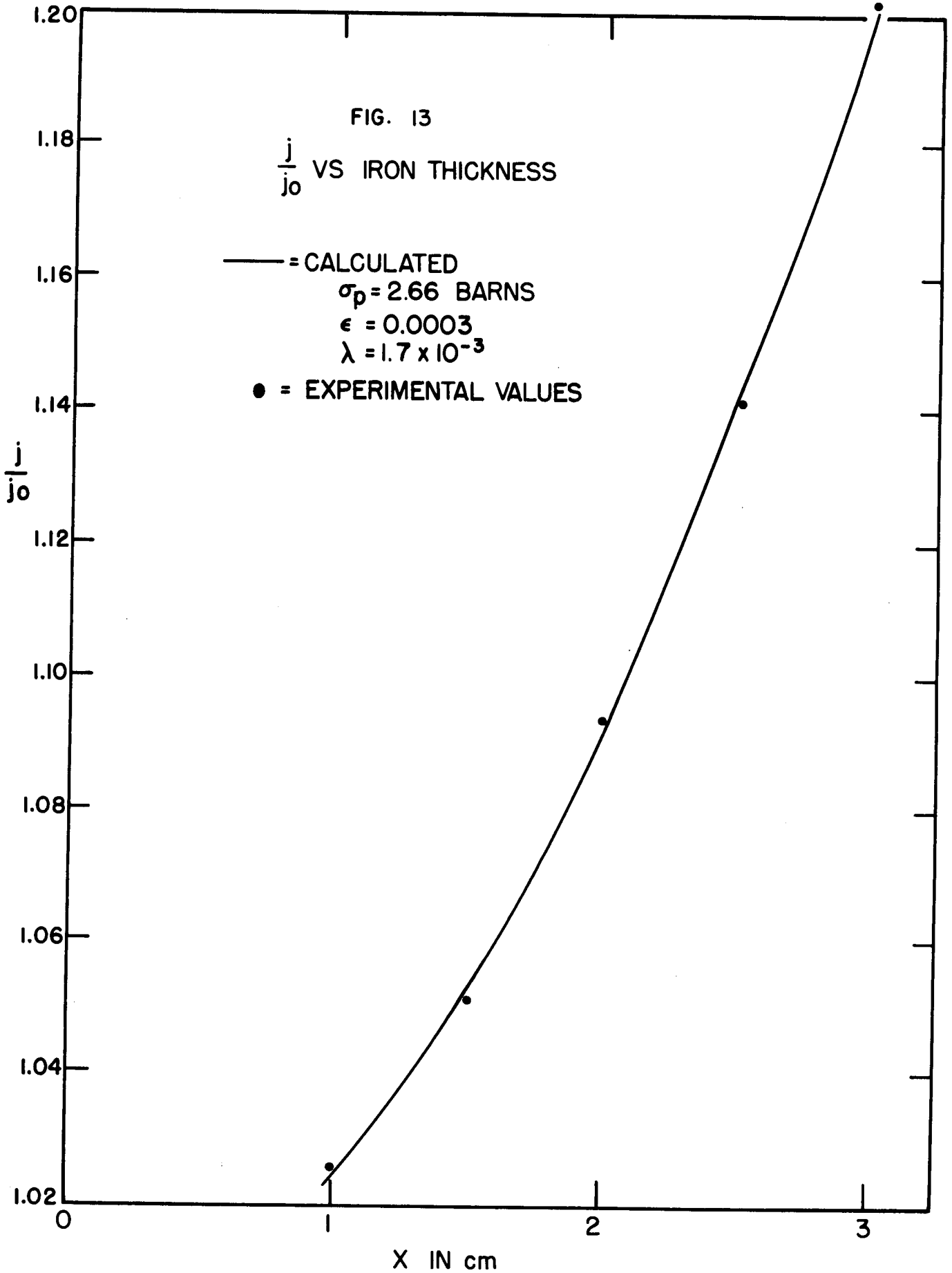

TABLE VII

λ (Å)	$\Delta j / j_0$ MEASURED	$\Delta j / j_0$ CORRECTED	σ_p
0.88	0.00534	0.00534	0.642
1.20	0.0283	0.0291	1.50
1.49	0.0533	0.0562	2.09
1.77	0.0848	0.0915*	2.66*
2.05	0.1379	0.1752	3.68
2.24	0.1698	0.2479	4.37
2.32	0.1689	0.2773	4.63
2.42	0.1223	0.1662	3.59
2.56	0.1339	0.2015	3.95
3.27	0.1372	0.4589	5.96

* Best-fit values.

The Miller indices of the sets of planes for which discontinuities in the polarization cross section occur are indicated at the appropriate wavelength in Fig. 12. Although experimental points are shown from 3.27 Å to 1.53 Å, most attention was directed toward attempting to follow the 211 discontinuity at about 2.334 Å, or 0.0151 ev. In spite of the fact that the third-order corrections are still rather large at this wavelength, the existence of the discontinuity is clearly shown by the data. The measurements suggest that with improved resolving power and very careful attention to third-order corrections, this discontinuity in the polarization cross section could be plotted with some accuracy, and that perhaps a unique choice could be made between the various form factors.

NEUTRON DIFFRACTION

C. G. Shull W. C. Koehler
E. O. Wollan W. A. Strauser

Polarization of Bragg-reflected Neutrons. According to the theory of magnetic scattering of neutrons by ferromagnetic materials, there should exist partial polarization in the neutrons scattered by a single ferromagnetic domain. This polarization should be a maximum when the magnetization in the domain is perpendicular to the plane of scattering. It also depends upon the relative values of the nuclear and magnetic scattering amplitudes, C and D, respectively, according to the formula

$$P = 2\left[\frac{C}{D} + \frac{D}{C}\right]^{-1}$$

When C is equal to D, the polarization becomes complete with only one spin state of the incident neutron beam being scattered.

For the case of Bragg scattering by Fe, the expected polarization in the strong 110 reflection is calculated to be 60%. Attempts have been made to measure this polarization by studying its passage through various samples of magnetized and unmagnetized analyzing blocks of iron. To get an intensity high enough, a single crystal of iron (96% Fe - 4% Si) was used to produce the polarized beam. The single crystal was grown from the melt by F. A. Sherrill of this Laboratory. A small section (1/8 in. by 1/8 in. by 5/8 in.) was cut from the ingot with the long axis along a 100 direction. It was mounted between the pole pieces of a permanent magnet so that an applied field of 4800 oersteds was directed along the long axis, 100, direction. Monochromatic neutrons (λ = 1.204 Å) were then reflected from internal 110 planes. This partially polarized beam was passed through one of several analyzing blocks of polycrystalline iron placed between the poles of an electromagnet capable of applying a magnetic field of about 8000 oersteds to the analyzing block. The two field directions (polarizer and analyzer) were kept parallel in all the experiments to avoid any spin flipping in the neutron beam.

Since the analyzing field was not strong enough to saturate the analyzing block, depolarization effects discussed by Halpern and Holstein[1] were present. The extent of the depolarization was determined by measuring the single transmission effect in the various blocks with unpolarized incident neutrons. It was not feasible to use the single crystal of Fe as the source of unpolarized radiation because of the extreme difficulty encountered in demagnetizing the single crystal. Accordingly, a nonferromagnetic crystal (Cu in 111 reflection) was used for this.

Measurements were then made of the single transmission effect in the analyzing block with polarized radiation from the Fe crystal and with unpolarized radiation from the Cu crystal. These two measurements permit calculation of the degree of polarization in the polarized beam.

As analyzing blocks, three blocks of thickness 3/4, 1, and 1-1/4 in. were cut from an Armco iron slab and three blocks of equivalent thickness from a cold-rolled steel slab. A polarization value was obtainable from the data for each block with the following results: 54%, 58%, and 55% for the Armco blocks and 30%, 23%, and 23% for the cold-rolled steel blocks. Within the individual sets the data are consistent, but there is a serious discrepancy between the values obtained from one set compared to those from the other set. Studies were then made on the analyzing blocks to establish the cause of this discrepancy. A grain-size analysis by R. J. Gray of the Metallurgy Division showed the grain size in the Armco blocks to be 250 μ, whereas in the cold-rolled blocks it was only 25 μ. Further studies on the neutron-diffraction spectrometer showed a very pronounced intensity variation around the Bragg rings for both samples, this being caused by large grain size in Armco and strong preferred orientation in the cold-rolled specimens. Thus the above discrepancy in polarization results could easily have been explained on the basis of nonuniform intensity in the Bragg rings. The theory of the single transmission effect is predicated on the basis of complete uniformity of scattering in azimuthal angle, and departures from this through orientation or grain-size effects can lead to erroneous results.

It is planned to restudy the polarization effects discussed above after obtaining analyzing blocks of suitable properties. All that can be said at the present time is that the Bragg-reflected beam from magnetized iron is polarized but the degree of polarization is uncertain.

Other ferromagnetic crystals are of interest in this connection where the degree of polarization is expected to be much higher. Cobalt and certain Bragg reflections from Fe_3O_4 should show almost complete polarization on the

(1) Halpern, O., and Holstein, T., "On the Passage of Neutrons through Ferromagnets," *Phys. Rev.* 59, 960 (1941).

basis of already measured nuclear and magnetic scattering amplitudes. It is planned to study these as soon as suitable analyzing specimens become available.

Scattering of Neutrons by Iron and Its Isotopes. According to Halpern and Johnson, the scattering of neutrons by an unmagnetized ferromagnetic substance is characterized by

$$F^2 = C^2 + 2/3(D^2 f^2)$$

where

F = the crystal-structure scattering amplitude of the magnetic ion

C = the nuclear scattering amplitude

D = the magnetic scattering amplitude

f = the magnetic form factor

The experimental investigation of the scattering of neutrons by ferromagnetic substances is of interest in problems involving the interaction of the neutron magnetic moment with magnetic ions, as, for example, in the production of polarized-neutron beams. The interpretation of such scattering experiments generally requires the knowledge of both the nuclear and magnetic scattering amplitudes, since, according to the equation above, the nuclear and magnetic effects both contribute to the experimentally determined quantity.

Since the magnetic scattering arises from the interaction of the neutrons with unbalanced magnetic moments of electrons in the 3d shell, it will have a form-factor dependence on angle determined by the distribution of the electrons responsible for the magnetic scattering.

By measuring the crystal structure amplitudes of iron over a range of scattering angles, it is then possible to determine the magnitude and angular dependence of the magnetic scattering as well as the angularly independent nuclear scattering.

Figure 14 shows the scattering data obtained from powdered iron. These data represent an average from several samples of iron prepared in different ways and of particle sizes ranging from very fine powders to coarse filings. The angularly dependent items of the data, which represent even at small angles only about 10% of the total differential scattering cross section, are due to magnetic scattering. The solid curve in the figure has been calculated using a formula of Halpern and Johnson for the magnetic scattering amplitude with numerical values for the form factor taken from the average of the curves

UNCLASSIFIED
DWG. 9799

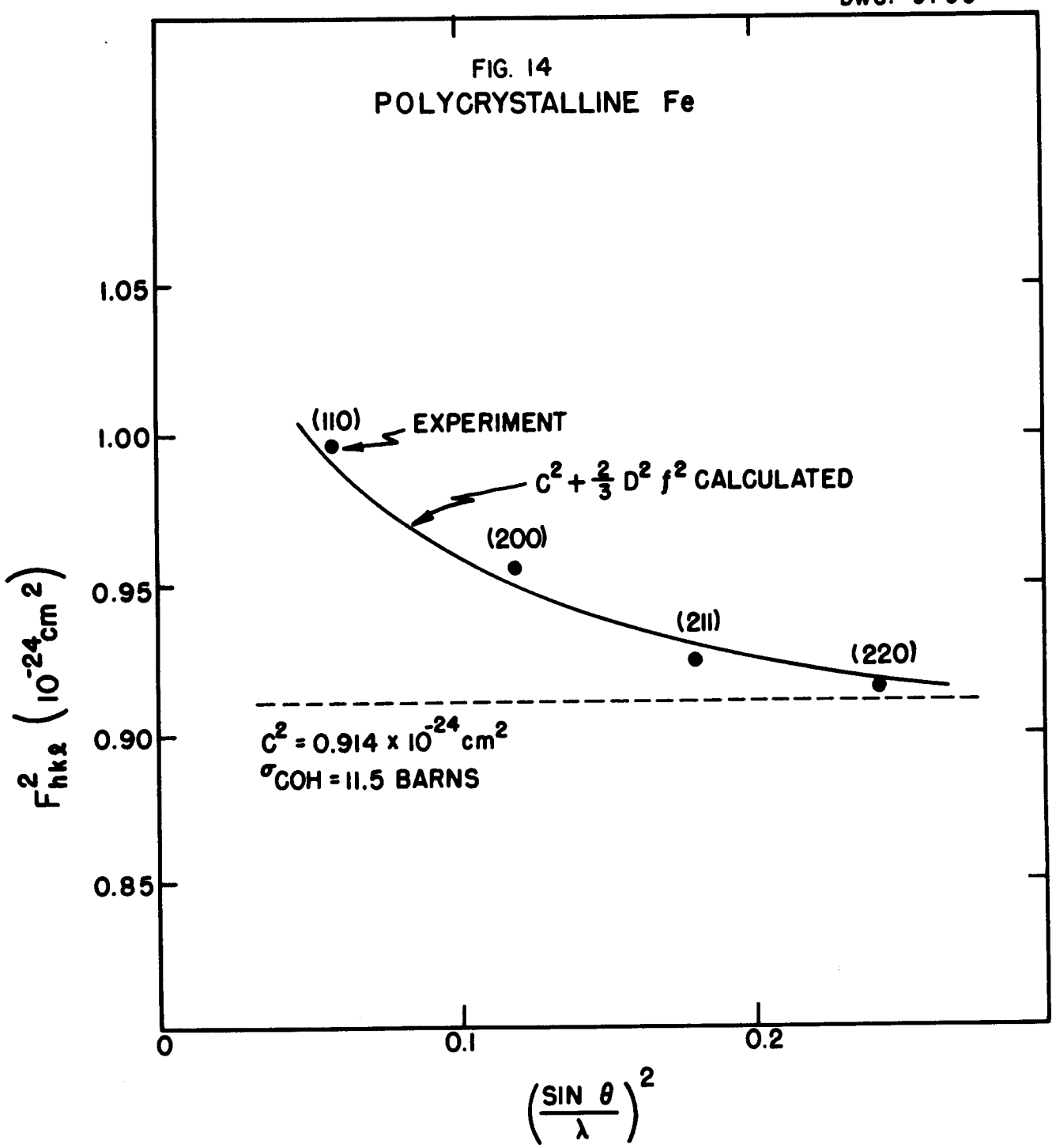

calculated by Steinberger and Wick[2] on the assumption of different boundary conditions for their wave functions. Good agreement is to be noted between the data and the average form-factor curve. At the present time, the experimental data are not capable of distinguishing between the two cases. The dashed horizontal line represents the residual nuclear cross section of normal iron. This nuclear cross section of 11.4 barns for normal iron is the weighted average of results obtained with several samples of both fine powders and coarse filings. Since we can expect the magnetic scattering amplitude and form factor to be independent of the mass of the nuclear scattering center, the investigation of isotopically enriched samples permits the variation of the nuclear scattering amplitude while leaving the magnetic amplitude unchanged. The results of measurements on unmagnetized cobalt were reported in ORNL-694 (*p.* 34), together with preliminary results for iron. The measurements on normal iron and samples of isotopically enriched iron have been extended and are reported here.

Samples of Fe_2O_3 of known enrichment in Fe^{54}, Fe^{56}, and Fe^{57} were obtained from the Stable Isotope Division at the Y-12 section of ORNL, and these samples were analyzed for purity by spectroscopic and X-ray-diffraction studies. Neutron-diffraction patterns were first obtained with the oxide samples in order to determine the scattering phases of the isotopes, and these samples, as well as a sample of normal iron oxide, were reduced to the metal powder, with which more extensive and accurate intensity studies of the diffraction patterns were made. The data for Fe^{56} were analyzed in the same way as for normal iron, and the magnetic intensity was found to follow, within experimental error, the same curve. For the other two samples, the quantity of material was limited and the cross sections were low so that only a few reflections were observed. The form-factor curve of Steinberger and Wick was fitted to the data and extrapolated to large angles to give the nuclear scattering amplitudes and cross sections. All the nuclear data are given in Table VIII. From the patterns of the oxide samples it is found that the phases of scattering are all positive.

(2) Steinberger, J., and Wick, G. C., "On the Polarization of Slow Neutrons," *Phys. Rev.* 76, 994 (1949).

TABLE VIII

Scattering Amplitudes and Cross Sections

ISOTOPE	COHERENT SCATTERING AMPLITUDES (10^{-12} cm)	COHERENT SCATTERING CROSS SECTIONS (barns)	TOTAL SCATTERING CROSS SECTIONS (barns)
Fe^{56}	0.999	12.6	12.6
Fe^{54}	0.42	2.2	2.2
Fe^{57}	0.23	0.64	2.0
Fe (directly)	0.956	11.5	11.4
Fe (from isotopic cross section)		11.2	

It may be seen that the cross sections of the three isotopes of Fe studied are all appreciably different from the potential scattering cross section. The large cross section of Fe^{56} appears to be due to a virtual resonance, since it is only for $E > E_r$ that constructive interference between potential and resonance scattering occurs. The small cross sections of Fe^{54} and Fe^{57} must correspond to destructive interference with positive energy resonances.

Of the three isotopes studied, only Fe^{57} may be expected to exhibit spin-dependent scattering. Total scattering cross sections for the four metal samples were obtained from transmission measurements using values of the isotopic absorption cross sections obtained by Pomerance.(3)

The total scattering cross sections of the even-even isotopes were found to be in good agreement with the coherent cross section, and they have been set equal to them in the table. The total cross section of Fe^{57} is approximately 2.0 barns, and the fact that this is considerably larger than the coherent-cross-section value of 0.64 barn shows the existence of strong spin dependence. Since the available sample was small, the accuracy in this measurement is only within about 20%.

(3) Pomerance, H., personal communication.

Crystal Monochromators. Rock salt has been used in the past as a monochromating crystal primarily because it is readily available in large pieces. It has been evident from the first, however, that rock salt is too perfect a crystal to constitute an efficient monochromator for neutron beams with the large angular spread required in order to obtain sufficient intensity. Large crystals of copper and lead which are now being grown in the laboratory by Mr. Sherrill show a mosaic spread of the order of a degree, and, since this is about the angular spread in the neutron beam, these crystals can be expected to constitute very efficient monochromators. Preliminary tests with copper and lead crystals of far from ideal size and shape have given an intensity increase of about a factor of 3 with little loss in resolution, and it is expected that with new large copper crystals which are now being prepared an additional increase in intensity of a factor of 2 can be readily obtained.

Tables of Trigonometric Functions. Tables of the trigonometric functions appropriate to the most commonly used sample geometries in neutron diffraction have been compiled by K. L. Robertson and W. L. Stair. These tables list the values of $\sin \theta$, $\sin 2\theta$, $\sin \theta \sin 2\theta$, and $\sin^2 2\theta$ for angles ranging from 2° to 45° at 2′ intervals.

HIGH-VOLTAGE ACCELERATOR PROGRAM

W. M. Good B. D. Kern
C. D. Moak

Reactions with Protons on B^{11}. The reaction B^{11} + protons has afforded an opportunity to become familiar with the 300-Kev Cockcroft-Walton generator at the same time that the generator was being used for ion-source and lens studies. The study of this reaction has also stimulated the construction of detection instruments which will be required for future work. The following reactions of protons on boron have long been known:

$$B^{11} + p \longrightarrow Be^{8*} + He^4 + 4.39 \text{ Mev} \qquad Be^{8*} \longrightarrow 2\,He^4 + 3.12 \tag{1}$$

$$\longrightarrow Be^8 + He^4 + 7.39 \text{ Mev} \qquad Be^8 \longrightarrow 2\,He^4 + 0.125 \tag{2}$$

$$\longrightarrow C^{12} + \gamma\ (12 \text{ Mev}) + \gamma\ (4 \text{ Mev}) \tag{3}$$

$$\longrightarrow C^{12} + \gamma\ (16 \text{ Mev}) \tag{4}$$

Since the Q of the reaction is spent in giving energy to both Be^8 and He^4, the energy of the α particle in the C^{12} center of mass is 2/3 Q. Likewise, the breadth of a Be^8 level will appear as a spread in energy of the α particles giving rise to that level, equal to 2/3 the width of that level in the C^{12} center of gravity. At these low bombarding energies (about 300 Kev), relatively high Q's, and for a target as heavy as B^{11}, the C^{12} is essentially at rest.

The first of the reactions mentioned above is followed in a time interval estimated at less than 10^{-20} sec by the breakup of Be^{8*} into two α particles. The excitation energy of Be^{8*} is released in the Be^8 center of mass and gives rise in the laboratory to α particles ranging in energy from about 0.5 to 4.5 Mev, depending upon the width of the Be^{8*} level. The second reaction yields a higher energy α particle of much narrower energy spread because of the smaller width of the Be^8 ground state. Be^8 is still unstable against breakup into two α particles; hence this mode of reaction is accompanied by a monokinetic α of about 5.82 Mev together with α's having energies ranging from about 0.9 to about 2.1 Mev.

A preliminary study has been made of the α-particle spectra from these reactions, using an electron collection chamber and differential pulse-height selection. In addition, it has been possible to obtain the yield with voltage of the groups of α's taken separately. From such yield curves and α-particle spectra it should be possible to make more certain assignments on the levels in C^{12} and Be^8 than has so far been possible with less powerful techniques.

For the results given here, the target was elemental boron evaporated to a thickness of about 5 kv onto a water-cooled tungsten backing. The electron collection chamber had a window about 1 cm in diameter, about 3 cm from the target, and at 90° to the beam. The window was 30 $\mu g/cm^2$ of Formvar, and aluminum absorbers in front of the window screened out the scattered protons.

Figure 15 shows the α-particle spectrum at a bombarding energy of 182.5 Kev. Some meaning is attached to the abcissa by the pulse height associated with the Pu α's, but it is otherwise arbitrary because no correction has been made for window or absorber thickness. In addition, the change in linearity with energy has not been thoroughly studied. Nevertheless there are clearly resolved the low-energy α's associated with leaving Be^8 excited and the high-energy α's leaving Be^8 in its ground state. Setting the spectrometer at pulse heights corresponding to the peaks of the short-range and long-range groups, the yield curves, (*a*) and (*c*), respectively, of Fig. 16 were obtained.

These two yield curves contain uncertainties in the voltage due to some uncertainty in the condition of the target. Curves (*b*) and (*d*), which are the yields of the first reaction on successive 24-hr periods, illustrate what is known to happen to a target with age. In addition, the voltage plotted is obtained from a precision resistor string and does not take into account the energy that the protons have when they leave the ion source. This energy is not precisely known at present. Taken as a whole, the results confirm the earlier work of Cockcroft[1] and von Ubisch.[2]

The γ rays from the third and fourth of the competing processes following proton capture by B^{11} are known to have energies of 16.6, 12.2, and 4.4 Mev. The spectrum of these γ rays is being studied with a scintillation spectrometer,

(1) Cockcroft, J. D., and Lewis, W. B., "Experiments with High Velocity Positive Ions. V. Further Experiments on the Disintegration of Boron," *Proc. Roy. Soc. London* 154, 246 (1936).

(2) "Alpha Particles from the Boron-Proton Interactions Obtained from Thin-boron Targets," *Kgl. Norske Videnskah Selskabs For.* 15, 71 (1942).

UNCLASSIFIED
DWG. 9803

FIG. 15

B" (p, 3 α)

α PARTICLE DISTRIBUTION

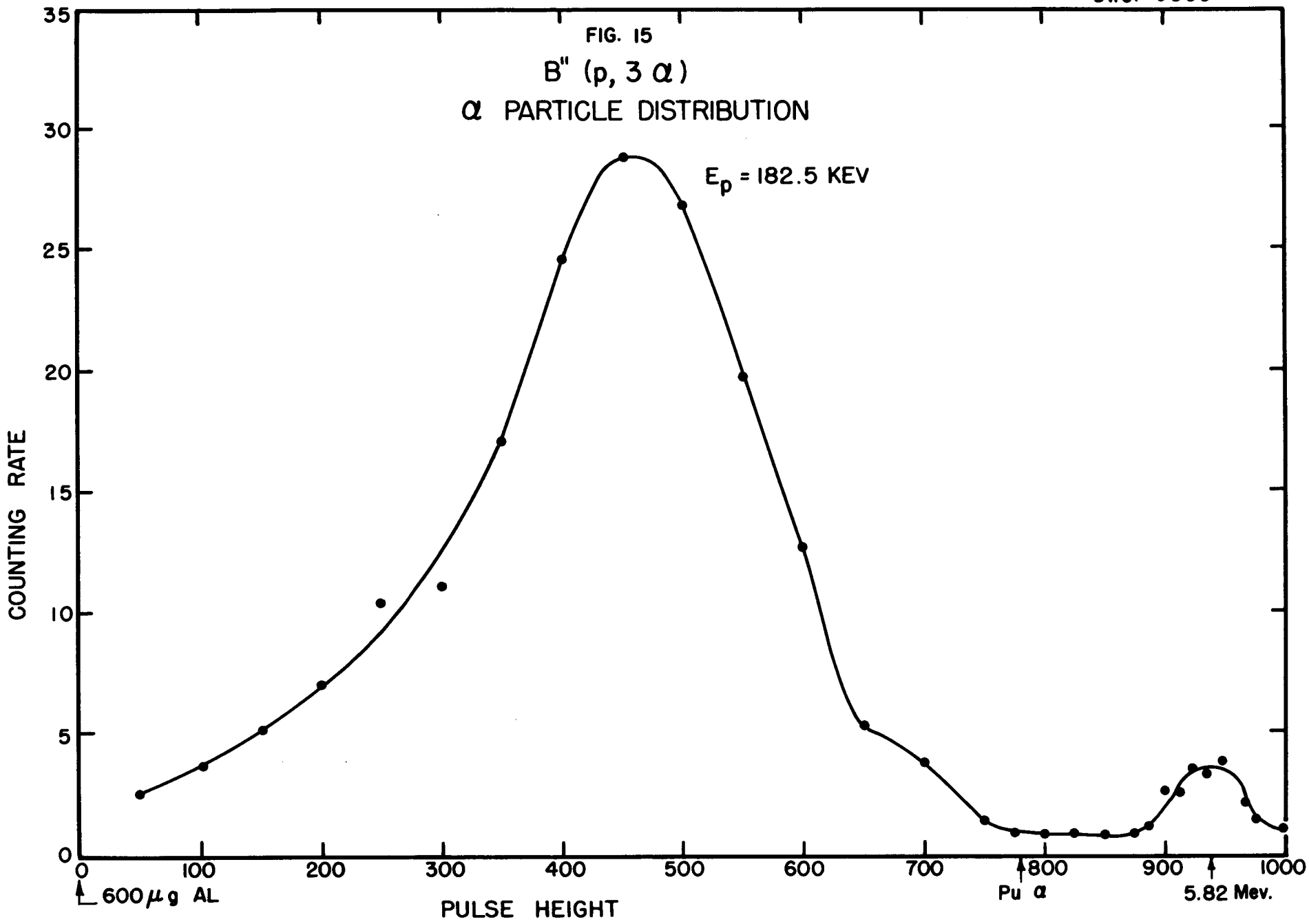

UNCLASSIFIED
DWG. 9804

FIG. 16

YIELD CURVES FOR THE $B^{11}(p, 3\alpha)$ REACTIONS; EFFECT OF TARGET CONTAMINATION

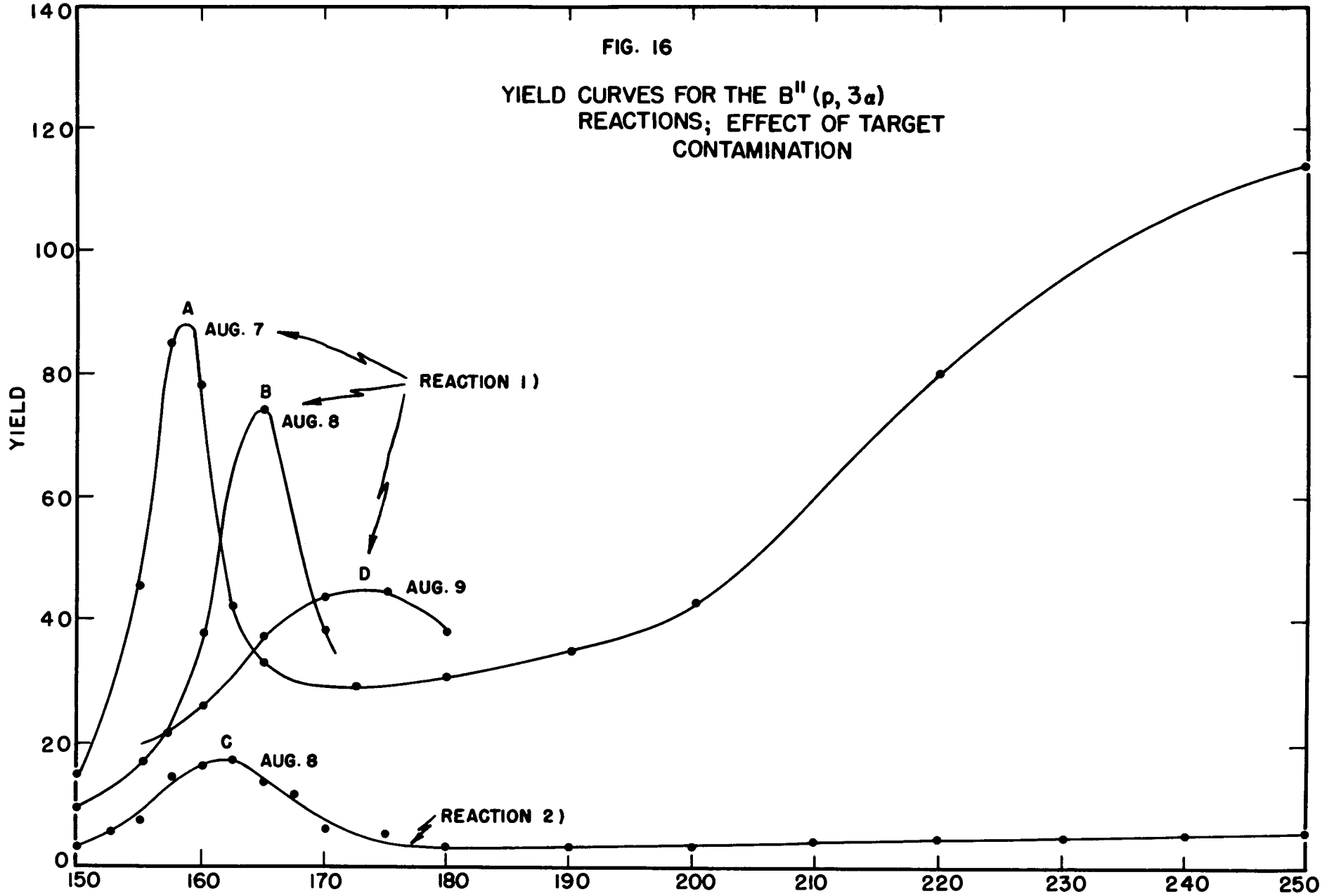

partly as a means to calibrate the spectrometer and partly to get new information about the rays. Specifically, a complete study is being made of the angular correlations of the γ rays with each other and with the beam, and the thin-target yield with energy of the γ rays taken individually is under investigation.

The spectrometer consists of a NaI crystal 1 in. by 1-1/2 in. diameter, an RCA 5819 photomultiplier tube, and a linear amplifier followed by a differential pulse-height selector. The differential number vs. pulse-height curve shows peaks which correspond to three γ rays, and the pulse-height calibration is linear within the present uncertainties of the instrument. The possibility seems promising of using such an instrument to single out γ rays in cases in which not too many γ rays are present.

Coincidences were obtained between the 12-Mev and 4-Mev γ rays, confirming what seemed certain, *viz.*, that the 12- and 4-Mev γ's take place in succession to the ground state of C^{12}. The 16-Mev γ ray is a direct transition. The thin-target yield with energy data are still provisional, but it seems reasonably certain that the 16-Mev and the 12-Mev γ rays show the same 163-Kev resonance and, in fact, the same yield with energy in the range 150 to 300 Kev. The emission of a γ ray from these levels to the ground state of C^{12} with $J = 0$ already indicates that the capturing level in C^{12} cannot be $J = 0$. Preliminary results on the γ-ray angular distributions are as follows: The 12-Mev γ ray has a distribution with the beam of the form $A + B \cos^2 \theta$ where $A = 0.82$ and $B = 0.18$ (Fig. 17). The 4-Mev γ-ray angular distribution with the beam is uncertain by the amount of 12 Mev radiation accepted by the spectrometer along with the 4 Mev radiation. Consistent data are not yet available on the γ - γ angular correlation between the 12-Mev and 4-Mev γ rays. The 16-Mev γ radiation appears isotropic within 10% with respect to the beam. These results were obtained on a thick target with a bombarding energy just above the resonance, *viz.*, 175 Kev.

UNCLASSIFIED
DWG. 9711

FIG. 17
ANGULAR DISTRIBUTION OF THE 12.2 MEV GAMMA-RAY FROM B'' + H' WITH RESPECT TO THE BEAM

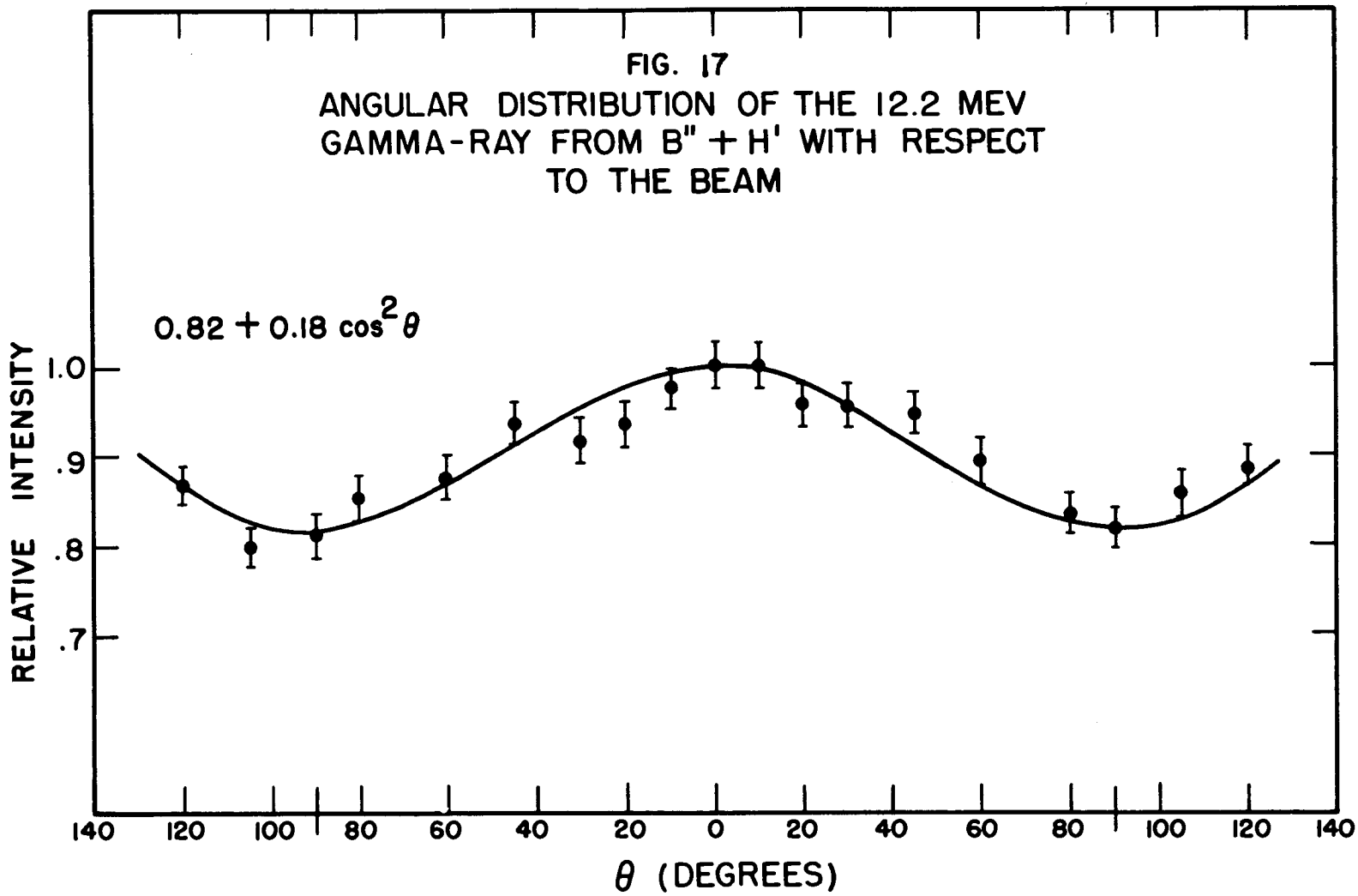

SEARCH FOR A PERMANENT ELECTRIC DIPOLE MOMENT OF THE NEUTRON

J. H. Smith

Recent considerations by Purcell and Ramsey[1] have indicated that direct measurement of the permanent electric dipole moments of nucleons or nuclei would be desirable. A search for such a moment in the neutron has therefore been undertaken as a joint program of Harvard University and this Laboratory.

The experiment is similar to the molecular-beam-resonance techniques of Rabi as modified by Alvarez and Bloch[2] for studying the magnetic moment of the neutron but further modified by employing the split-oscillating-field technique suggested by Ramsey.[3] This allows the use of a much longer (6-ft) homogeneous magnetic field with proportional increase in sharpness of the resonance. It also allows a vacuum absorber containing a high-voltage condenser to be placed in the region between the oscillating fields. The neutrons pass through this electric field of 10^5 volts/cm, and, if the neutron has a permanent electric dipole moment, a reversal of the direction of this electric field should result in a shift of the magnetic dipole resonance.

The apparatus is working satisfactorily. Resonances are observed with a half-width of only 600 cycles. No shift of the resonance has been observed upon application of the electric field, which would indicate the existence of an electric dipole moment greater than the electronic charge multiplied by 10^{-18} cm.

Work to increase the accuracy of the experiment is continuing.

The work is under the direction of Profs. E. M. Purcell and N. F. Ramsey of Harvard.

(1) Purcell, E. M., and Ramsey, N. F., "On the Possibility of Electric Dipole Moments for Elementary Particles and Nuclei," *Phys. Rev.* 78, 807 (1950).

(2) Alvarez, L. W., and Bloch, F., "A Quantitative Determination of the Neutron Moment in Absolute Nuclear Magnetons," *Phys. Rev.* 57, 111 (1940).

(3) Ramsey, N. F., "A Molecular Beam Resonance Method with Separated Oscillating Fields," *Phys. Rev.* 78, 695 (1950).

THERMAL NEUTRON DIFFUSION IN WATER

F. J. Sisk

In order to study in a precise way the diffusion of thermal neutrons in water, the following problem was attacked both experimentally and theoretically: What is the thermal neutron flux distribution in water (23°C) in the vicinity of an infinite-plane black absorber (cadmium) situated at $x = 0$ when the asymptotic flux (far from the plane) is given by $e^{\kappa x}$?

This situation was realized experimentally to a good approximation in the large water tank on top of the thermal column of the Oak Ridge Graphite Reactor. The neutron flux distribution was measured by activation of small, thin indium foils at various distances below a circular cadmium plate. In order to normalize the results to constant incident current, two monitor foils at fixed positions were also exposed for each run. In this way the flux depression due to the cadmium plate was rather accurately determined as a function of distance from the plate. At $x = 0$ the normalized flux was measured and found to be 18.3% of what it would have been with the plate removed.

The theoretical approach to the problem consisted in setting up the integral equation of transport theory with an exponential integral kernel for this situation and carrying through a solution with assumed eigenvalue $\Sigma_s/2\Sigma$ by a numerical iteration method.

Excellent agreement between the observed and theoretical flux distributions is obtained with $\Sigma_s/2\Sigma = 0.496$. This provisional value, together with the measured value of $\kappa = 0.373\ \mathrm{cm}^{-1}$, leads to the following values for the equivalent scattering and absorption cross sections (per hydrogen atom) for water: $\sigma_s \approx 45$ barns, $\sigma_a \approx 0.25$ barn. Additional refinements in the calculations may change these values slightly.

Further details will be found in a complete report now in preparation on the experiment and calculations. This work will be submitted as a dissertation for the M.S. degree to the U.S. Naval Academy Postgraduate School.

THEORETICAL PHYSICS

M. E. Rose S. D. Drell*
J. M. Jauch* G. B. Arfken, Jr.
L. C. Biedenharn, Jr.

Introduction (M. E. Rose). The principal developments since the appearance of the last quarterly report are concerned with the internal conversion problem. It had been planned originally to have the numerical work done at the Computation Laboratory at Harvard University on the Mark III. However, when this proved to be impossible, the work was held in abeyance. Recently, tentative plans with the Bureau of Standards were discussed, and a conference was held with Dr. Albert Cahn of the Los Angeles branch of the Bureau; it now appears quite likely that the work on the L-shell internal conversion can and will be done on the Western Automatic Computer. In this connection the work of last summer on the methodology of the problem was re-examined, and certain improvements in starting values for the numerical integration of the wave equation for the bound-state case were effected.

The matrix elements used in the K-shell internal conversion were tabulated at the Computation Laboratory at the request of the writer. These matrix elements are needed in connection with two additional problems:

(1) The reduction of the γ-ray flux due to the presence of extranuclear electrons. The emerging γ ray is absorbed by the K electron, which goes to an intermediate state and returns to the K shell by a quantum emission. This is a higher order effect which might conceivably affect the value of the internal conversion coefficients when the latter are large. Drs. J. B. French at Massachusetts Institute of Technology and G. Goertzel at New York University have made some study of this effect.

(2) In a cascade transition involving isomeric states one possible mode of decay is by successive emission of a γ ray and a conversion electron, in either order. The theory of the angular correlation for this process was worked out by Dr. D. Ling (now at the University of Kansas) in 1948 but was never published because, without the above-mentioned matrix elements, it was impossible to obtain reliable numerical values for the coefficients in this angular correlation. A joint publication with Dr. Ling is now in the planning stage.

* Summer visitor.

A considerable amount of work was done by Dr. S. D. Drell on problems which arise in the Van de Graaff program and by Dr. J. M. Jauch on low-temperature problems. This work is described below. It is also described in part elsewhere, in ORNL-792 by S. D. Drell and in ORNL-813 by J. M. Jauch. It is pertinent to mention that, in connection with the low-temperature program, the writer has re-examined the formula obtained for the nuclear alignment (see AECD-2119) with the purpose of determining whether a number of effects hitherto unconsidered could be important. These effects are intermediate hyperfine structure coupling, quadrupole coupling, and quenching of orbital angular momentum and hyperfine structure anisotropy. All these effects, in the worst cases, do not appreciably affect the formula previously given.

Theoretical Problems Concerning Paramagnetic Substances (J. M. Jauch*). The problem of quenching of the orbital motion of a paramagnetic ion was investigated, and a simple systematic treatment of this problem was developed with the methods of quantum mechanics.

The theory was then applied to the problem of the Cu-Tutton salts and $CuSO_4 \cdot 5H_2O$ where Polder's results for the anisotropy of the g factors can be easily derived with this method. In the course of this work it was observed that there exists a large interaction between the Cu ions in the undiluted salt, which must be of the superexchange type. There are four independent physical phenomena which confirm this interaction:

(1) The fact that the susceptibility follows a Curie-Weiss law with a Weiss constant $\theta = +0.7°K$

(2) The observed anomaly of the specific heat at about 1°K found by Ashmead

(3) The confluence of the magnetic resonance absorption lines corresponding to the two kinds of ions in the unit cell into one single line

(4) The phenomenon of "exchange narrowing" observed in the magnetic resonance absorption

The first two effects allow a rather accurate determination of this constant and give a value of about 1 cm^{-1}. The last two effects can be estimated

*Summer visitor.

only very roughly and give a value of 0.15 cm^{-1}. It is not certain whether this last estimate can still be considered in agreement with the first.

As a last problem the hyperfine structures of the Mn^{++} and Cu^{++} ions were investigated. In both these cases previous theories were in disagreement with experiment, giving zero splitting for Mn and a splitting for Cu which varies in the opposite direction with the g factor. For the Mn case an explanation recently proposed by Abragam is probably correct. It is shown, however, that this explanation fails in the case of Cu and that the true explanation of the discrepancy is to be found in the reversal in sign for the spin part of the hyperfine interaction in a "positive hole" such as exists in a $3d^9$ configuration. The value for $\Delta E_{\parallel} / \Delta E_{\perp}$, that is, the hyperfine structure splitting in the directions parallel and perpendicular to the tetragonal axis, is found to be about 6 experimentally, about ½ with the old theory, and about 5 with the new theory here proposed.

Internal Conversion (S. D. Drell*). The approximate analytic formulas for electric dipole and quadrupole and magnetic dipole conversion from the K and L_I shells were compared with precise machine values obtained by Reitz for the K shell and by the University of Toronto Computing Laboratory. K- to L_I-shell conversion ratios obtained from approximate formulas were found to be bad for large values of Z, being in error by as much as a factor of 7 for the electric quadrupole case at 150 Kev and $Z = 92$. This work was carried out only to get an idea of how much faith can be put in currently available K to L conversion ratios until Dr. Rose's tables for L-shell conversion become available.

Zero-Zero Transitions (S. D. Drell*). In the decay of a nucleus from an excited level of zero spin to a lower lying state of zero spin with no parity change, an orbital electron will be ejected from its path about the nucleus, or, if the one excited level of the nucleus is higher than $2mc^2$ above the other level, an electron-positron pair may be created as well. It is significant that in these zero-zero no-parity-change transitions the perturbing fields which induce the internal conversion or pair formation exist only within the nucleus and vanish identically outside the nuclear radius. Because of this unique property of zero-zero transitions it is of particular interest to consider the effect of finite nuclear radius on the rates of internal conversion and of pair formation for such a process. This effect was studied by

*Summer visitors.

using the methods of Dr. M. E. Rose to obtain wave functions for relativistic Dirac electrons in the field of a finite charge distribution. In particular, a K- to L-shell conversion ratio can be given which is independent of the nuclear matrix elements. (It was found to equal the square of the product of the normalization constants for initial and final electron states for the K conversion divided by the same quantity for the L conversion.) This ratio agrees to within 10% with the result obtained by using point Coulomb functions for the electrons. Experimental agreement and estimates for the nuclear matrix elements were also discussed in the course of this work.

Reactions (S. D. Drell*). Several reactions which were accessible to experimental study by the Van de Graaff group were analyzed. In particular it was felt that α-particle and γ-ray angular distributions would yield valuable information concerning excited levels in the intermediate compound nucleus of ${}_6C^{12}$ formed by proton bombardment of ${}_5B^{11}$. For example, it would be desirable to ascertain if the (p,α) reactions proceed through the same levels of the compound carbon nucleus as do the (p,γ) reactions and to specify spin and parity for these levels.

Consider a nuclear process

$$P + A \longrightarrow B + Q \tag{1}$$

Particle P with spin p hits particle A with spin a. After the reaction, particle Q with spin q and recoil B with spin b emerge. Analysis is made in the center-of-mass system, assuming that we are in the region where the reaction can be approximated by considering it to be induced in the main by just one orbital momentum wave L of the incident wave. Thus at low energies waves of higher L are less effective, because of smaller overlap of wave functions, in inducing a reaction. It may be remarked here that the concept of "compound nucleus" is always applicable if it is introduced and employed no more specifically than in connection with angular momentum and parity conservation. That is to say, by virtue of the restrictions customarily placed on nuclear Hamiltonians with regard to their properties of rotation in configuration and spin space, angular momentum is conserved throughout a nuclear reaction.

The general conclusion of Yang[1] is that in the reaction (1), restricted as indicated above to being induced by one value of L, the angular distribution

*Summer visitor.

(1) Yang, C. N., "On the Angular Distribution in Nuclear Reactions and Coincidence Measurements," *Phys. Rev.* 74, 764 (1948).

of the outgoing particles in the center-of-mass system is an even polynomial of cos θ with maximum exponent not higher than $2L$. θ is the angle between incident and scattered particles:

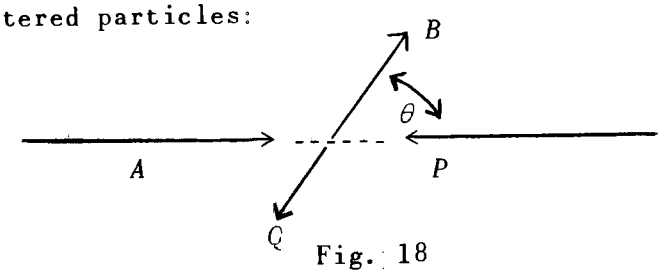

Fig. 18

In order to calculate relative values for the coefficients a_{2i} in the expansion

$$W(\theta) = \sum_{i=0}^{L} a_{2i} \cos^{2i}\theta$$

for the angular distribution which applies for any specific nuclear reaction, models must be constructed for the individual interaction mechanisms.

No restriction or specialization is implied if the reciprocity theorem of nuclear reactions is invoked to describe the reaction reversed in time to (1), namely,

$$B + Q \longrightarrow P + A \tag{2}$$

The reciprocity theorem states that

$$\frac{\sigma_{PQ}}{\lambda\!\!\!^{-}_{P}{}^{2}} = \frac{\sigma_{QP}}{\lambda\!\!\!^{-}_{Q}{}^{2}}$$

and its validity implies merely that the Schrodinger equation describing process (1) has a solution for $t \longrightarrow -t$. If $\overline{L}$ describes the maximum relative orbital momentum (of the incident plane wave, in the center-of-mass system, which describes $B \neq Q$) responsible for reaction (2), Yang's theorem puts $2\overline{L}$ as the upper limit on the complexity of the angular distribution in the nuclear reaction. Yang's theorem can thus be extended by saying that $W(\theta)$ is an even polynomial in cos θ with maximum exponent not higher than the smaller of the numbers $2L$ and $2\overline{L}$.

L and $\overline{L}$ can be related by calling j the total spin angular momentum of the incident wave $A + P$ and $\overline{j}$ the same quantity for $B + Q$. By angular momentum conservation, then,

$$\underset{\rightarrow}{L} + \underset{\rightarrow}{j} = \overline{\underset{\rightarrow}{L}} + \overline{\underset{\rightarrow}{j}} = \underset{\rightarrow}{J}$$

where J denotes the angular momentum (total) of the compound state. This statement on the maximum complexity of the angular distributions in a nuclear reaction will be more restrictive than Yang's theorem in the following type of reaction: The $\underset{\rightarrow}{L}$ and $\underset{\rightarrow}{j}$ in the incident beam combine in antiparallel orientations to form a resonance level in the compound nucleus with a low value of $\underset{\rightarrow}{J}$. This then will be the effective parameter in determining the maximum complication in the distribution of outgoing particles.

For bombarding energies higher than or of the order of 10 to 20 Mev, several L values of the incident wave may be important in inducing the reactions, and interference terms between the several compound levels formed will give rise to odd powers of cos θ in the distribution. In applying the continuum theory to describe the intermediate compound state, the odd powers of cos θ will disappear, and the reaction will appear to be symmetric about $(\pi/2)$ if, with Wolfenstein, we assume arbitrary phase for the many compound states through which the reaction may occur. All Coulomb effects are neglected in discussing these reactions in the center-of-mass system.

Consider next the following type of process of interest:

$$A + P \longrightarrow B + Q + C \tag{3}$$

The nature of this three-body breakup, that is, whether the three particles emerge simultaneously or in successive steps, will affect the energy spectrum and may affect the particular angular distribution observed. It will, however, have no effect on the theorems stated below.

Theorem I: If a wave of relative orbital momentum L is responsible for initiating the reaction, the distribution of any one of the outgoing particles B, Q, and C with respect to incident beam P will be an even polynomial in cos θ with maximum exponent $2L$, where θ is the scattering angle in the center-of-mass system. This result is contained in Yang's theorem.

Theorem II: Consider the angular correlation between any two of the outgoing particles in reaction (3), say, between B and C. If particle B emerges with total angular momentum J_B and C with J_C, then the distribution of particles B relative to C will be a polynomial in $\cos\theta_{BC}$ of maximum exponent $2|J_<|$, where $|J_<|$ represents the smaller of $|J_B|$ and $|J_C|$ and θ_{BC} is the angle between particles B and C.

These theorems may be used in discussing reactions of possible interest:

$$_5B^{11}(p,\alpha)\,_4Be^8 \longrightarrow \alpha + \alpha$$

$$_5B^{11}(p,\gamma)\,_6C^{12}$$

$$T\,(T,2n)He^4$$

$$T\,(p,\gamma)He^4$$

Of the reactions occurring when $_5B^{11}$ is bombarded with protons, the following four are of interest:

$$_5B^{11} + p \longrightarrow (_6C^{12*}) \longrightarrow \begin{array}{l} _4Be^{8*} + \alpha_S \\ \searrow \alpha + \alpha \end{array} \qquad (a)$$

$$\longrightarrow \begin{array}{l} _4Be^{8} + \alpha_L \\ \searrow \alpha + \alpha \end{array} \qquad (b)$$

$$\longrightarrow \alpha + \alpha + \alpha \qquad (c)$$

$$\longrightarrow {}_6C^{12} + \gamma \qquad (d)$$

In the $(p,3\alpha)$ reaction, mode (a) is predominant, *i.e.*, the most probable channel for occurrence of the process is the one in which a short-range α_S is emitted, leaving a Be^8 nucleus with 2.8 Mev excitation energy; this in turn decays to two α particles. Mode (b), the emission of a long range α_L followed by decay of the Be^8 in its ground state to two α's, is less probable. Mode (c), the simultaneous decay into three α's, is exceedingly rare.

Wheeler's analysis[2] of α - α scattering suggests that the 2.8-Mev excited level in ${}_4Be^8$ might be ${}^1S_0$ state. The ground state of even-even nucleus ${}_4Be^8$ is also thought to be ${}^1S_0$, with even parity. The ${}^1S_0$ excited level must have even parity if it is to decay to two particles of zero intrinsic spin, such as α particles. This is because a compound level cannot decay to products of vanishing intrinsic angular momentum if it has odd parity and even angular momentum or even parity and odd angular momentum. (Oppenheimer and Serber[3] suggested ${}^1D_2$ as the configuration of the excited level in ${}_4Be^8$.) Shell theory indicates that the ground state of ${}_5B^{11}$ is an odd ${}^2P_{3/2}$ state. Since the α_S and α_L are observed to emerge spherically symmetrically about the incident proton beam, it is consistent with Yang's theorem to assume the reaction to be induced by S protons. (Cross-section variation with change of bombarding energy might throw more light on this point.) For the intermediate ${}_6C^{12}$ excited states, then, the total angular momentum J will have magnitude 1 or 2. Angular momentum conservation may be written

$$\vec{J} = \vec{\Lambda}_1 + \vec{\Lambda}_2 + \vec{\Gamma}$$

where $\vec{\Lambda}_1$ and $\vec{\Lambda}_2$ are the orbital momenta for the two α's emitted in the Be^8 decay and Γ is the orbital momentum of the first emitted α [in mode (a) or (b)]. Coincidence measurements between the two α's resulting from the Be^8 decay should give a distribution which is a polynomial in the cosine of the angle between them with maximum possible exponent of twice the smaller of $|\vec{\Lambda}_1|$ and $|\vec{\Lambda}_2|$. For the distribution between the originally emitted α and either of the others, there should be observed a polynomial of maximum power equal to twice the smaller of $|\vec{\Gamma}|$ and either $|\vec{\Lambda}_1|$ or $|\vec{\Lambda}_2|$.

Study of the yield curves of the γ's resulting from disintegration mode (d) can yield information as to whether they come from the same levels as those responsible for the α decay. Angular distribution studies of the γ's will tell, by Yang's theorem, the minimum orbital momentum component of the incident wave which is responsible for inducing the reaction. Thus, any anisotropy will rule out the possibility of S protons inducing the reaction.

(2) Wheeler, J. A.; "The Alpha-particle Model and the Properties of the Nucleus Be^8," *Phys. Rev.* 59, 27 (1941); "Interaction Between Two Alpha Particles and the Properties of Be^8" (abstract), *Phys. Rev.* 59, 108 (1941).

(3) Oppenheimer, J. R.; and Serber, R.; "Note on Boron Plus Proton Reactions," *Phys. Rev.* 53, 636 (1938).

In the (p,γ) reaction on tritium, Los Alamos reports a $\sin^2$ distribution of γ's with a small but finite component at 0°. It has been suggested by Christy that the $\sin^2$ component comes from a $^1P_1 \longrightarrow {}^1S_0$ transition in He^4. The 0° component can be attributed to a $^3P_1 \longrightarrow {}^1S_0$ transition which gives rise to a $(1 + \cos^2)$ distribution. The entire reaction appears to be initiated by p-wave protons. A check with scintillation counters to ascertain the reality of the 0° component is desirable.

(n,α) coincidences in the $T(T,2n)He^4$ reactions can indicate minimum angular momentum assignments in accord with Theorem II. The distribution of outgoing α's with respect to the incident triton beam direction will fix a minimum orbital angular momentum assignment by Theorem I.

Angular Dependence in Gamma Emission (G. B. Arfken, Jr., and L. C. Biedenharn, Jr.). Preliminary experiments by Dr. Good and coworkers on $B^{11}(p,\gamma)C^{12}$ have shown strong anisotropy of the 4- and 12-Mev γ's but less than 10% anisotropy of the 16-Mev crossover γ ray. In this connection an investigation was undertaken to determine what restrictions could be set on the angular dependence of one γ from a given level if a second γ from the same level was found to be isotropic. It is believed that a theorem may be stated as follows:

Let J be the total angular momentum of an excited level and a_m the population of the mth magnetic sublevel. Assume $a_m = a_{-m}$ as would be the case for formation of the compound state from a plane wave. Let L be the multipolarity of the emission γ with projections M. Then, for $L \geqslant J - \frac{1}{2}$, isotropy of the γ ray requires that all levels of J be equally populated and, therefore, that all γ radiation from J be isotropic. In particular the condition $L \geqslant J - \frac{1}{2}$ is always satisfied when the lower level is $J = 0, \frac{1}{2}$.

This is a limited converse of the well-known theorem that radiation from a level in which the sublevels are equally populated is isotropic. The necessary condition is readily obtained by noting that the angular dependence of an Lth order multipole is a series of powers of $\cos^2\theta$ up through $\cos^{2L}\theta$. Requiring that $\cos^2\theta, \ldots, \cos^{2L}\theta$ terms have zero coefficients gives L conditions. Equating the angular independent terms gives one additional constraint, which has been shown equivalent to normalization. For integral J and for $J' = J + \frac{1}{2}$, there are $J + 1$ independent level populations. Hence, the necessary condition is that $L \geqslant J$ for integral J or $L \geqslant J'' - \frac{1}{2}$ for any J''. If

$J + 1$ conditions are independent (sufficiency condition), then the solution is unique and must be a_m = constant independent of m. A general proof that the $L + 1$ conditions are independent has not been given. For $L > J$ or $J' - \frac{1}{2}$, there are more constraints than independent variables; therefore some degeneracy must exist. The theorem has been verified by direct calculation for a number of special cases of interest. It should be noted that while pure multipole radiation has been assumed, the results are independent of the electric or magnetic character of the multipole.

A more complete general proof is being sought, and extensions to include particle emission are being developed.

Collecting Efficiency in Neutron Decay Studies (L. C. Biedenharn, Jr.). The chief source of error in the measurement of the neutron half-life by Snell *et al.*[4] is the determination of the efficiency of collection of the decay protons. The possibility of a better determination of the efficiency from the geometry of the system is being investigated. It was necessary to study the β-proton directional correlation as a preliminary step in this determination, and only this phase of the work has been completed.

For an allowed transition, which is presumably the case, the electron-neutrino correlation is well known to have the form, for pure invariants,

$$1 + n\beta \cos \theta_{e,\nu} \tag{3}$$

where $n = -1(S,P)$; $+1(V)$; $1/3\ (T)$; $-1/3\ (A)$; and $\beta = v/c$ (electron). Momentum and energy-conservation considerations permit the conversion of this expression into an expression involving the angle ϕ between the electron and proton. It is assumed that the proton takes up negligible energy, an assumption that has already been made in obtaining Eq. (3). (A calculation of the expected electron-proton correlation on a more rigorous basis was performed during the course of this work by E. Greuling and led to the conclusion that the above procedure is satisfactory.)

The electron-proton angular correlation is then found to be

(4) Snell, A. H., Pleasonton, F., and McCord, R. V., "Radioactive Decay of the Neutron," *Phys. Rev.* 78, 310 (1950).

$$g(\phi,E) = \left\{ 1+n\cdot\beta\cdot\left[\pm\cos\phi\left|1-\frac{E(E+2)}{(E_0-E)^2}\sin^2\phi\right|^{1/2} - \frac{\sqrt{E(E+2)}}{(E_0-E)}\sin^2\phi\right]\right\}$$

$$\cdot\left|2\frac{\sqrt{E(E+2)}}{(E_0-E)}\cos\phi \pm \frac{1+\frac{E(E+2)}{(E_0-E)^2}\cos 2\phi}{\left|1-\frac{E(E+2)}{(E_0-E)^2}\sin^2\phi\right|^{1/2}}\right|$$

where E is the kinetic energy of the electron and E_0 is the maximum kinetic energy. The signs are correlated and are to be taken

$$- \text{ for } E < \frac{E_0^{\,2}}{2(E_0+1)}$$

$$+ \text{ for } E = \frac{E_0^{\,2}}{2(E_0+1)} \Longrightarrow \pi/2 \leq \phi \leq \pi$$

$$+ \text{ and } - \text{ for } E > \frac{E_0^{\,2}}{2(E_0+1)} \Longrightarrow \cos^{-1}\left[-\left|1-\frac{(E_0-E)^2}{E(E+2)}\right|^{1/2}\right] \leq \phi \leq \pi$$

It will be seen that this expression is double-valued for $E > E_0^{\,2}/2(E_0+1)$. This is not surprising and is readily interpretable in terms of momentum conservation.

Before embarking on calculations with this correlation function it is useful to examine it in some elementary cases. Consider the relative number of protons, $G(\phi)$, emitted at an angle ϕ with respect to the electron direction. This function is equal to

$$G(\phi) = N^{-1}\int_0^{E_0} dE\ (E_0-E)^2(E_0+1)\sqrt{E(E+2)}\ g(\phi,E)$$

where N is a normalizing factor. $G(\phi)$ can be obtained as a sum of elliptic integrals and elementary functions, but, for a first orientation, we place $p_e = E$ and obtain an approximate $G(\phi)$

Table IX shows $G(\phi)$ at several points, the effect of the assumed type interaction (n), and a comparison with the exact (numerically evaluated) $G(\phi)$ for $n = 0$.

TABLE IX

ϕ	$G(\phi)$ (approximate)	$G(\phi)$ (exact, with $n = 0$)
0	$0.010 - n(0.010)$	0.006
$\pi/4$	$0.016 - n(0.011)$	0.008
$\pi/2$	$0.0303 - n(0.015)$	0.021
$3\pi/4$	$0.139 - n(0.0009)$	0.132
π	$1.10 + n(0.49)$	1.66

It will be noted that (1) there is a rather strong back-to-back correlation of the electron and proton, and (2) the effect of the type interaction appears not too important in the region where the distribution is at a maximum ($\sim 3\pi/4$, since the solid angle vanishes at π). It is to be expected that the effect of n in the exact $G(\phi)$ is comparable to its effect on the approximate $G(\phi)$.

By integrating the approximate $G(\phi)$ we find the approximate fraction of the particles emitted that have ϕ between two given angles. Table X lists some values of $F(\phi)$, where $F(\phi)$ is the fraction of protons emitted making an angle ϕ or less with respect to the electron.

TABLE X

ϕ	$F(\phi)$ (approximate)
0	0
$\pi/2$	$0.109 - n(0.0781)$
$3\pi/4$	$0.395 - n(0.138)$
π	1.000

The angle (with respect to the back-to-back direction) such that half the protons emitted lie within a cone of this half-angle is found to be approximately $30° + n(10°)$.

The laborious application of this distribution in angle to the proton trajectories has yet to be done. In view of the strong back-to-back correlation of the electron and proton (which increases for higher electron energies) it might be supposed that an experimental elimination of the efficiency might result from placing the proton and electron counters back-to-back, selecting only high-energy electrons, and extrapolating to unit efficiency. This scheme is quite impractical in view of the great difficulties already experienced with obtaining sufficient intensity.

PHYSICS OF SOLIDS

PHASE TRANSITION ON NEUTRON BOMBARDMENT

M. A. Bredig

In the theory of the effects of fast neutron bombardment in solids the assumption of thermal spikes, *i.e.*, conversion of neutron energy into lattice vibrations, plays a major role. On the other hand, the effects observed have also been compared with those produced in solids by cold-working. The experiment described below was the first in a series designed to study these effects by observing solid-phase transformations.

Lead oxide, PbO, is one of the many substances which occur in various crystal modifications and undergo a structural transformation on heating. Like a few of these, it also exhibits the interesting behavior of transforming on cold-working (grinding) from a metastable structure into a stable one. Its orthorhombic yellow form is stable above 587°C but is metastably preserved on slow cooling even below that temperature. On plastic deformation, such as in grinding, the yellow crystals are converted into tetragonal red ones. The mechanism of this process is thought by the writer to be similar to that of production of twinning in crystals by mechanical deformation and dissimilar to the "catalytic" or nucleating effect produced by cold-working, as, for example, in the transformation of white into gray tin.

The results of exposing the yellow form, and, in another instance, the red modification, to fast neutron bombardment might show whether thermal spikes occur sufficiently to raise the temperature locally, *i.e.*, in volume elements of the order of 10^{-18} cm^3 or less, to above 600°C, or whether the atoms are "pushed" into more stable positions in a manner similar to the transformation resulting from cold-working. Other processes such as chemical decomposition or production of an amorphous phase are also possible.

One sample consisting of approximately 1 g of the yellow form and another sample representing the red form were exposed for one week in a torpedo hole of the X-10 graphite reactor. X-ray-diffraction patterns made before and after irradiation did not reveal any changes in phase composition. Preparations are being made to repeat the experiment in the Chalk River pile or in the MTR mock-up. It is expected that this new experiment will furnish more significant results.

X-RAY DIFFRACTION AND CRYSTAL STRUCTURE

M. A. Bredig B. S. Borie, Jr.*
R. M. Steele F. A. Sherrill

Remote Control X-ray-diffraction Spectrometer for High-level Radioactive Specimens (M. A. Bredig, B. S. Borie, Jr.*). A General Electric X-ray spectrometer, which will be modified for use in one of the concrete-shielded cells of the new hot laboratory, has been ordered from the manufacturer. The special engineering design group is engaged in the detailed design of alterrations of this instrument for use with a bent-crystal monochromator and with remote control, in accordance with the plans described in the preceding quarterly report (ORNL-782, p. 89).

Determination of the Crystal Structure of the Tutton Salts (B. S. Borie, Jr.,* M. A. Bredig). The crystal structure of cobalt ammonium sulfate hexahydrate and its many isomorphs has been investigated by Hofmann.[1] He found that the monoclinic unit cell contains two molecules and that the space group is $P2_1/c$. A set of positions for the atoms was proposed such that cobalt ions or analogous metal ions are at 000, ½½0, and the rest of the atoms occupy sets of fourfold general positions. However, as has been pointed out by Wyckoff,[2] Hofmann's parameters could hardly be correct since they require oxygen atoms in adjacent sulfate groups to be as close together as 2.10 Å.

This group of salts has interesting magnetic properties which depend on the crystal structure. These properties have been under investigation for some time by the low-temperature physics group, and it was felt that the structures should be re-examined.

A rotation photograph and a zero-layer Weissenberg photograph for rotation about the *c* axis were made using copper radiation filtered through nickel foil. Intensities were estimated visually from the Weissenberg photograph and reduced to structure factors. Some differences between the values observed and those predicted by Hofmann's structure were found.

A Fourier synthesis of the electron density as projected onto the *xy* face of the unit cell is now being prepared. The experimentally observed magnitudes

---

* Metallurgy Division.

(1) Hofmann, W., "Die Struktur der Tuttonschen Salze," *Z. Krist.* 78, 279 (1931).

(2) Wyckoff, R. W. G., *Crystal Structure*, supplement to second edition, p. 92, Interscience Publishers, Inc., New York.

of the structure factors and the structure-factor signs predicted by Hofmann's structure (most of which are probably right) were used. It is hoped that the electron density map will yield enough information about the true atomic positions for correction of errors in the structure-factor signs and obtaining of accurate atomic coordinates. If this turns out to be the case, the procedure will be repeated for rotation about another crystallographic axis, which should provide enough information for determining a complete set of parameters.

Line-broadening in Electron-bombarded Copper-Beryllium Alloy (M. A. Bredig and B. S. Borie, Jr.*). G. E. Evans and V. L. DiRito submitted a 10-mil foil of α-quenched Cu-Be which had been irradiated in the 2-Mev Van de Graaff accelerator with 1.3 Mev electrons. Their experiment is described elsewhere in this report (p. 87).

Line-broadening was measured on the etched and unetched surface of the specimen with the new Norelco high-angle X-ray-diffraction spectrometer, using filtered copper $K\alpha$ radiation, and the 331 reflection of the cubic face-centered lattice at $2\theta = 140°$, where the $K\alpha$ doublet was fully resolved. The increase in the half-width of the reflections amounted to approximately 35%. An apparent large and as yet unexplained simultaneous drop in the integrated intensity of the reflections on irradiation may be connected with preferred orientation or with recrystallization texture, but it requires further consideration. Precipitated body-centered cubic-phase Cu-Be was not observed, nor were any lines of oxidation products (BeO, CuO, or the like) detected in the unetched specimen.

Search for Hypothetical Cubic Modification of Beryllium Oxide (M. A. Bredig). It has been pointed out previously (ORNL-37 and 176) that there is a possibility that beryllium oxide, BeO, would be found to occur under suitable conditions in a second, face-centered cubic modification, similar to ZnS. In accordance with the conclusions derived by V. M. Goldschmidt from observations on ZnS, CdS, and CdSe, such a cubic form would be expected to be stable at lower temperatures than the hexagonal structure, the only one known at present in BeO. While more commonly the higher symmetrical structure is the high-temperature form, there are numerous exceptions.

In the case of the polymorphism of the cubic zincblende—hexagonal-wurtzite type, it is suggested here that it is the decrease with rising temperature in

* Metallurgy Division

the screening, by the tetrahedrally arranged ions of opposite charge, of the field of the central ion which leads to the attraction, at elevated temperatures, of a fifth ion (the increase in coordination number at elevated temperatures has been discussed by Bredig[3]) in something like a "sphere of coordination" slightly less than second and to a slight repulsion of three of the ions in the first sphere of coordination. The distance of this fifth ion in BeO, for example, is 2.73 Å as compared with 3.15 Å for the other nine ions of the second sphere of coordination (and with 1.66 Å and 1.64 Å for three ions and one, respectively, in the first sphere of coordination). The repulsion of three of the nearest neighbors leads, then, in BeO to an increase in their distance from the central ion by approximately 1%.

In ZnS it is possible to transform the hexagonal, high-temperature form, when metastably preserved by cooling, into the cubic, low-temperature form by plastic deformation, *e.g.*, by grinding in a mortar. The plastic properties of crystals are a function of temperature. Conversion into a more stable form by plastic deformation is possible if the critical shear stresses that result in such a transformation are, at a given temperature, lower than the critical stresses resulting in rupture. Critical stresses for rupture, slippage, and twinning have been considered as functions of temperature (see, for example, C. S. Barrett[4]) while similar considerations for transformation have not been noticed in the literature by the writer. With respect to the problem of the existence of a cubic form of BeO there appeared to be a slight possibility, though not much probability, that the relationship of critical stresses for rupture, slippage, twinning, and transformation (if any was possible thermodynamically) might change favorably with temperature. Grinding at room temperature and at a temperature near that of liquid air has not produced a cubic structure in BeO. Grinding at elevated temperature is still to be tested, since it is imaginable that a transition temperature exists in the wide range up to the melting point (2200°C) but it must be sufficiently low to explain sluggishness and absence of an actual inversion (hexagonal $\longrightarrow$ cubic) on mere annealing.

Two experiments have been carried out, one at 500°C, the other at 900°C. BeO was heated in a small mullite mortar mounted inside a vertical tube

---

(3) Bredig, M. A., "High Temperature Crystal Chemistry, etc.," *J. Phys. Chem.* 49, 537 (1945).

(4) Barrett, C. S. *Structure of Metals*, Fig. 34, *p.* 324, McGraw-Hill Book Company, Inc., New York, 1943.

furnace. By means of a pestle, to which a 2-ft long stainless steel tube was attached as a handle, the beryllium oxide was ground for several minutes, a time long enough to produce noticeable amounts of transformation in other substances such as PbO, ZnS, or CaC_2. X-ray-diffraction examination of the powder did not reveal any trace of a cubic phase. This negative result may be due to the failure of BeO to assume cubic structure at any temperature or to the unfavorable relationship of the critical shear stress for transformation to that of the other processes at the temperatures at which tests have been made thus far. This latter seems highly probable. In fact, it may be noted that the substances in which transformation, from a metastable to a stable structure, can be achieved by plastic deformation are the exceptions rather than the rule (ZnS, PbO, AgI, CaC_2). They have in common the presence of highly polarizable ions, *i.e.*, $S^{=}$, I^{-}, $C_2^{=}$, Pb^{++}; and polarizing ions, *i.e.*, Zn^{++}, Ag^{+}, Ca^{++}, and $O^{=}$. While Be^{++} is a highly polarizing cation, $O^{=}$ possesses only a medium degree of polarizability. It may be just below the limit necessary to produce the appropriate relationship of critical shear stresses.

It is believed that under these circumstances even the negative result of the two simple experiments performed is of some significance.

High-temperature Crystal Structure of Uranium Dicarbide (M. A. Bredig). The carbides (MeC_2) of calcium, strontium, and barium exhibit enantiotropic transitions, from tetragonal symmetry at low temperatures to cubic symmetry at high temperatures, at 450, 370, and below 200°C, respectively.(5) The lattice dimensions increase regularly with the atomic number as the transition temperatures decrease, as shown in Table XI.

TABLE XI

CARBIDE	LATTICE CONSTANTS		TRANSITION TEMPERATURE (°C)
	a_0	c_0	
UC_2	4.97	5.95	?
CaC_2	5.48	6.37	450
SrC_2	5.81	6.68	370
BaC_2	6.22	7.03	200

(5) Bredig, M. A., "The Polymorphism of Calcium Carbide," *J. Phys. Chem.* 46, 801 (1942).

On the other hand, the lattice constants of UC_2 are almost 10% smaller than those of CaC_2. This is the more remarkable, since the lattice constant of cubic, NaCl type UO (4.92 Å) is considerably larger than that of CaO (4.78 Å). In the sulfides of similar structure the relationship is intermediate, *i.e.*, 5.67 Å for CaS and 5.47 Å for US, but there is already a considerable decrease in the uranium compound. This is an indication of the very different nature of the binding forces active in the uranium compounds.

If the forces between the $C_2^{=}$ anion and a U^{++} cation were similar to those between the alkaline earth metal cations and the $C_2^{=}$ ion, a transition from tetragonal to cubic symmetry might be expected to occur in UC_2 below 700°C. Metallographic examination of ThC_2 (Wilhelm[6]) has indicated that there may be a transition to a different phase in this compound at some high temperature. X-ray-diffraction patterns at elevated temperatures might be obtained to prove the occurrence of a transition into a cubic form in UC_2 and ThC_2. The rare earth metal dicarbides are also tetragonal at room temperatures and are expected to change into a cubic modification at higher temperatures. In all these cases oxidation and reaction with adsorbed water or with the walls of a quartz capillary would produce an oxide film which would be difficultly penetrable by X rays of energies suitable for diffraction measurements. The use of neutron diffraction appears as the logical way to overcome this difficulty.

A platinum-wire resistance furnace was built which permitted heating a powdered specimen inside a quartz tube of 3/8 in. diameter to approximately 1300°C while a neutron beam was being diffracted.* In a preliminary test run the diffraction peaks corresponding to the 002, 111, and 200 planes of the tetragonal lattice of UC_2 appeared unchanged at 920 and 1250°C.

It appears, then, that the forces active between uranium and $C_2^{=}$ ions are indeed different from, *i.e.*, stronger than, those between the noble-gas-type Ca^{++} cation and the $C_2^{=}$ ions, leading to a higher temperature of conversion (if any occurs). After another furnace for higher temperature has been built, the experiments will be extended to higher temperatures and to various

(6) Wilhelm, H. A., of Ames, Iowa, at AEC Metallurgy Conference at Pittsburgh, January, 1949.

* The neutron spectrometer of H. A. Levy and S. W. Peterson employing a neutron wavelength of 1.15 Å was used. Their help, as well as C. G. Shull's valuable advice, is gratefully acknowledged.

rare earth metal dicarbides. These studies are expected to shed some light on the role in the interionic binding with the $C_2^{=}$ ions of the one, two, and four extra valence electrons, as in lanthanum, cerium, and uranium dicarbide, respectively, which is also reflected in the metallic (electronic) conductivity of these compounds.

Growing of Single Crystals (F. A. Sherrill). Single crystals of copper grown in the furnace described previously were found by H. A. Levy and S. W. Peterson to be of great value in neutron diffraction. Intensities were found increased by a factor of 5, probably because of a favorable mosaic structure of the crystal used. For use with a neutron energy of maximum intensity in the epithermal range, reflection at the 111 plane is favored, and a Pfankuchen angle of 7° for "focusing," is recommended. It appears that crystals having the desired orientation within 5° are more readily obtained by keeping the crucible stationary and lowering the temperature of the furnace than vice versa. By slicing in half a crystal whose cross section tapers down from 15/16 in. to 3/4 in. over a length of 4 in. and mounting the two halves together, a large crystal surface can be obtained for monochromatizing and focusing a primary neutron beam of large cross section. Lead crystals of similar size and orientation have also been grown in graphite crucibles. Crystals of an iron-silicon alloy (5% Si) were grown in a stabilized zirconia crucible to a considerably smaller size, but they are large enough to be usable. One large single crystal of nickel has also been obtained, but difficulties were encountered in several cases with "boiling," or, rather, gas evolution, from the melt.

Miscellaneous X-ray-diffraction Work. (R. M. Steele). About 225 samples were submitted for X-ray analysis; 95% have been identified.

The Metallurgy Division submitted numerous samples in connection with liquid metals corrosion and uranium alloy research. A few samples (standard mixtures) were submitted to determine what percentage of Fe_3C could be detected in the presence of α Fe.

The Chemistry Division submitted problems involving crystallite size observations. Also, X-ray patterns of niobium and tantalum oxides and phosphates were determined for the Chemistry Division. Miscellaneous samples originated from the homogeneous reactor research; others, such as ND_4DF_2, ND_4B_2, and LiOD originated from the neutron-diffraction work.

A number of samples from the Physics Division included α Cr, Cr_2O_3, Ni_3Mn, and PbO in connection with neutron diffraction and radiation damage research.

HEAVY POSITIVE ION BOMBARDMENT STUDIES

G. E. Evans and J. W. Schwartz

Work on the preliminary design, construction, and bench-testing of a positive ion source for the Cockcroft-Walton and Van de Graaff generators is essentially complete. The present source has produced a total positive ion current of 0.8 ma, using solid sodium chloride as a source of sodium ions.

The various components of the ion source are shown schematically in Fig. 19. The outer casing is of pyrex, employing commercially available 5-in. flanges grooved for "O" ring seals. The sodium chloride charge is placed within the stainless steel furnace, and the NaCl vapor produced escapes through a 4-mm hole in the bottom of the furnace. The furnace is maintained at a potential of about 2000 volts positive with respect to the filament and is heated by electron bombardment. The electron beam also serves to ionize the NaCl gas in the region between the filament and furnace. At present, ordinary 100-watt G.E. light-bulb filaments are being used, which easily supply sufficient emission to heat the furnace. (Electron emission currents above 200 ma can be obtained for rapid heating, while 50 ma is adequate to maintain the furnace temperature in the operating range.) A hollow nickel cylinder, 1 cm in diameter, directly beneath the filament serves as an electrostatic lens, and its potential is maintained at the mean potential of the a-c filament voltage. The positive ion beam is further focused by an aperture lens of stainless steel maintained about 4000 volts negative with respect to the cylinder lens. About 10 cm below the 4-mm aperture of the bottom lens, a 3-cm copper disk collects the positive ion current.

To study the focusing characteristics of the lens system, the standard electrolytic tank technique was employed. Large-scale models of the furnace and lens elements were suspended in a tank of water. The lenses were raised to chosen potentials by means of a voltage divider and a small audio-frequency oscillator constructed for the purpose. The potentials of various points on the water surface were measured by balancing against a known audio-frequency

FIG. 19
HEAVY POSITIVE ION SOURCE

UNCLASSIFIED
DWG. 10003

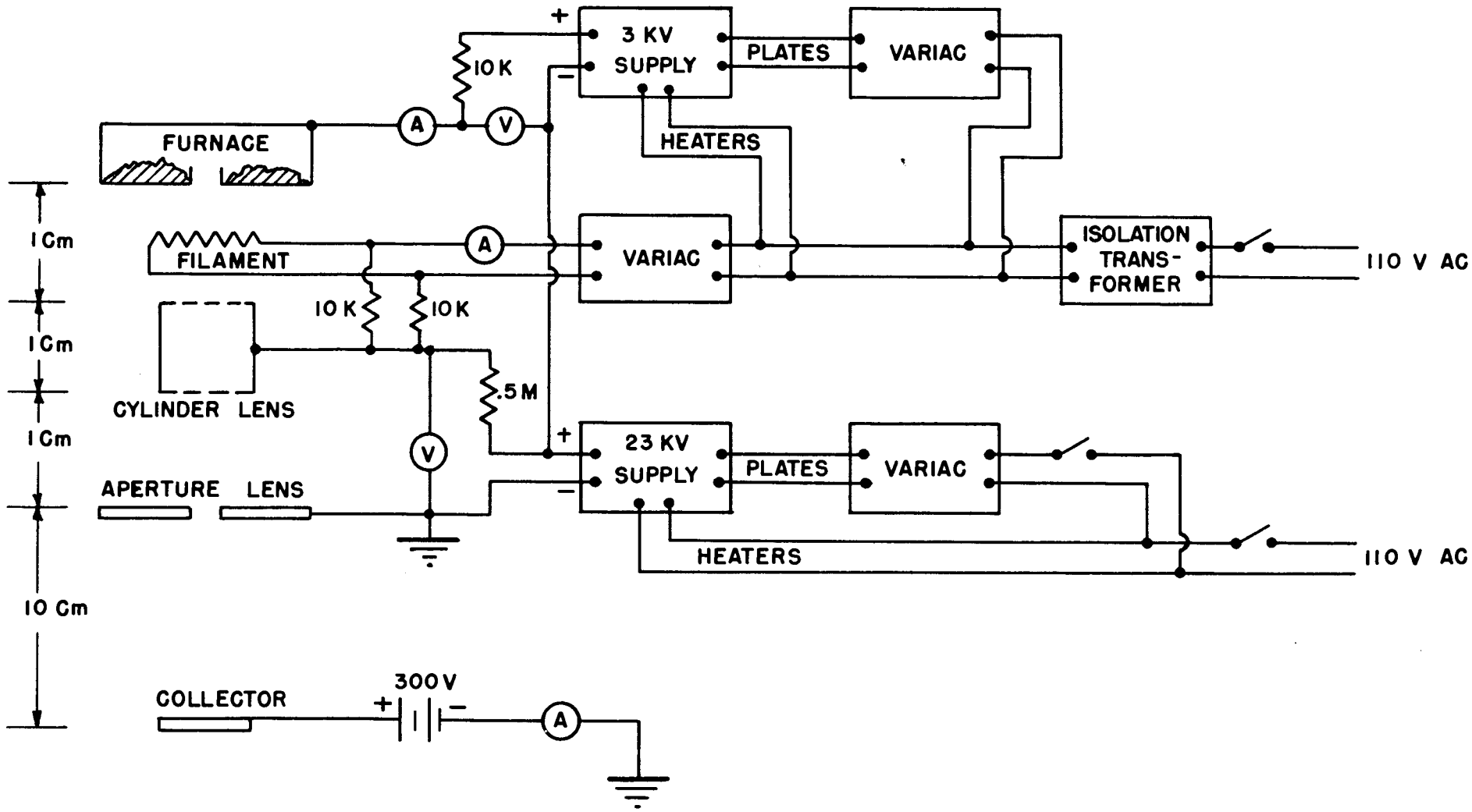

voltage, using an oscilloscope as a null detector. The equipotential curves thus determined were transferred to large sheets of paper, using an aluminum alloy pantograph and a magnetically operated marking pen. It was determined that for a suitable geometry for the lenses, focusing could be obtained with the bottom aperture lens at 0 volts, the cylinder lens at 8000 volts, and the furnace at 10,000 volts. A power supply was then constructed giving variable voltages of this order of magnitude.

A schematic diagram of the power supply is also shown in Fig. 19. The power supply allowed the cylinder lens to operate at a maximum of 23 kv above ground, but arcing in the ion source reduced the maximum usable voltage to less than 8 kv. The filament a-c voltage is tied to the cylinder lens by two 10,000-ohm resistors. The input voltage for the filament variac and the 3-kv power supply is obtained from a 110-volt isolation transformer. The 3-kv power supply is designed to supply 1 kw at 3000 volts, but in use a maximum of 200 watts at 2000 volts has been found adequate. The entire power supply is mounted in a grounded cabinet to eliminate shock danger from the chassis of the 3-kw supply which floats at high voltage above ground.

A vacuum supply has been built using a VMF-20 diffusion pump and a Duo-seal fore pump. Aided by a liquid-air trap, this is capable of maintaining a vacuum of 2×10^{-5} mm Hg under normal operating conditions. The maximum pressure at which the ion source will operate satisfactorily is about 4×10^{-5}.

The maximum ion current which has been obtained is 820 μa. The source has been operated at an ion current of 100 μa over a period of several hours without adjustment of voltages and shows negligible variation in the ion current. Raising the potential of the collector electrode to +300 volts produces less than 4 μa drop in ion current, showing that neither secondary electron emission nor collection of low-energy positive ions contributes significantly to the measured ion current.

The source is now being redesigned to permit more rapid alignment of components and to suppress sparking. The new design will incorporate a much lighter weight furnace to permit rapid heating. The operating characteristics of the present source indicate that the positive ion current is limited primarily by the amount of ionization of the NaCl vapor. Attempts are being made to focus the electron beam at the aperture of the furnace, so as to produce a much greater concentration of positive ions within the volume contributing to the beam.

ELECTRON BOMBARDMENT OF Be-Cu

G. E. Evans and V. L. DiRito

Some 10-mil Be-Cu foil containing about 2.15% Be was obtained from Dr. D. S. Billington. This foil was cut into circles about 2-1/8 in. in diameter to be used as test samples, while the scrap piece connected at the bottom was used as a reference sample. The samples were cleaned of all oxide coatings and degreased. Two samples have been bombarded with electrons in the Van de Graaff apparatus at 1.3 Mev and 1.33 Mev, respectively, using the technique described in ORNL 694, *p.* 69.

After bombardment, the test samples were cut into strips about 1/16 in. by 1-3/4 in. by 10 mils. The ends were polished, and accurate size measurements were made, using a measuring microscope.

Resistivity measurements were then made using a standard resistivity circuit. The greatest portion of time was spent in the design and construction of a resistivity circuit which would reproduce readings in the 0.01-ohm range with an error less than 0.5%. Insufficient data have been taken at present to allow definite conclusions to be drawn.

SEMICONDUCTOR BOMBARDMENT RESEARCH

J. W. Cleland J. H. Crawford, Jr.
K. Lark-Horovitz* J. C. Pigg
F. W. Young

Experiments on Cuprous Oxide.

(1) *Bombardment on Cu_2O Plates.* The experiments on the effect of pile radiation on the electrical properties of Cu_2O have been extended. As previously reported[7] Cu_2O plates bombarded in a high fast flux region of the X-10 pile show a conductance behavior similar in many respects to that exhibited by Ge. Experiments have been carried out to investigate this behavior in greater detail.

* Consultant from Purdue University.

(7) Cleland, J. W., Lark-Horovitz, K., Crawford, J. H., Jr. and Pigg, J. C., "Semiconductor Bombardment Research," *Physics Division Quarterly Progress Report for Period Ending June 15, 1950*, ORNL 782, 71 (Oct. 4, 1950).

Two low-resistivity (~ 500 ohm-cm) polycrystalline Cu_2O plates were prepared from plates of very high resistance (~ 10^5 ohm-cm) obtained from S. J. Angello by annealing in air for 24 hr at ~ 950°C and quenching in air to room temperature. These were bombarded in a water-cooled experimental hole in a high fast flux region. The conductance was followed carefully during the first 24 hr of bombardment, readings being taken at 15-min intervals. During this period the conductance decreased more than two orders of magnitude. A linear plot of conductance vs. bombardment time at constant pile power for one sample is shown in Fig. 20 for the first 1½ hr of bombardment. Owing to the initial temperature increase, the initial portion of the curve is not very suitable for analysis because of the very large temperature coefficient of conductivity of Cu_2O. However, using estimated temperature corrections from conductivity measurements before bombardment, the curve was corrected approximately to constant temperature and the initial portion from 0 to 20 min was essentially linear. The curve appears to be hyperbolic in form. A more detailed analysis is now underway.

One of these samples was followed until the conductance minimum was passed. The same behavior was observed as that previously reported (ORNL-782, *p.* 71).

In addition, during these experiments conductance behavior was carefully observed during pile shutdowns to ascertain the degree of annealing of the radiation damage. The conductance invariably dropped during these shutdowns because of the drop in temperature and possibly because of the decrease in intensity of the γ radiation field. However, on pile startup the conductance returned to the value before the shutdown, and there was no detectable evidence of annealing under these conditions.

Another experiment has been carried out in an unsuccessful attempt to determine whether there is a transition from P-type to N-type conduction associated with the conductance minimum. The sign of the Seebeck coefficient of the thermoelectric power is the same as the sign of the current carrier. An apparatus was constructed with which a known temperature gradient could be produced across a Cu_2O plate in the pile, thus allowing in-pile thermoelectric measurements to be made. However, owing to large residual emf's across the sample without the temperature gradient, such measurements were impossible. These interfering residual fields are at the present thought to be caused mainly by poor contact to the sample and to improper shielding of the sample leads. Refinements of technique and apparatus should eliminate these difficulties.

UNCLASSIFIED
DWG. 10004

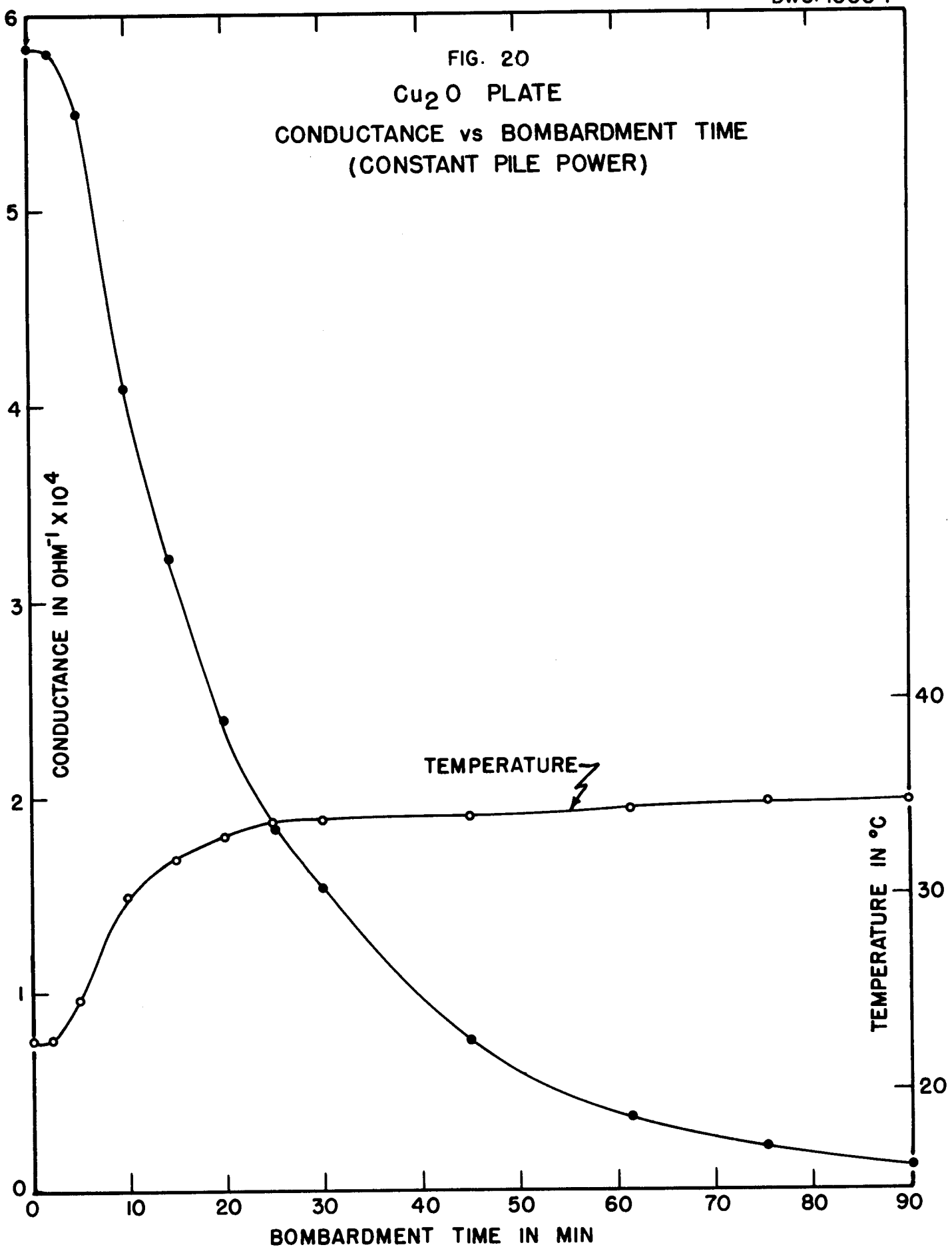

(2) *Cu_2O Single Crystals.* In the last quarterly report (ORNL-782, *p.* 74) mention was made of attempts to prepare single crystals of Cu_2O of a size suitable for bombardment work. The method used was that of Englehard.[8] A single copper crystal was suspended in air in a furnace at temperatures between 950 and 1000°C. The temperature was oscillated between the limits with a period of about 2 hr. The total heating periods for various samples ran from 24 to 48 hr. In every case polycrystalline oxide layers were obtained with grain size of about 1 mm^3. This work will be extended at a later date using thinner copper crystals and carrying out the oxidation at a lower temperature and at lower oxygen pressures.

(3) *Cu_2O Rectifiers.* Another indication of carrier type is the direction of rectification. The direction of easy carrier flow is from semiconductor to the metal. Thus, if a change in type occurs, one would expect either a change in direction of rectification or, if the barrier is not suitable for N-type rectification, ohmic behavior.

The results of bombardment studies on several commercial rectifier units have been reported previously. These units showed no reversal of rectification direction and no exact ohmic character even after 12 days of bombardment. Since nothing was known concerning the method of preparation and the characteristics of the oxide film used in these rectifiers, this work has been extended using rectifier disks prepared by S. J. Angello at Westinghouse under similar conditions to those used in the preparation of the above-mentioned Cu_2O plates.

One of these units was followed until lead insulation broke down. Complete current voltage characteristics were taken periodically during the exposure. A plot of the current at 1 volt and at 0.1 volt in the forward and back directions as a function of bombardment time is shown in Fig. 21. It is interesting to note that after six days of bombardment the unit becomes almost ohmic at 1 volt while at 0.1 volt there is some evidence of a reversal of the direction of rectification.

At the present time a second unit is being exposed. By using a more refined setup, it is hoped that the unit can be followed for a longer period of time before the insulation breaks down.

---

(8) Engelhard, E., "Elektrisches und optisches Verhalten von Halbleitern 9," *Ann. Physik* 17, 501 (1933).

UNCLASSIFIED
DWG. 10005

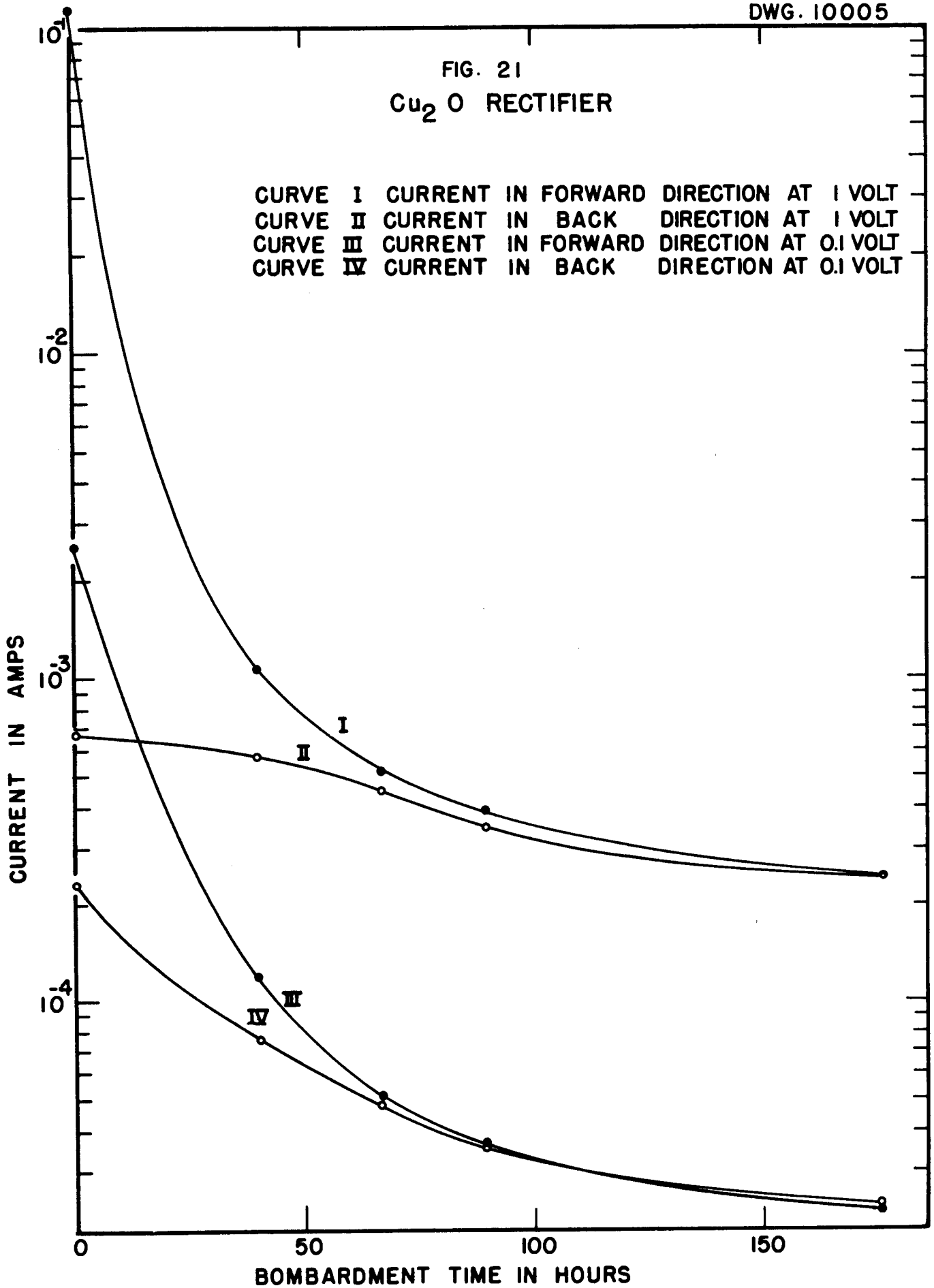

Experiments on Germanium.

(1) *Impurities Introduced by Thermal Neutron Capture.* A preliminary report on this experiment was made in the last quarterly report (ORNL-782, *p.* 75). Thermal neutron capture by Ge isotopes produces predominantly As and Ga end products; As is an N-type impurity, and Ga a P-type impurity. It has been shown[9] that an excess of Ga over the amount of As is produced, which contributes to the P-type character of the material. This transformation from N-type to P-type Ge has been followed in a stepwise fashion in the following manner: A high-resistivity N-type Ge sample was bombarded for short periods of time in the pneumatic tube. When activity had decayed sufficiently, the sample was annealed in a vacuum (10^{-5} mm Hg) for 24 hr at 450°C to remove any effects due to fast neutron damage. After this treatment the Hall constant and resistivity were measured as a function of temperature. The region around the transition point, the quasi-intrinsic point, was carefully studied; data concerning this region were reported in the last quarterly report (ORNL-782, *p.* 75). Subsequent bombardments have carried the material into the P-type range. The results after conversion are shown in Fig. 22.

This experiment is being carried out as a basis for a check on the theory. By means of such irradiations the effective impurity concentration can be varied at will in the direction toward P type. Consequently, the variation of the Fermi level as a function of effective impurity concentration can be determined experimentally and compared with the values calculated from the theory. A report on such an analysis will be made at a later date.

The variation of the concentration of current carriers as a function of irradiation time is shown in Fig. 23.

(2) *Rate of Annealing of Lattice Damage.* Preliminary experiments on the rate of annealing of lattice damage produced in Ge by fast neutrons are underway. One Ge sample was bombarded to the minimum conductivity at dry ice temperature and stored at this temperature to minimize annealing. After the activity of the sample and holder had decayed to a safe level, the conductivity was followed as a function of time at a constant temperature of 30.2 ± 0.1°C. An increase in conductivity with time was observed. Unfortunately, the experimental accuracy was not sufficient to allow determination of either

(9) Cleland, J. W., Lark-Horovitz, K., and Pigg, J. C., "Transmutation-produced Germanium Semiconductors," *Phys. Rev.* 78, 814 (1950).

UNCLASSIFIED
DWG. 10006

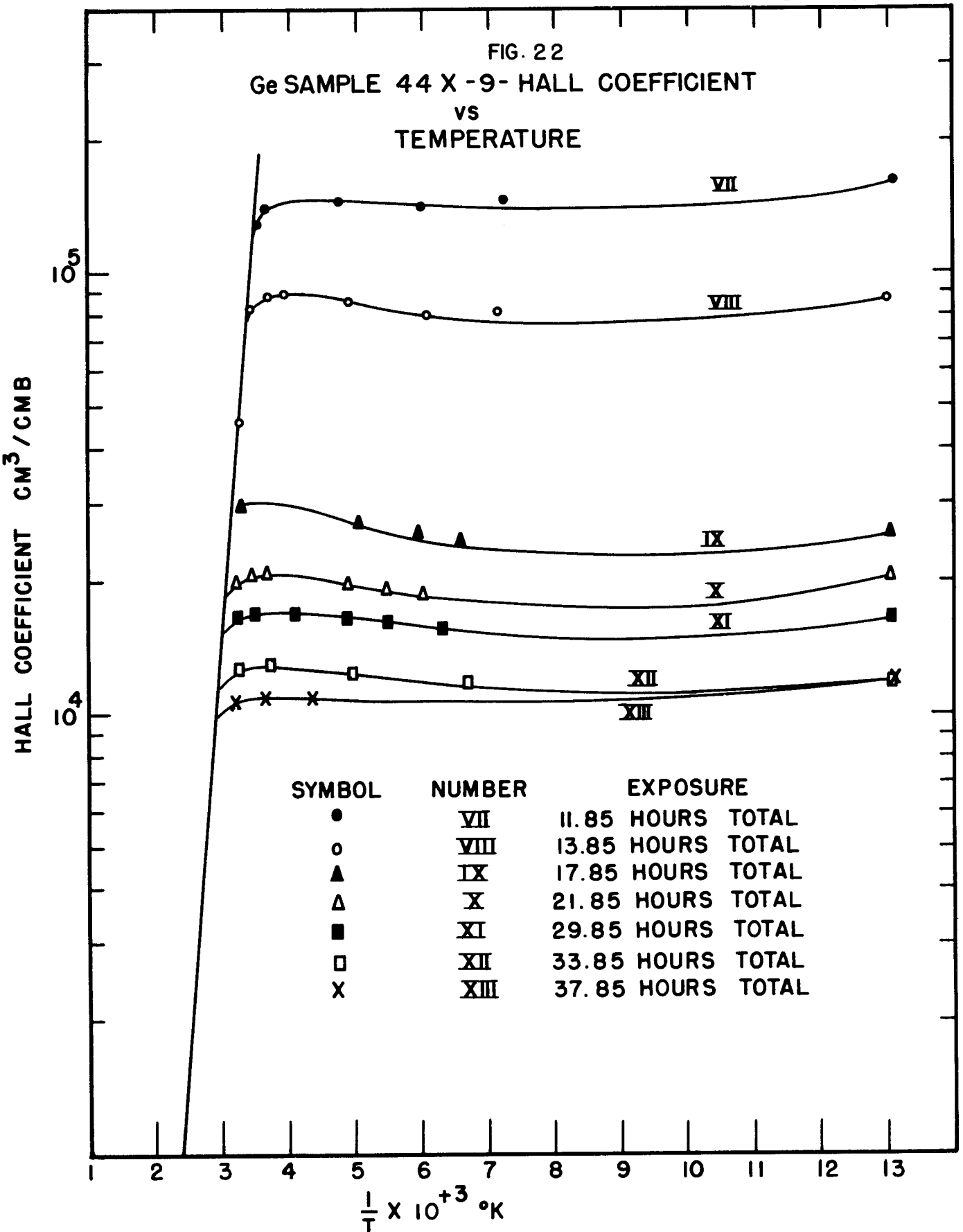

UNCLASSIFIED
DWG. 10007

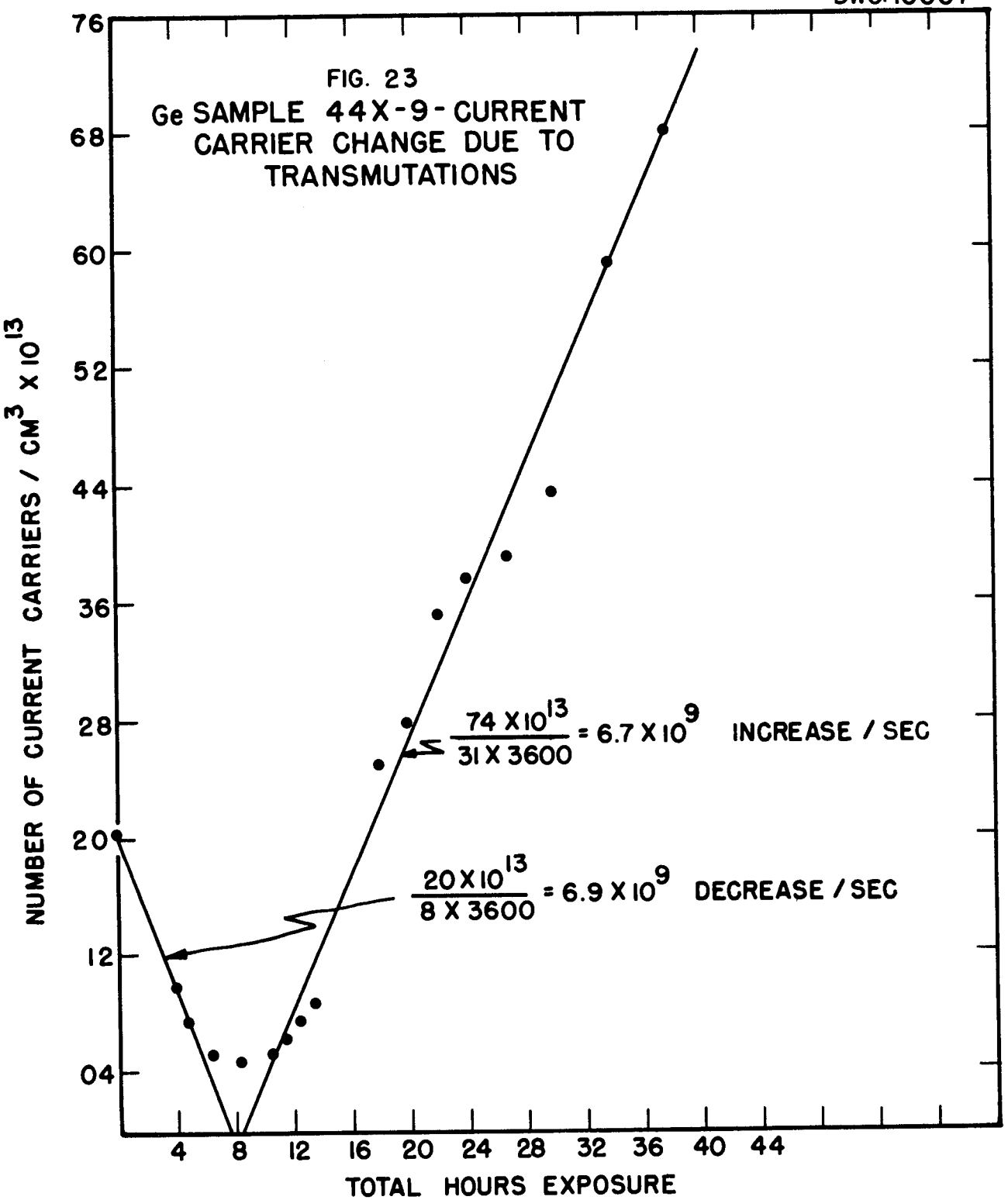

the order of the process or the rate constant. However, a plot of log σ vs. time indicates that probably a number of processes are taking place simultaneously, since there are at least two distinct kinks in the curve. The experiment was repeated at a higher temperature (~ 50°C), but no change in σ at that temperature could be determined. However, on cooling to room temperature a sizable change was evident. Examination of the log σ vs. $1/T$ curve made previously shows that above room temperature the conductivity lies on the intrinsic slope and is due to intrinsic electrons. Thus in this range the conductivity is insensitive to changes in available impurity concentration.

In view of this difficulty in measuring the rate of annealing in N-type material near the conductivity minimum, all further annealing studies will be carried out on high-resistivity P-type material which has been bombarded to produce P-type material well out of the intrinsic range.

PHYSICS OF SOLIDS NEW HOT LABORATORY

S. E. Dismuke and D. S. Billington*

The designs of cells 4, 5*a*, 5*b*, and 6 are essentially complete. Many features are similar to those found in the Argonne National Laboratory cells in which the Argonne Master Slave Manipulator is also used. The windows will be filled with zinc bromide solution.

Since the cell structure is to be very flexible, the cell walls will be made of high-density concrete blocks held together by a weak mortar. The doors will move on tracks. Cell 4 will have a movable roof.

By simply moving the doors back and forth and simultaneously changing the length of the walls separating the cells, the depth of the cells can be varied easily.

Figures 24 and 25 give details of these cells.

CRYOSTAT FOR PILE IRRADIATIONS

R. P. Metcalf

The design of the cryostat has been gone over with the Engineering Department in the light of experience with the two cryostats which have now

* Metallurgy Division.

UNCLASSIFIED
DWG. 10022

FIG. 24
PHYSICS OF SOLIDS CELL SECTION

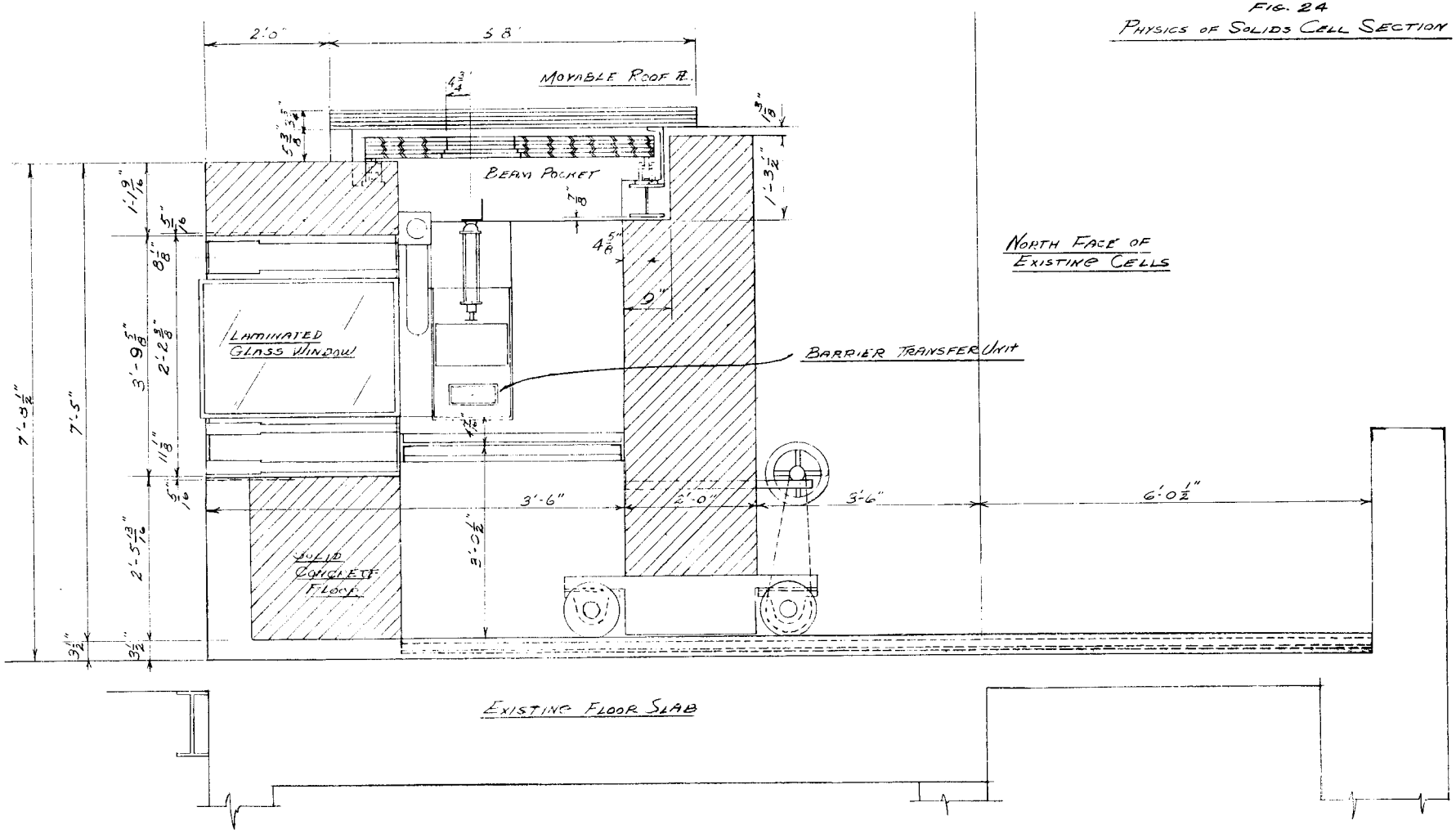

UNCLASSIFIED
Dwg. 10023

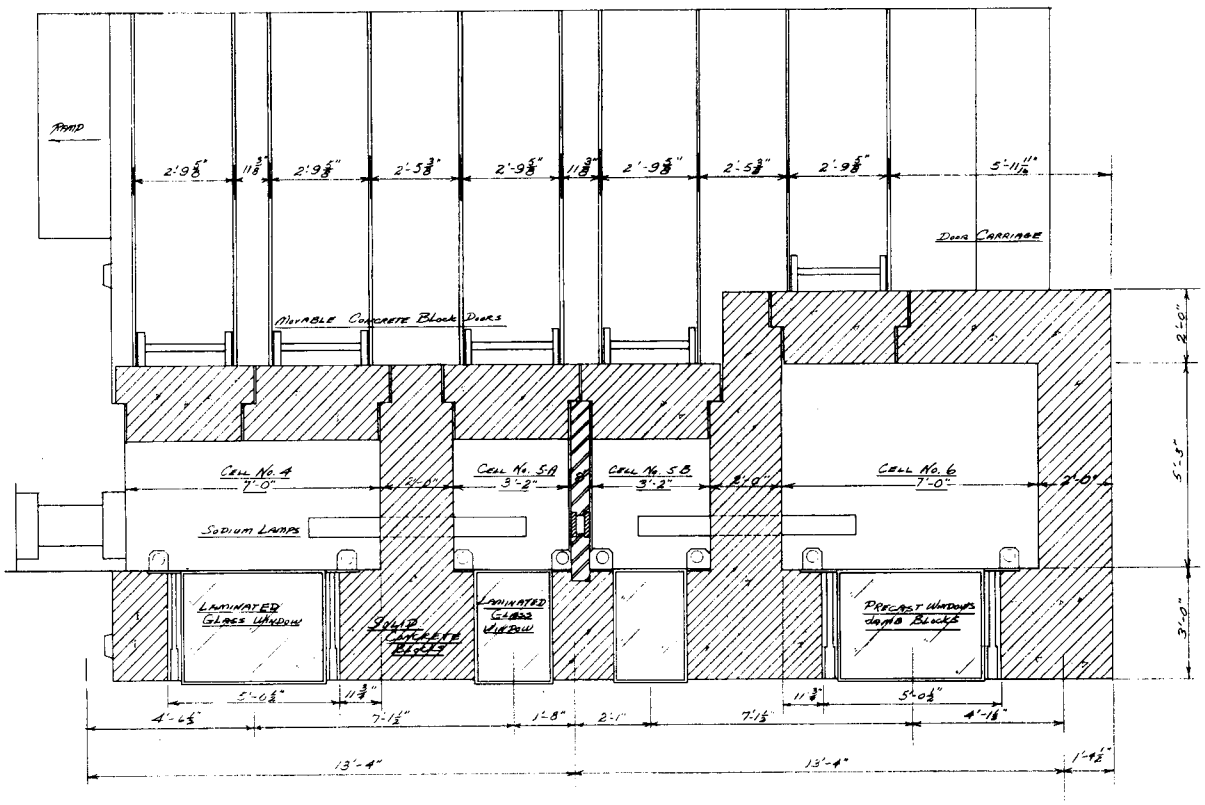

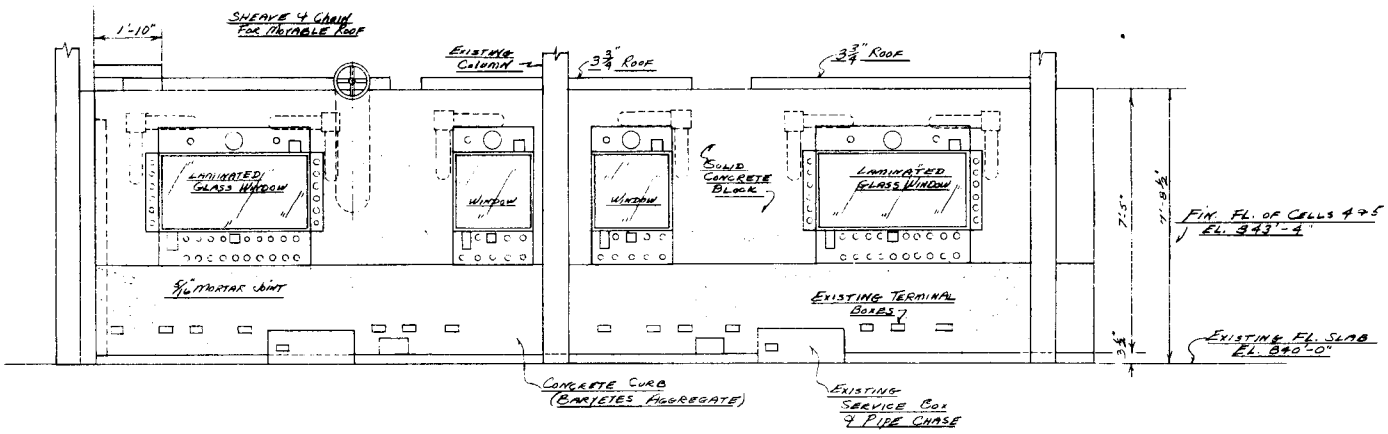

FIG 25
PHYSICS OF SOLIDS BUILDING, SECTION OF CELLS 4 & 5
SCALE 1/8" = 1'-0"

been built and bench-tested. A number of minor changes have been made which should make the cryostat easier to build and more durable. The new drawings have been transmitted to the machine shop, and construction of a new cryostat is being started.

The helium refrigerator, which supplies the cold helium gas for cooling the cryostat, has undergone several repairs and modifications which should improve its performance.

BONDED WIRE RESISTANCE STRAIN GAGES

M. R. Goodman

As mentioned in the preceding quarterly progress report, ORNL-782, specimens of annealed copper, 2S aluminum, and Nilvar, 6 in. by ½ in. diameter, were inserted in the pile in the water-cooled neutron converter hole No. 51 and maintained at 34°C. Radiation damage effects and dimensional changes were observed by means of special bakelite-bonded 100-ohm SR-4 gages that were cemented to the specimens. The specimens and gages were irradiated for an *nvt* of 3.0×10^{18} fast neutrons/cm^2. Data were taken, and graphs of strain vs. *nvt* and strain vs. time were plotted. The resulting curves appear as Figs. 26 through 31.

The curves appear to be a combination of exponential change, straight lines, and erratic behavior. For copper the total change during irradiation was about -500×10^{-6} in./in. strain. The change for 2S aluminum was about -350×10^{-6} in./in. strain and for Nilvar was about -290×10^{-6} in./in. strain. All changes indicated that a contraction had taken place.

The interpretation of the experimental results is incomplete. However, one or more of the following factors can contribute toward the changes observed:

1. Possible radiation damage to the bakelite in which the wire strain gage is embedded.
2. Possible radiation damage to the bakelite cement holding the strain gage to the specimen.
3. Possible radiation damage to the 0.001-in. constantan strain gage wire.
4. Breakdown of strain gage insulation resistance.
5. Actual radiation damage to the specimen itself, which, of course, the strain gage is supposed to indicate.

UNCLASSIFIED
DWG. 9937

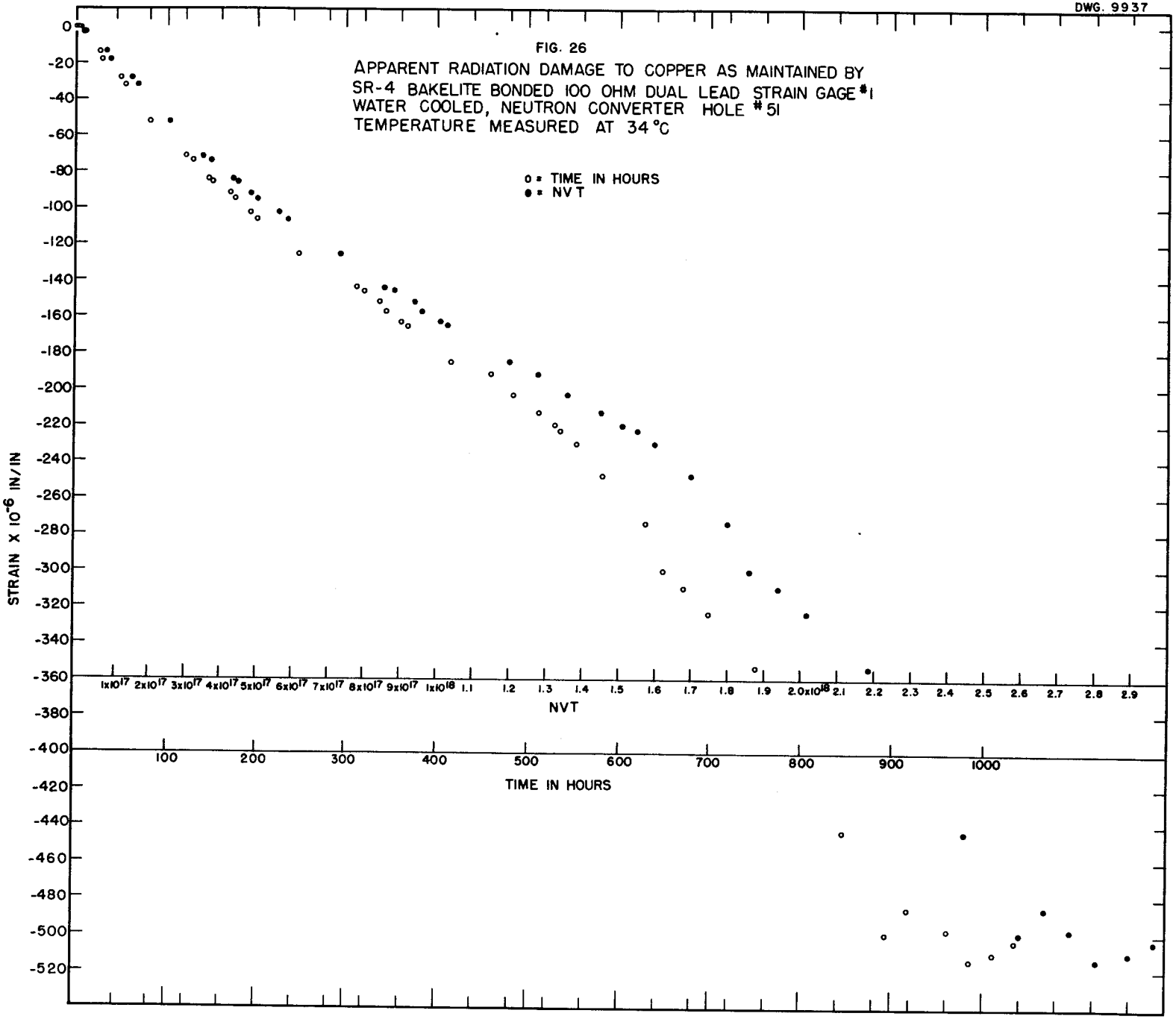

FIG. 26
APPARENT RADIATION DAMAGE TO COPPER AS MAINTAINED BY SR-4 BAKELITE BONDED 100 OHM DUAL LEAD STRAIN GAGE #1 WATER COOLED, NEUTRON CONVERTER HOLE #51 TEMPERATURE MEASURED AT 34 °C

UNCLASSIFIED
DWG. 9938

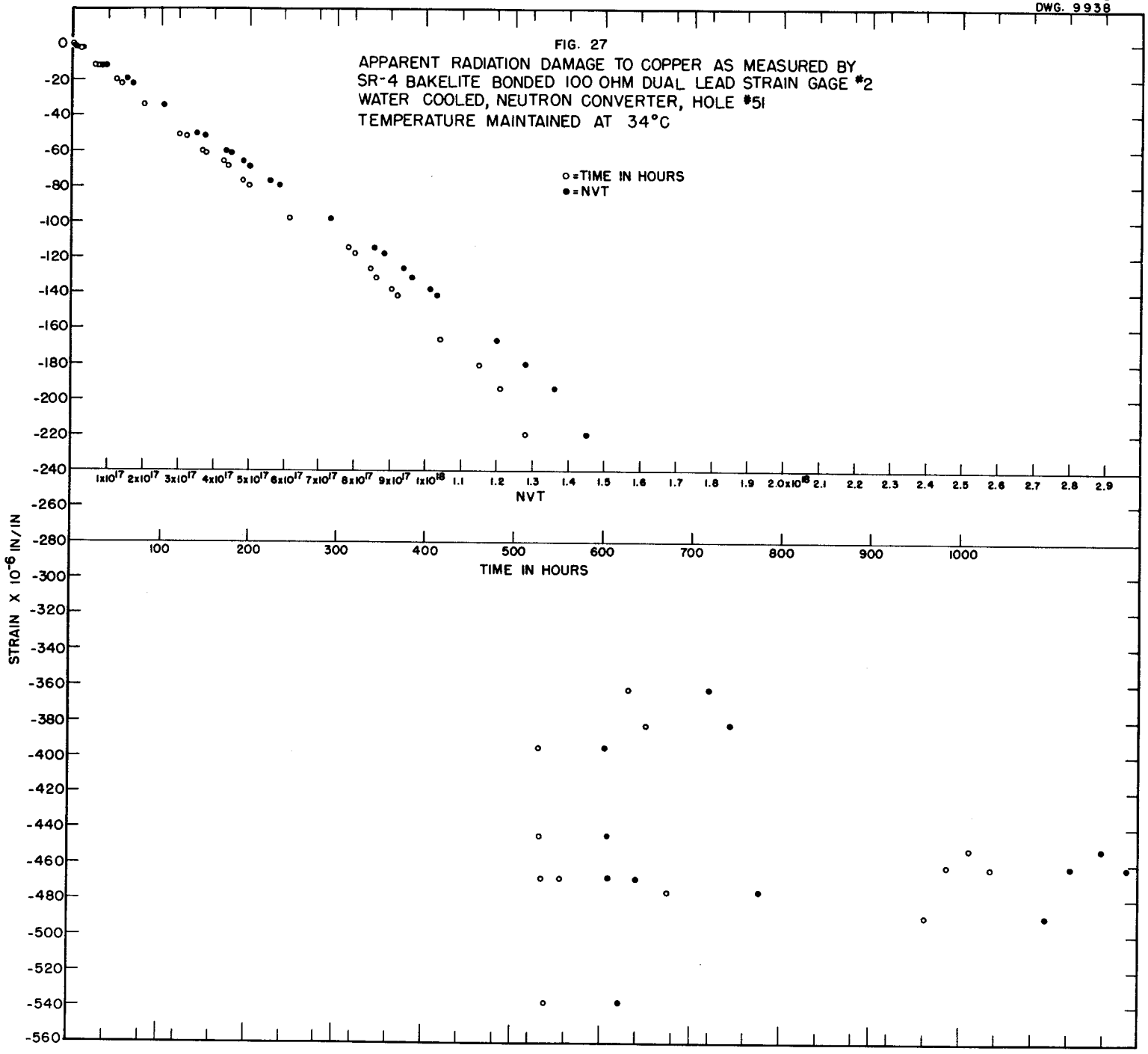

FIG. 27
APPARENT RADIATION DAMAGE TO COPPER AS MEASURED BY SR-4 BAKELITE BONDED 100 OHM DUAL LEAD STRAIN GAGE #2 WATER COOLED, NEUTRON CONVERTER, HOLE #51 TEMPERATURE MAINTAINED AT 34°C

UNCLASSIFIED
DWG. 9939

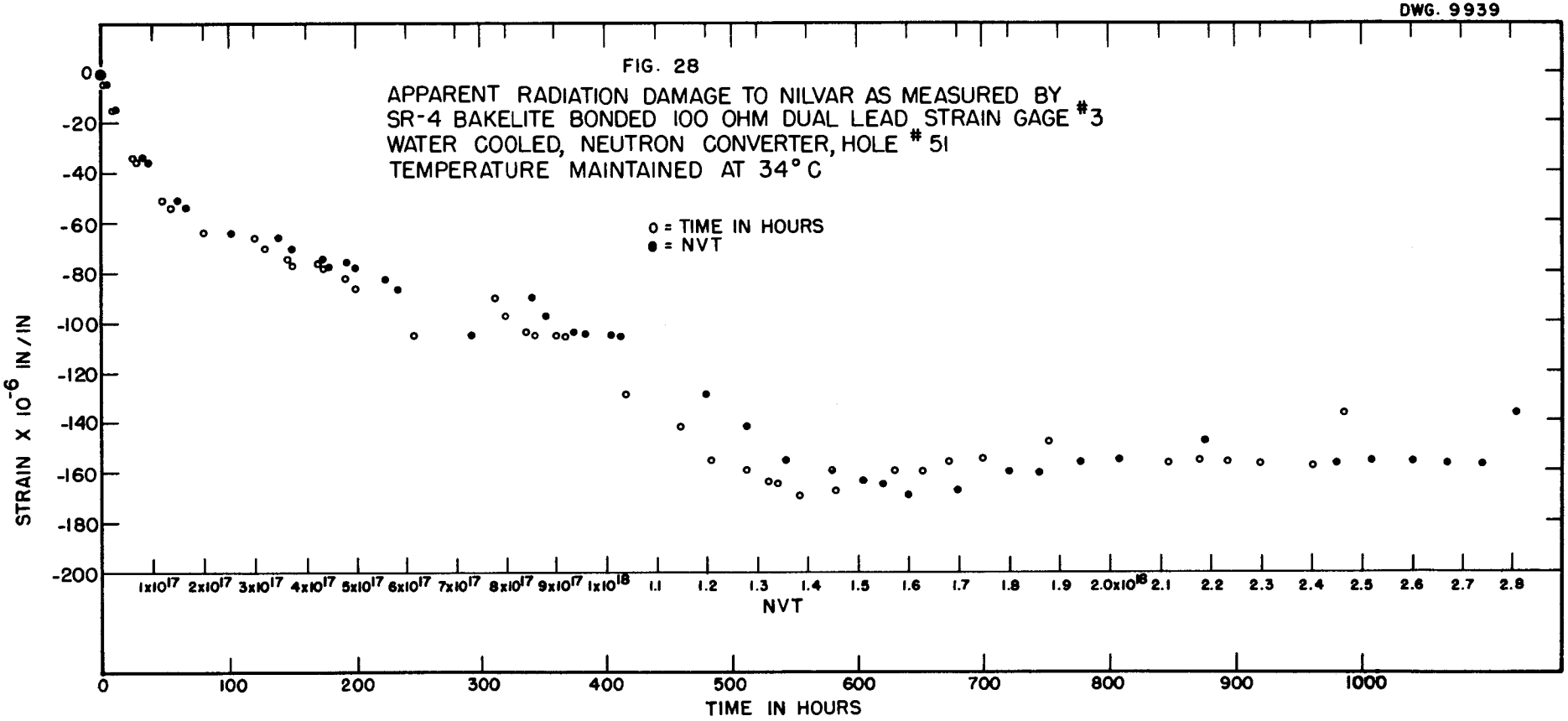

UNCLASSIFIED
DWG. 9940

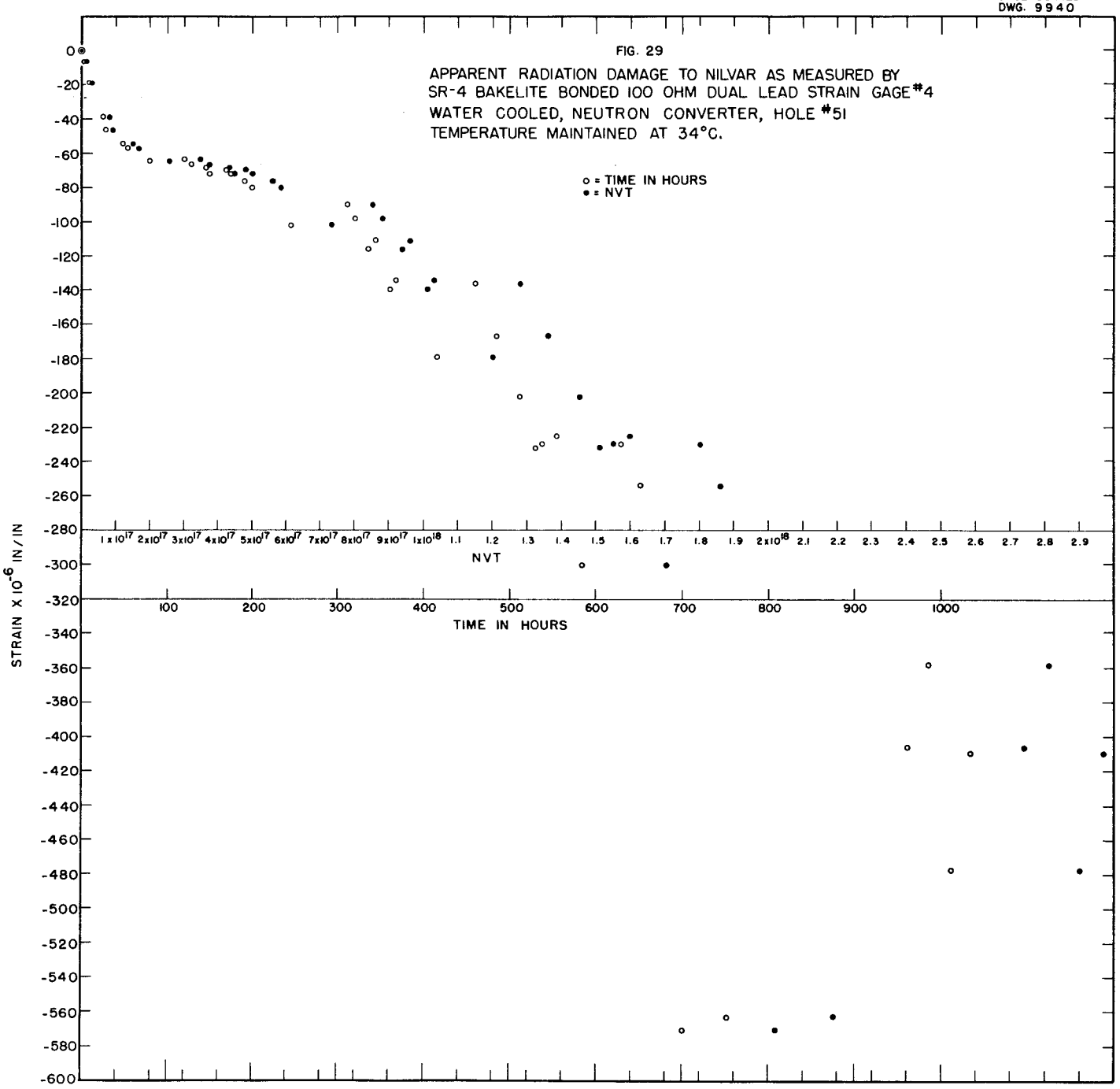

FIG. 29

APPARENT RADIATION DAMAGE TO NILVAR AS MEASURED BY SR-4 BAKELITE BONDED 100 OHM DUAL LEAD STRAIN GAGE #4 WATER COOLED, NEUTRON CONVERTER, HOLE #51 TEMPERATURE MAINTAINED AT 34°C.

UNCLASSIFIED
DWG. 9941

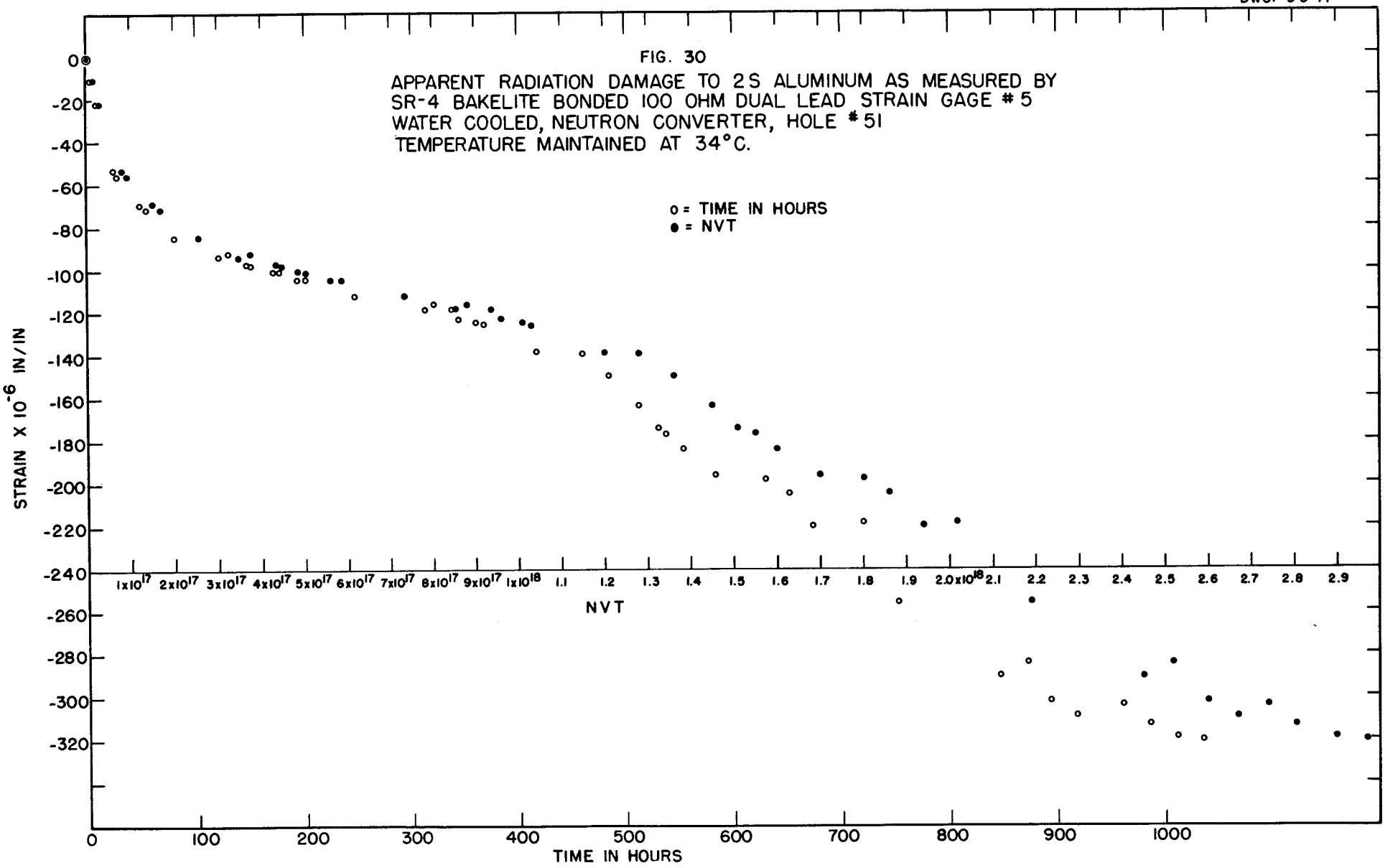

FIG. 30
APPARENT RADIATION DAMAGE TO 2S ALUMINUM AS MEASURED BY SR-4 BAKELITE BONDED 100 OHM DUAL LEAD STRAIN GAGE # 5 WATER COOLED, NEUTRON CONVERTER, HOLE # 51 TEMPERATURE MAINTAINED AT 34°C.

UNCLASSIFIED
DWG. 9942

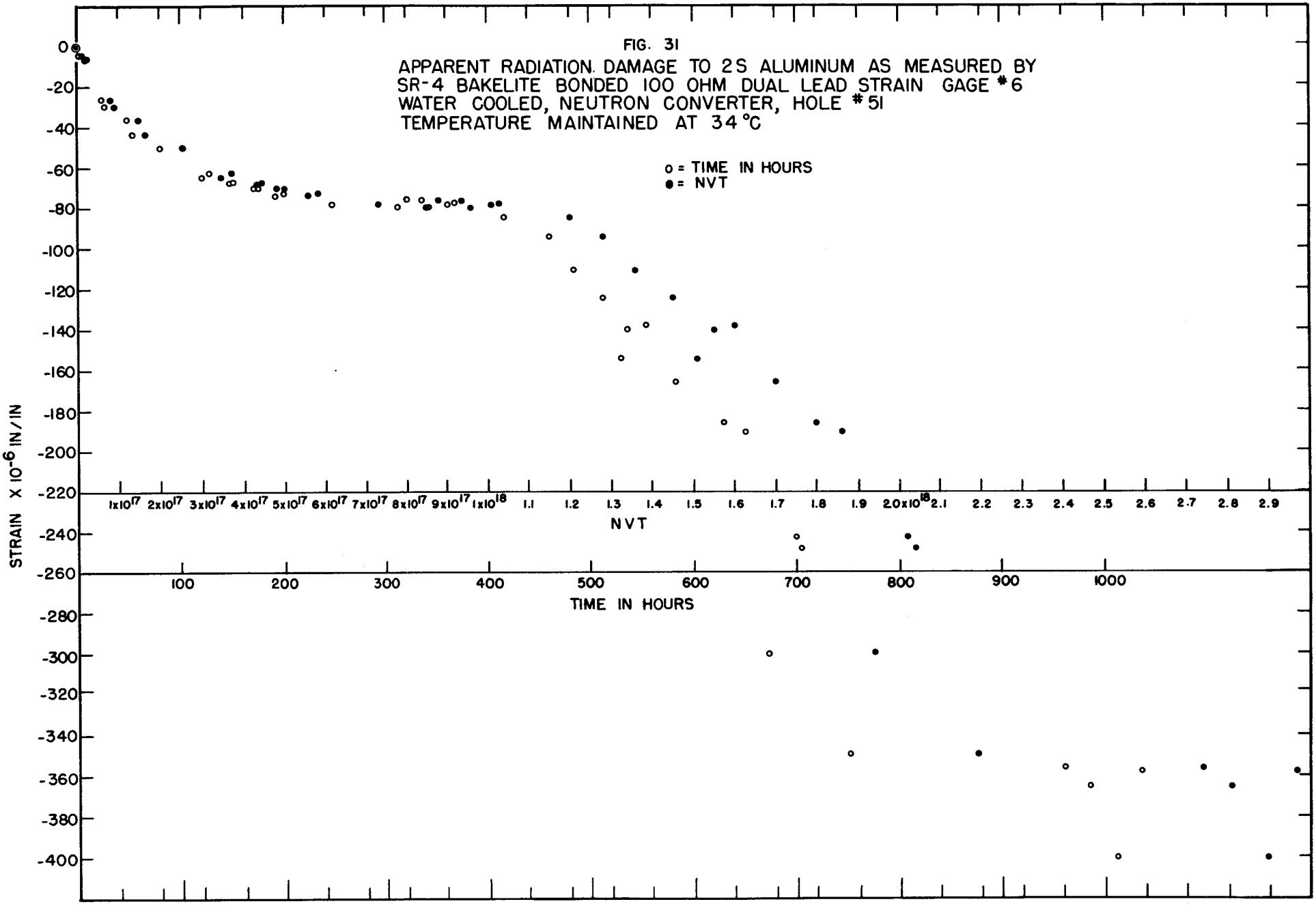

FIG. 31
APPARENT RADIATION DAMAGE TO 2S ALUMINUM AS MEASURED BY SR-4 BAKELITE BONDED 100 OHM DUAL LEAD STRAIN GAGE #6 WATER COOLED, NEUTRON CONVERTER, HOLE #51 TEMPERATURE MAINTAINED AT 34 °C

The previous history of the gages used (ORNL-707) in addition to in-pile experiments on bakelite and bakelite cement (reported in previous Physics Division quarterly reports) would seem to indicate that the strain gages should function satisfactorily in radiation fields of at least moderate intensity. However, the in-pile insulation resistance of the strain gages used in the present experiment decreased from greater than 10^9 ohms to a range varying from 1.5×10^5 to 2.0×10^4 ohms. Calculations indicate that the lowest gage insulation resistance of 2.0×10^4 ohms could cause an apparent radiation damage of about -625×10^{-6} in./in. strain. This would come about if it were assumed that the leakage path shunted the gage across its end. The chance that the leakage is in such a place as to cause an effect this great is very small.

There were times during the in-pile experiments when the readings giving apparent radiation damage were either too great to be measured by the bridge employed or were too erratic to record. Only the stable readings, repeated within 1×10^{-6} in./in. strain, were plotted in Figs. 26 through 31. Nevertheless some graphs still indicate periods of erraticness. The exact cause for such fluctuating readings is not at present known. Perhaps a loosening of the gage-to-specimen bonding or some sort of chemical interaction might account for the strange behavior observed. Such possibilities might even account for a large part of the apparent total dimensional change in the specimens irradiated.

Tensile testing work by C. A. Mossman (ORNL development engineer) on pile irradiation of bakelite strain gages on aluminum indicated that on four out of five specimens the bond between the strain gages and the specimens was broken. However, no change in insulation resistance was found (it remained greater than 10^9 ohms). Observations at close hand of our own specimens will have to wait until they cool down from radioactivity and are safe to handle and inspect.

Experiments are now planned to differentiate clearly between possible strain gage irradiation damage and actual irradiation damage to the specimen. Essentially these experiments will consist in machining appropriate specimens of copper, 2S aluminum, and thin sheet gage bakelite material to an accuracy of 0.0001 in. or better. All three dimensions will then be measured at many specially engraved marks to an accuracy of 0.00001 in. by means of an electrolimit gage. Specimens will then be annealed, remeasured, irradiated in the pile, and then again measured. In addition to the significance of these

experiments in their own right, it is hoped that the resulting dimensional changes will permit a proper evaluation of the meaning of the data contained in Figs. 26 through 31.

EFFECT OF PILE RADIATION ON PERFORMANCE OF ELECTRICAL LEADS

J. C. Pigg

A knowledge of the characteristic behavior of lead insulation is necessary for the proper evaluation of data obtained during in-pile experiments involving electrical measurements. Consequently, measurements of lead insulation resistance for a number of commercial specimens of lead wire were made during prolonged exposure. The conditions of the experiment approximate the most severe conditions encountered in the usual in-pile measurements of electrical resistance in the X-10 reactor.

Several wires with different types of insulation were wound around a conductor. The assembly was anchored by means of a graphite torpedo in the center of the pile through a central fuel channel. The insulation resistance was measured periodically by measuring the resistance between the various wires and the central conductor with a vacuum-tube megohmmeter. The specimens tested, chosen so as to be representative of most of the commerical types usually encountered, were (1) unbonded Ceroc, (2) Formex, (3) nylon braid with fiber filler on No. 22 Belden hookup wire, (4) polyethylene high voltage, (5) shielded 2S-aluminum wire with polyethylene insulation, and (6) enameled glass braid on Leeds and Northup duplex copper constantan thermocouple wire. The results of the experiment are summarized in Table XII.

The complete breakdown of the Ceroc and Formex is probably due either to a cracking or a flaking off of the insulation at a point which came in contact with the central conductor. This is borne out by the fact that intermittently during the exposure period both specimens did show resistances of the expected order of magnitude. The results definitely indicate that polyethylene insulation is the best material for long-period in-pile measurements, while for periods of about one week ordinary nylon braid is probably sufficient.

This work is being continued. In addition, tests of thermocouple behavior under long-term pile exposures are in progress.

TABLE XII

SPECIMEN	INITIAL RESISTANCE (ohms)	RESISTANCE AFTER TWO MONTHS OF CONTINUOUS BOMBARDMENT (ohms)	REMARKS
Ceroc	2×10^{10}	0.0	Shorted out after 4 days
Formex	3×10^{10}	0.0	Shorted out after 1 day
Nylon braid	3×10^{10}	1×10^{6}	Little change after 15 days
Polyethylene	3×10^{10}	1×10^{9}	Little change after 3 days
Polyethylene (2S-Al shielded)	3×10^{10}	1×10^{9}	Little change after 3 days
Glass braid L and N copper constantan	3×10^{10}	4×10^{5}	Slow change over entire period